



UNIVERSITÀ
DEGLI STUDI
FIRENZE

PhD in
Industrial Engineering

CYCLE XXXVI

Silencing the Noise: Advanced Active Noise Control
for Automotive and Outdoor Environments using FxNLMS
algorithm

Academic Discipline (ING-IND/15) 2023/2024

Doctoral Candidate

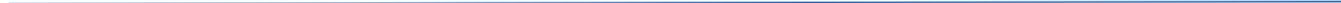
Massimo Generoso Buttarazzi

Supervisor

Prof.ssa Monica Carfagni

Coordinator

Prof. Giovanni Ferrara



The consultation of the thesis is free. Unless a specific authorization is obtained from the author, the thesis can be, however, downloaded and printed only for strictly personal purposes related to study, research and teaching, with the explicit exclusion of any use that has – even indirectly – a commercial nature

Contents

CONTENTS	3
ABSTRACT	7
ACKNOWLEDGEMENTS	9
PUBLICATIONS	10
LIST OF FIGURES	11
LIST OF TABLES	13
LIST OF ACRONYMS	14
LIST OF SYMBOLS	15
CHAPTER 1	17
1.1 Basic principles of Acoustics	18
1.1.1 The Physics of Sound Waves	18
1.1.2 Principles of Pure Tones, RMS Pressure and Sound Strength	19
1.1.3 Crafting Plane Sound Waves	21
1.1.4 Complex Sound Waves with Regular Patterns	22
1.1.5 Complex Sound Waves without Regular Patterns	23
1.1.6 Decibel Scale and Sound Intensity Analysis	25
1.1.7 Spatial Distribution of Sound Sources	27
1.2 Acoustic Properties: Reflection, Diffraction, and Refraction	27
1.3 Methods for Minimizing Undesirable Sources	29
1.3.1 Active Control Methods-Basic principles of ANC	30
1.4 Literature Review on Adaptive Algorithms	31
1.4.1 Least Mean Square (LMS) Algorithm	31
1.4.2 Normalized Least Mean Square (NLMS) Algorithm	34
1.4.3 The Exponentially Weighted Recursive Least Square (RLS) Algorithm	37
1.4.4 Filtered-x Least Mean Square (FxLMS) Algorithm	39
1.4.5 Feedforward Active Noise Control Systems	43

1.4.6	Feedback Active Noise Control Systems	47
1.4.7	Secondary Path Estimation	53
1.4.8	Acoustic Feedback Estimation	56
1.4.9	Hybrid Active Noise Control Systems	57
1.4.10	Multi Channels ANC systems	59
1.4.11	Deep Learning for Single-Multi Channels ANC systems	61
1.5	Motivation	64
1.6	Contributions	65
1.7	Thesis outline	67
CHAPTER 2		68
ANALYSIS OF POSSIBLE ALGORITHMS FOR ACTIVE NOISE CONTROL OF SIREN NOISE INTO AN AMBULANCE		68
CHAPTER 3		70
AN ACTIVE NOISE CONTROL SYSTEM FOR REDUCING SIREN NOISE INSIDE THE AMBULANCE.		70
CHAPTER 4		72
AMBULANCE SIREN ACTIVE NOISE CANCELLATION: REFERENCE SYNTHESIS AND SWITCHING FXLMS ON REAL-TIME TARGET HARDWARE		72
CHAPTER 5		74
ACOUSTIC SOURCE ARRAY FOR NOISE REDUCTION IN POWER STATIONS - AN ACTIVE NOISE CONTROL APPLICATION		74
5.1	Introduction to Electromagnetically Induced Acoustic Noise	75
5.1.1	The Magnetostriction Phenomenon	75
5.1.2	An Active Noise Control solution applied to an Electric Reactor	77
5.1.3	Design Assumptions for the Canceling Acoustic Field to be generated.	78
5.2	Proposed Solution: Distributed Secondary Sources Used for Antinoise Generation (virtual modelling)	79
5.2.1	Simulations for Analyzing Acoustic Fields	80
5.2.2	Identifying the optimal placement points for error microphones	83
5.3	Creation of Antinoise Field with an ANC algorithm	86
5.3.1	Feedforward FxNLMS with Reference Synthesis System	86
5.4	Field tests results	87
5.4.1	Field pre-tests results	87

5.4.2	Experimental results	90
5.5	Conclusions	90
	CHAPTER 6	91
	THESIS CONCLUSION	91
6.1	Thesis' Results	92
6.2	Future work	93
	REFERENCES	94
	APPENDIX A	99



Abstract

Active Noise Control (ANC) is a possible technique for reducing noise in the surroundings of appliances, consumer electronics, industrial equipment, mainly emitting in the low frequency range. The ANC technique is based on the cancellation of an noise control filters by generating an anti-noise using electronically controlled speakers. Noise reduction filters are applied to the control signal before being emitted by the speakers, which is how sound waves that are identical to amplitude but in opposition in phase compared to the unwanted noise are produced. Adaptive algorithms are used to update those noise control filters.

This thesis discusses the development of ANC algorithms that have been applied to both indoor and outdoor environments. The proposed algorithms are based on the Filtered-x Normalized Least Mean Squares (FxNLMS), typically employed for active noise cancellation problems. In particular, ANC techniques are employed for two specific applications and signals: the first one considers the reduction of a complex, but a priori known, signal (e.g. the siren of an ambulance), while the second one refers to a stationary pure tone noise produced by large industrial machinery (e.g. the emission of an electric reactor).

For the ambulance siren's case the objective was to protect drivers from the noise reaching inside the cabin, as they are exposed to loud and repeated sounds during field operations for extended periods of time. Environmental noise reduction, and particularly the noise generated by emergency vehicles, has been the focus of increased interest in the last decade due to its negative impact on people's physical and mental health. One of the most promising noise-mitigating solutions is the implementation of intelligent systems whose acoustic performance is actively controlled. The algorithms were first implemented in a Single Input Single Output (SISO) configuration, which served as a step towards a multichannel architecture. The adaptive filtering system consists of an error microphone and a control (secondary) loudspeaker, without employing a reference microphone to detect the noise that needs canceling, as the signal to be attenuated is known in advance.

Referring to the reduction of stationary noise produced by large industrial machines, the activity has been mainly focused on electric reactors, operating within a local electric substation, implementing active noise control techniques designed for noise reduction of the stationary, pure tone, humming noise they generate during operation. Such noise has been characterized, modeled, and investigated as a relevant case study of interest.

Finally, experimental activities were conducted to demonstrate the effectiveness of the developed control logic for both the SISO and Single Input Multiple Outputs (SIMO) configurations.

For all the above studies and application, the chosen approach involved actively intervening at the noise sources themselves to reduce their impact, rather than merely attenuating the noise downstream.

The results showed that intelligent noise cancellation system could achieve almost complete noise reduction within designated areas of interest, highlighting the successful performance of the systems studied and implemented.

Keywords: Active Noise Control (ANC), Filtered-x Normalized Least Mean Squares (FxNLMS), Adaptive filtering, Feedforward ANC.

Acknowledgements

I would like to express my gratitude to my tutor Dr Francesco Borchì, and supervisor Professor Monica Carfagni, for the constant support, availability, and kindness. Moreover, I want to thank the Acoustics Laboratory of Florence University for the opportunity to carry out the experimental activity and for the kindness of every person involved; finally, thanks to the whole Team Innovation Products and Processes (TIP), and in particular to Professor Rocco Furferi for encouraging me throughout my studies. Last but not least, special gratitude goes to my family and loved ones for constantly supporting me on this unforgettable journey.

Massimo Generoso Buttarazzi

October 2023

Florence (Italy)

Publications

Journal publications

1. **Buttarazzi, M. G.**, Bartalucci C., Borchì F., Carfagni M., and Paolucci L.. "Analysis of Possible Algorithms for Active Noise Control of Siren Noise into an Ambulance." In *International Conference on Design, Simulation, Manufacturing: The Innovation Exchange*, pp. 630-640. Cham: Springer International Publishing, 2021.
2. **Buttarazzi, M. G.**, Borchì F., Mambelli A., Carfagni M., Governi L., Puggelli L., "An active noise control system for reducing siren noise inside the ambulance", *Design Tools and Methods in Industrial Engineering III*. ADM 2023. Lecture Notes in Mechanical Engineering. Springer, Cham. https://doi.org/10.1007/978-3-031-52075-4_31 2024.
3. **Buttarazzi, M. G.**, Borchì F., Mambelli A., Carfagni M., Governi L., Puggelli L., "Ambulance Siren Active Noise Cancellation: Reference Synthesis and Switching FxLMS on Real-Time Target Hardware," (2023). (Under-Review on ADM-Springer International Publishing)

List of Figures

Figure 1. 1: Frequency-Wavelength.....	18
Figure 1. 2: Production of sound waves by a vibrating piston.....	18
Figure 1. 3: Example of the acoustic spectrum.....	23
Figure 1. 4: Cosine Series Plus Noise in time domain.....	24
Figure 1. 5: diffraction effect.....	29
Figure 1. 6: reflection and refraction effect.....	29
Figure 1. 7: LMS algorithm block diagram.....	31
Figure 1. 8: Resulting denoised sinusoid for each filter.....	35
Figure 1. 9: Calculated learning curves for the LMS and NLMS adaptive filters.....	36
Figure 1. 10: Predicted and actual LMS curves.....	37
Figure 1. 11: Negative feedback diagram RLS.....	38
Figure 1. 12: Fx-LMS Algorithm.....	39
Figure 1. 13: MSE behavior of the Fx-LMS.....	42
Figure 1. 14: Feed-forward configuration of single channel ANC system.....	44
Figure 1. 15: The results of the coefficients when apply Least Mean Square algorithm.....	46
Figure 1. 16: Report the results of Noise Residue, Noise Signal and Control Signal of the feedforward ANC system.....	47
Figure 1. 17: Feed-back configuration of single channel ANC system.....	48
Figure 1. 18: Adaptive feedback ANC system block diagram.....	49
Figure 1. 19: The results of the coefficients when apply Least Mean Square algorithm.....	51
Figure 1. 20: Report the results of Noise Residue, Noise Signal and Control Signal of the feedback ANC system.....	52
Figure 1. 21: ANC system with secondary path modeling (Eriksson’s method).....	54
Figure 1. 22: Using filter noise to generate impulse response, true secondary path impulse response.....	55
Figure 1. 23: Secondary Path Impulse Response Estimation.....	56
Figure 1. 24: Block diagram of single-channel ANC system with.....	57
Figure 1. 25: Block diagram of hybrid ANC system with combination of feedback ANC and feedforward ANC.....	58
Figure 1. 26: J reference microphones, K secondary sources and M error microphones make up the structure of a multichannel feedforward ANC system.....	59
Figure 1. 27: Block diagram of multichannel ANC system with J reference microphones, K secondary sources and M error microphones.....	60
Figure 1. 28: Block diagram of the multichannel active noise control system with J reference microphones, K secondary sources and M error microphones.....	61
Figure 1. 29: Single channel diagram of the deep ANC approach.....	62
Figure 1. 30: Single channel diagram of CRN based deep ANC.....	62
Figure 1. 31: Diagram of (a) deep MCANC approach, and (b) CRN based deep MCANC. P and S denoted primary and secondary paths. Superscripts (r) and (i) denote real and imaginary parts of signals, respectively....	63
Figure 5. 1: a) ferromagnetic material magnetic domain individual orientation with no external magnetic field; b) magnetostriction process in ferromagnetic material domains; c) resulting outcome of magnetostriction process in ferromagnetic material domains [4].....	76
Figure 5. 2: Diagram illustrating how increasing the number of domains can lower the external demagnetizing field and hence lower the magnetostatic energy.....	77
Figure 5. 3: Gradual tilt of molecular dipoles in a Bloch wall (B) to satisfy adjacent domains (A) and (C).....	77
Figure 5. 4: Primary source and control surface at 20 meters (note a series of secondary sources located near the reactor, represented by the black dots around the reactor).....	80
Figure 5. 5: a) Emission from the primary source b) Detail of the emission on the "vertical" plane.....	80

Figure 5. 6: a) Emission with Active Control 9x1 b) Detail of Vertical Plane Control	81
Figure 5. 7: a) Emission with Active Control 6x2 b) Detail of Vertical Plane Control	81
Figure 5. 8: Primary source and control surface at 20m with firewalls.	82
Figure 5. 9: a) Primary source emission b) Detail of Vertical Plane Control	83
Figure 5. 10: a) Emission with Active Control 9x1 b) Detail of Vertical Plane Control	83
Figure 5. 11: a) Emission with Active Control 6x2 b) Detail of Vertical Plane Control	83
Figure 5. 12: Full implant model. ANC microphones assumed area highlighted in red.	84
Figure 5. 13: ANC off.	84
Figure 5. 14: ANC on.	85
Figure 5. 15: SPL vs Distance from the Reactor.	85
Figure 5. 16: Graph of SPL along the segment where the placement of ANC microphones was assumed between the ANC On and ANC Off.	85
Figure 5. 17: Basic building block to generate a synthetic reference signal, $x_s(n)$, for a sine tone at 100Hz.	86
Figure 5. 18: Schematic representation of the system with 3 reactors and 3 error microphones, each paired with respective secondary acoustic speakers.	87
Figure 5. 19: Attempts to Replicate Attenuation System.	88
Figure 5. 20: Attempts to Reproduce the Cylindrical Noise Source (Tried with Control Boxes Both Outside and Inside the Cylinder of Figure 5.19).	88
Figure 5. 21: A laboratory configuration is shown, where the noise source is connected to the real-time target audio output. This setup emphasizes the primary and secondary acoustic paths, represented as $P(z)$ and $S(z)$, along with the highlighted "zone of silence."	88
Figure 5. 22: Configuration with sinusoidal tone at 100 Hz.	89

List of Tables

Table 1. Comparison of the algorithms discussed.....	43
---	----

List of Acronyms

ANC	Active Noise Control
LMS	Least Mean Square
NLMS	Normalized Least Mean Square
RLS	Recursive Least Mean Square
Fx-LMS	Filtered Least Mean Square
Fx-NLMS	Filtered Normalized Least Mean Square
FIR	Finite Impulse Response
IIR	Infinite Impulse Response
MSE	Mean Square Error
MMSE	Minimum Mean Squared Error
EMSE	Excess Mean Squared Error
TDOA	Time Difference of Arrival
DSP	Digital Signal Processing
ZoS	Zone of Silence
SISO	Single Input Single Output

List of Symbols

$d(n)$	Desired response/output of primary path
$E\{ \}$	Expectation operator
$e(n)$	Residual Error/Error Signal
f	Signal frequency
$P(z)$	Primary path transfer function
$S(z)$	Secondary path transfer function
$W(z)$	Noise control filter
$\hat{S}(z)$	Estimated secondary path transfer function.
$p(n)$	Impulse response of primary path
$s(n)$	Impulse response of secondary path
$w(n)$	Impulse response of noise control filter
$\hat{s}(n)$	Impulse response of estimated secondary path
$\hat{p}(n)$	Estimated secondary path transfer function
$x(n)$	Reference signal
$y(n)$	Control signal
*	Linear convolution
$v(n)$	Auxiliary noise
n	Time index
$R\{ \}$	Autocorrelation matrix factor
$\ -\ ^2$	Square of the Euclidean norm
λ	Forgetting factor
μ	Step size parameter
D	Delay parameter
Σ	Summatory
$\hat{P}_x(n)$	Power Estimate
L	Length of the filter
$\hat{s}_m y$	Coefficients of the FIR filter



Active Noise Control (ANC) is a powerful technology aimed at reducing or eliminating unwanted noise in different environments. It makes use of sophisticated technology and algorithms to actively cancel out unwanted sounds. Destructive interference is the underlying principle behind ANC.

ANC systems can successfully reduce or cancel undesired sounds by producing an anti-noise signal that is identical in amplitude but in anti-phase to the incoming noise.

Here is a comprehensive overview of Active Noise Control (ANC) techniques, along with an explanation of the underlying acoustic principles that underpin active control. Then, the contributions and research objectives for each of the two applications of interest—stationary pure tone noise generated by huge industrial machinery and complex signals with known a priori characteristics—are emphasized. Lastly, summaries of the upcoming chapters are given.

1.1 Basic principles of Acoustics

The study of sound is the focus of the field of acoustics in physics, such as mechanical waves that travel through a solid, liquid, or gaseous media because of object vibrations. Understanding sound waves and their properties – frequency, wavelength, velocity, and intensity – is one of the fundamental of acoustics.

A noise wave is a disturbance that propagates through space, carrying energy and momentum from one point to another, with a specific direction of propagation sound waves are therefore longitudinal waves. In *Figure 1. 1*, a classic example of a sinusoidal signal is depicted, highlighting the wavelength on the x -axis and intensity and distance on the y -axis.

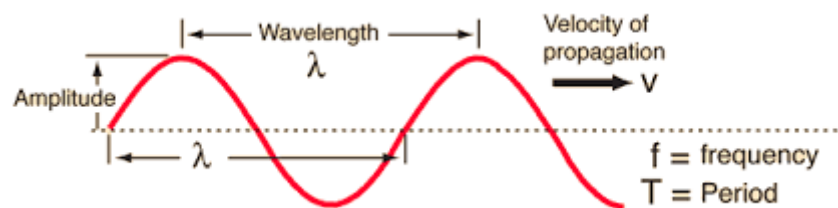


Figure 1. 1: Frequency-Wavelength.

1.1.1 The Physics of Sound Waves

Based on empirical evidence, vibrations generated by a membrane or any other surface at a specific frequency propagate through the atmosphere and are interpreted as sound when they reach our ears. A piston moving in reciprocating rectilinear motion at the mouth of a tube with rigid walls, as shown in *Figure 1. 2*, can serve as an explanatory example and produce sound.

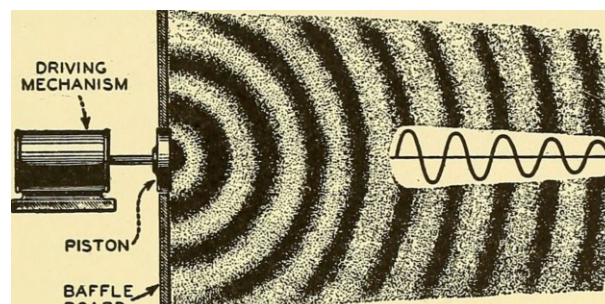


Figure 1. 2: Production of sound waves by a vibrating piston.

Compression and rarefaction occur in the air in contact with the piston. A sound wave is produced by a pressure disturbance that occurs inside the tube. Three distinct phases can be identified in the sound propagation system: emission, propagation, and reception. Propagation is the process by which movement is communicated and spreads across the fluid medium surrounding the body functioning as the source, whereas emission is the process by which a sound source creates excitation in an elastic medium by transferring mechanical energy. The pressure wave that makes up sound always follows a series of compressions and rarefactions and propagates according to different laws. Finally, reception is the process by which the sound is detected and converted into a physiological sensation (human ear) or into a measurable signal (measuring instrument) [1].

1.1.2 Principles of Pure Tones, RMS Pressure and Sound Strength

As it is well-known, sound propagation occurs only if there is an elastic medium (solid, liquid, or gas) for it to travel through. A specific type of sound wave is a plane progressive wave, where all particles within a plane in space move in a single direction with equal velocity and pressure. A typical source is a piston moving inside a tube of indefinite length (thus the motion is in one direction only) with angular velocity $\omega = \cos t = 2\pi f$. Consequently, the plane wave propagating in the tube is also sinusoidal in nature and is described by the equation of propagation:

$$p(x, t) = p_{max} \cos (\omega t - kx + \delta) \tag{1.1}$$

This is the equation of a progressive wave, meaning a wave that advances in the direction of increasing x with the passage of time. Similarly, a regressive wave will have a similar relationship to the above but with a positive sign for the term kx and δ represent phase angle.

Since sound pressure is a time- and space-varying quantity, it is useful to take its average value into account. However, a simple arithmetic average would produce a null result, which does not match the actual sound experience because sound pressure is a fluctuating quantity that revolves around zero. Because of this, effective sound pressure (P_e), which is always guaranteed to be different from zero, is introduced. P_e is the square root of the temporal average of squared values.

$$p_{RMS} = \sqrt{\int_0^T p(x, t)^2 dt}$$

(1.2)

In the case of a plane wave, this relationship holds:

$$p_{RMS} = \frac{p_{max}}{\sqrt{2}}$$

(1.3)

Considering an infinitesimal volume element of the medium, it is observed that as it oscillates around its equilibrium position, both its kinetic and potential energy vary. Along the x-axis, instantaneous power $W(t)$ travels through the normal surface A to the direction of wave propagation.

Instantaneous sound intensity $I(t)$:

$$I(t) = \frac{W(t)}{A}$$

(1.4)

Considering that instantaneous power can be expressed as the product of the force acting on the element by the instantaneous velocity, we derive, by calculating the average:

$$I = \frac{1}{T} \int_0^T p * u dt$$

(1.5)

Making considerations regarding the velocity with ρ_0 (medium density), c (propagation velocity in the medium), and substituting the effective pressure, we obtain:

$$I = \frac{p_{RMS}^2}{\rho_0 * c}$$

(1.6)

Therefore, with the relationship between effective RMS pressure and maximum

pressure for the case of the a plane wave, this equation represent it:

$$I = \frac{p_{max}^2}{2\rho_0 * c} \quad (1.7)$$

The product $\rho_0 * c$, known as acoustic impedance z , denotes the resistance that a material presents to the acoustic flow resulting from an applied sound pressure to the system. It is an intrinsic property of the medium through which the wave propagates.

It can be stated that sound intensity is a vector quantity, and its magnitude depends on the power of the source, the distance from the source to the receiver, and the characteristics of the medium through which the wave propagates.

1.1.3 Crafting Plane Sound Waves

Considering two plane sound waves propagating along the x-direction, each generating a disturbance at point x, respectively $d_1(t)$ and $d_2(t)$, if these disturbances overlap, the total pressure $p(t)$ will result from the sum of their effects. If the frequencies and maximum pressures of the two waves are identical, it would result:

$$d_1(t) = p_{max,1} * \cos(\omega_1 t + \delta_1) \quad (1.8)$$

$$d_2(t) = p_{max,1} * \cos(\omega_2 t + \delta_2) \quad (1.9)$$

Therefore, the square of the RMS pressure will be:

$$p_{RMS}(t) = p_{RMS_1} + p_{RMS_2} + 2 p_{RMS_1} p_{RMS_2} * \cos(\delta_1 - \delta_2) \quad (1.10)$$

The phase difference $(\delta_1 - \delta_2)$ between the two waves will provide different

outcomes. If the difference is equal to 0, meaning the two waves are in phase, we get $p_{RMS}^2 = 4 * p_{RMS_1}^2$, whereas if the difference is $\frac{\pi}{2}$, meaning the waves are in antiphase, we get $p_{RMS}^2 = 0$. Therefore, the sound wave could be completely cancelled out if an identical wave with a phase shift of $\frac{\pi}{2}$ is overlaid on it. RMS pressure from the composition of N random waves is typically equal to the total of the RMS pressures from each individual wave.

1.1.4 Complex Sound Waves with Regular Patterns

Multiple harmonically correlated frequency components are a defining feature of periodic complex sounds. The human ear perceives sounds differently, even when they have the same frequency and different waveforms [1]. The timbre of a sound is a property that the ear attributes to it. Fourier's theorem states that the sum of a specific number of sinusoidal or harmonic components can be used to represent a periodic disturbance:

$$p(x, t) = p_{max,1} \cos(\omega t + \delta_1) + p_{max,2} \cos(2\omega t + \delta_2) + \dots \quad (1.11)$$

Where:

- ω is fundamental pulsation.
- $2\omega, 3\omega$ are the higher harmonics.
- δ_1, δ_2 are phase angles.

Analyzing a wave's frequency spectrum is essential since it defines a wave's properties and how the human ear interprets them. One must perform a sound wave frequency analysis to identify these characteristics. The Fourier Transform, which assumes different forms based on the kind of signal being studied, is the foundation of this research. Nevertheless, the signal is seen by all Fourier Transform variants as a combination of a specific number—often even an unlimited number—of sinusoidal components operating at various frequencies.

The sound spectrum for stationary periodic sounds, or signals made up of waves with characteristics repeating over a fundamental period T , is made up of the fundamental frequency, $f_0 = 1/T$, and a range of frequencies that are multiples of the fundamental and are referred to as harmonics.

Only those frequency components in a spectrum that are whole number multiples of

the fundamental frequency—also referred to as harmonics—are included in the harmonic spectrum. The harmonics are depicted by a segment whose length is proportional to the square of the effective pressure (RMS) $p_{RMS,i}^2$ at the frequency associated with the respective harmonic, as illustrated in the *Figure 1. 3*.

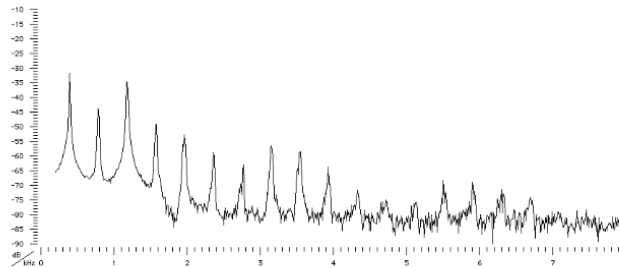


Figure 1. 3: Example of the acoustic spectrum.

This demonstrates, for example, how notes generated by various musical instruments can appear diverse even when they share the same basic frequency. The two instruments are believed to have different tones because of the only difference between them being the amplitudes of the harmonics that make up the two complex waves.

1.1.5 Complex Sound Waves without Regular Patterns

Aperiodic complex sounds lack this regularity and do not have a distinct base frequency, in contrast to periodic sounds, which are distinguished by a regular sequence of repetitions throughout time and a distinct basic frequency. These noises are produced when different frequencies of sound waves collide since there is no set harmonic order for the sound waves. When compared to periodic sounds, these noises are typically seen as more complicated and unexpected, and they are frequently labeled as noise. The sound of burning wood crackling, the continual hum of city traffic, or the whisper of wind through leaves are a few examples. These sounds have a distinct timbral nature since the spectrum analysis does not disclose the distinct peaks associated with harmonics, which are typical of periodic sounds. Instead, it reveals a continuous range of frequencies as depicted in the *Figure 1. 4*:

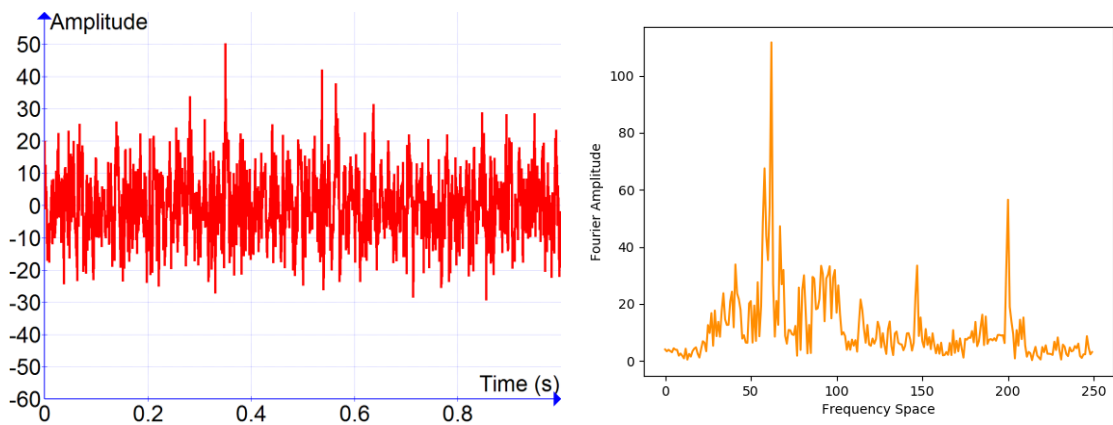


Figure 1. 4: Cosine Series Plus Noise in frequency and time domain.

Noise as a spectral characteristic shows a continuous distribution of infinite frequencies instead of discrete frequencies in harmonic relationships. Instead of identifying individual harmonic frequencies, the noise spectrum is usually examined using frequency bands, which are created by dividing the whole acoustic spectrum into intervals known as bands.

Analyzing an acoustic signal's spectrum entails determining how sound energy is distributed across different frequency bands. By applying particular filters to block frequencies outside of these ranges—high-pass filters are used to block lower frequencies, and low-pass filters are used to block higher frequencies—one can determine the effective sound pressure level within each frequency range, which is defined by a lower frequency limit (f_1) and an upper frequency limit (f_2). Octaves and one-third octaves are the most widely used divisions for this kind of study.

An octave interval is the range of frequencies between two frequencies, f_1 and f_2 , where f_2 is exactly twice f_1 in the context of musical acoustics. The relationship $f_c = \sqrt{f_1 * f_2}$ indicates that the ratio of the bandwidth to the central frequency f_c stays constant inside each octave. To break down octaves even further, one can further subdivide them into intervals of one-third octaves, which have three different ranges in each.

The application of the constant bandwidth band division approach to frequency analysis is covered in this paragraph, with an emphasis on the investigation of vibrations in equipment and structures. It highlights how useful this method is for carrying out in-depth and complex vibration assessments, which are essential for comprehending the behavior and structural integrity of machinery, buildings, bridges, and other engineering systems. The paragraph emphasizes that narrow band division is especially useful for higher frequencies, allowing for more exact

analysis compared to one-third octave or octave bands, even if it is beneficial for both low and high frequencies. This implies that narrow bands are better than wider bands for obtaining more accurate results in high-frequency vibration investigations [2].

1.1.6 Decibel Scale and Sound Intensity Analysis

Vibrations originating from a sound source are transmitted through the medium in the form of waves and then impact the eardrum membrane in the ear. For these vibrations to be considered as sound, that is, perceptible to the human ear, they must have a frequency ranging between **20 Hz** and **20 kHz**, which are the sensitivity limits of the human auditory system, defining the so-called audible range.

However, these limits have only statistical significance, as they can vary from individual to individual and with age. Moreover, higher frequencies, close to **20 kHz**, may only be perceived by a listener at a young age, but the sensation is often accompanied by a feeling of discomfort.

Oscillations at frequencies lower or higher than this range no longer elicit any auditory sensation and are respectively referred to as infrasound and ultrasound: seismic waves are an example of infrasound, while ultrasound can be produced, for instance, by the elastic vibrations of a quartz crystal induced by resonance through the application of an alternating electric field (piezoelectric effect) [2].

In practical acoustic problems, given the vast range of variables involved (such as frequency and power), it is not convenient to express acoustic quantities like sound pressure, power, and intensity in absolute values.

It is preferred to express these quantities by taking the logarithm of the ratio between them and certain reference values assumed as "zero" levels.

This system has proven useful because the logarithmic scale compresses numerical values, and because the intensity of auditory sensations is approximately proportional to the logarithm of the stimulus rather than its absolute value.

In acoustics, therefore, for energy quantities, it is common to adopt the sound level expressed in decibels (dB), defined as the decimal logarithm of the ratio between the value in question and the reference value.

In the next formulas are described the fundamentals level of the description of the acoustics phenomena:

➤ Sound power Level L_w :

$$L_w = 10 \log \frac{P_w}{P_0} \text{ (dB)} \quad (1.12)$$

where P_w is the sound power considerate ($Watt$) and P is the reference sound power ($10^{-12} Watt$)

➤ Sound Intensity Level L_i :

$$L_i = 10 \log \frac{I}{I_0} \text{ (dB)} \quad (1.13)$$

where I is the sound intensity under consideration (W/m^2) and I_0 is the reference sound intensity ($10^{-12} W/m^2$)

➤ Sound Pressure Level L_p :

$$L_p = 10 \log \frac{p^2}{p_0^2} = 20 \log \frac{p}{p_0} \text{ (dB)} \quad (1.14)$$

where p is the sound pressure considered (Pa) and p_0 is the reference sound pressure ($2 \times 10^{-5} Pa$)

One of the obstacles in defining noise occurrences in quantitative terms is from the necessity to quantify them, which are usually variable. Equivalent continuous sound level, or L_{eq} , was developed as a solution to this problem. This is the amount of a continuous, steady noise that would be similar in terms of its negative consequences to the fluctuating noise that is being evaluated. In essence, it conveys the noise's average energy level across the given time span. It is more accurately described as the level of constant, continuous noise that, over the same duration, would produce the same amount of sound energy as fluctuating noise. The formula of the equivalent level is:

$$L_{Aeq} = 10 \log \frac{1}{T} \int_0^T (p_A(t)/p_0^2) dt \quad (1.15)$$

where T represents the duration of the noisy emission (and thus the reference time interval), $p_A(t)$ is the instantaneous value of the sound pressure, using A-weighting, and p_0 is the reference sound pressure value.

1.1.7 Spatial Distribution of Sound Sources

An entity that can produce waves with properties like amplitude, frequency, and duration is called a source. The waves this source emits propagate within an elastic media when it comes in contact with it. The waves released by the source propagate directionally at high frequencies, which correspond to short wavelengths, affecting only restricted and geometrically defined portions of the medium. Waves become less directed as frequency decreases, and eventually waves with almost spherical wavefronts encompass the entire medium at low frequencies. Furthermore, the importance of secondary wave emissions that occur laterally, including transverse and surface waves, increases **Errore. L'origine riferimento non è stata trovata.**

1.2 Acoustic Properties: Reflection, Diffraction, and Refraction

When a sound wave encounters any material, its energy interacts with the material in several distinct ways, dividing into:

- **Reflected Energy:** a part of the energy contained in the sound wave is reflected into its original environment. This phenomenon is called reflection. The acoustic impedance mismatch between the encountered substance and the sound's propagation medium (such as air) determines the degree of reflection. Smooth, hard surfaces tend to reflect more sound than porous, squishy surfaces.
- **Transmitted Energy:** a further fraction of the energy of the sound wave travels through the substance and out the other side. Along with thickness and density, the material's acoustic impedance determines how much energy is transmitted. In general, materials that are thicker and denser transmit less sound energy than those that are thinner or less dense.
- **Absorbed Energy:** finally, the substance itself absorbs some of the energy. Because of internal friction and the viscoelasticity of the material, the absorbed energy is transformed into heat. To acoustically insulating an area, absorption is especially crucial since it lessens the quantity of sound energy reflected, which lowers reverberation and enhances sound quality. Acoustic

foam and rock wool are two examples of porous or fibrous materials that are particularly good at absorbing sound.

The way that the energy of a sound wave is distributed among its three categories—reflected, transmitted, and absorbed—determines the acoustic characteristics of the material, the surrounding environment, which in turn affects how sound is perceived, and the wavelength and angle of incidence of the sound wave.

The following explores different scenarios dependent on the thickness of the barrier T and the wavelength of the sound wave λ :

- $T \gg \lambda$: when the obstacle is significantly larger than the wavelength of the incident vibration, it sharply reflects the waves back according to the principles of geometric acoustics, thereby creating a well-defined reflected beam. Consequently, beyond the obstacle, an equally well-defined transmission zone is formed.
- $T \ll \lambda$: when the obstacle is significantly smaller than the incident wavelength, it acts exactly like an elementary Huygens-Fresnel source, dispersing waves over space and going completely undetectable.
- $T \approx \lambda$: diffraction phenomena cause the reflected wave to spread out in a diverging cone when the obstacle's dimensions are similar to the incident wave's wavelength. Within this cone, the wave propagates in many directions.

Diffraction is a phenomenon that occurs when the wavelengths are comparable to the thickness of the obstacle they encounter; for smaller wavelengths, corresponding to higher frequencies, the phenomenon is less evident. To understand how diffraction is generated, we must consider that each point on the wavefront acts as a point source, and as we've seen before, waves overlap. If there are N sources on a straight wavefront and we consider the superposition of the waves they generate, it can be observed that the resulting wave is also a straight wavefront. In the following Figure 1. 5, the different behavior for a sound source emitting waves at high frequencies and at low frequencies, where the phenomenon of diffraction occurs.

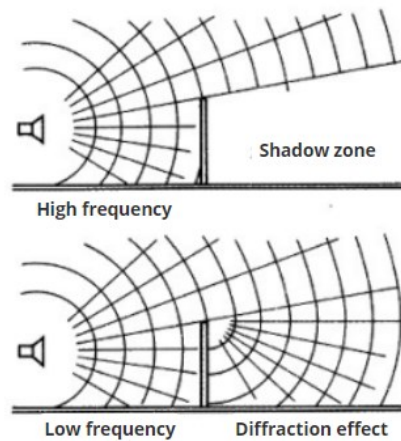


Figure 1. 5: Diffraction effect.

When waves move from one medium to another, they *refract*, whether they are sound or light waves. This is because the waves move through different materials at different rates. The wave's path will diverge at the interface where the two media meet since continuity needs to be preserved. The wave's changes in direction and speed when it transitions from one medium with a refractive index to another are what produce this divergence. The refractive index difference between the two materials determines the degree of refraction; larger differences cause the wave's path to change more noticeably Figure 1. 6.

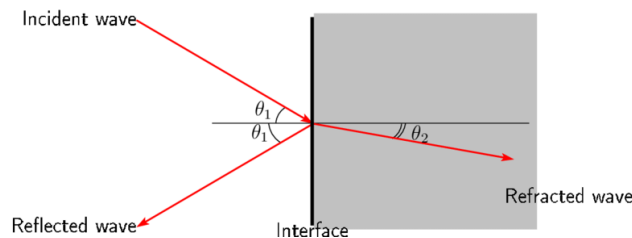


Figure 1. 6: Reflection and refraction effect.

1.3 Methods for Minimizing Undesirable Sources

Over the years, the use of noisy mechanical and electronic devices has increased exponentially in our daily lives. This has resulted in elevated levels of stress that have a negative impact on our health and productivity. Currently, available methods to mitigate this noise/stress issue are categorized as active and passive. Passive methods, such as concrete barriers, perform well at higher frequencies but become impractical at lower frequencies as the dimensions of these structures need to be

designed, constructed, and selected based on the wavelength of the noise under consideration [4].

In summary, passive techniques are generally based on vibration-damping technology, sound-absorbing materials, sound-insulating techniques (e.g. sound insulating box), and diffraction phenomenon (e.g. noise barriers), while to reduce undesired sound waves using active noise control techniques relies on the application of noise cancellation devices.

1.3.1 Active Control Methods-Basic principles of ANC

Active noise control (ANC) is the preferred choice for addressing low-frequency noises [5]. Due to its effectiveness, ANC is widely used in various industries, such as automotive and consumer audio, to enhance user experience by reducing ambient noise. Proper management of phase and amplitude of the cancellation signal is crucial for successful implementation of ANC [6]. Recently, active noise control (ANC) has experienced significant success in commercial products such as automobiles, headphones, and mobile phones, as well as demonstrated impressive results in various other applications, including aircraft cabin noise reduction, magnetic resonance imaging scanners, incubators, and air conditioning ducts [7].

Given that noise sources in both open and enclosed contexts are prone to time-varying fluctuations, the cancellation of the primary noise often depends on the distance and phase of the canceling noise. The fundamental noise's amplitude, frequency, and phase, change because of these alterations. By modifying key parameters of the classic cancellation algorithms (variations of the FxLMS in our cases) such as the step-size, input data correlation, and leakage factor, adaptive filters are used to handle these time-varying difficulties in real-time. These adaptive filters adjust to the input signal, but the input affects how they respond in terms of frequency.

The capacity of adaptive filters to dynamically change their bandwidth in response to changes is one of its key characteristics. Least-Mean-Square (LMS), Normalized Least-Mean-Square (NLMS), Recursive Least Squares (RLS), and Filtered Least Mean Square (FxLMS) are some of the common methods employed [8]. FxNLMS, combining NLMS and FxLMS above, was the algorithm used in the research study that produced the best outcomes and struck the ideal balance between the different algorithms.

The aim of the present research was to identify and implement active control algorithms for actual systems.

1.4 Literature Review on Adaptive Algorithms

Adaptive algorithms are widely used in signal processing and automatic control because they can effectively track slowly varying systems by utilizing time-invariant models. In the scientific literature [9] [10], a group of researchers has focused on analyzing and evaluating the performance of the adaptive algorithm known as LMS (Least Mean Square) using the mean square error as an evaluation metric. This study is based on the ability to have a priori knowledge of the received data and to acquire information during the execution process related to the operating environment of the algorithm. Then, different adaptive filters based on the mean square error are investigated and discussed.

1.4.1 Least Mean Square (LMS) Algorithm

The Least Mean Square (LMS) algorithm, developed by Widrow and Hoff in 1959 [11], is an adaptive algorithm that makes use of the steepest descent gradient-based technique [12]. The gradient vector's estimates from the supplied data are used by the LMS method. The least-squares method (LMS) is an iterative process that incrementally corrects the weight vector in the direction of the gradient vector's inverse to arrive at the minimal mean square error. In comparison to other methods, the LMS algorithm is relatively straightforward; it does not call for the calculation of a correlation function or the inversion of a matrix. In the following Figure 1. 7 shows the diagram of a typical adaptive filter, LMS.

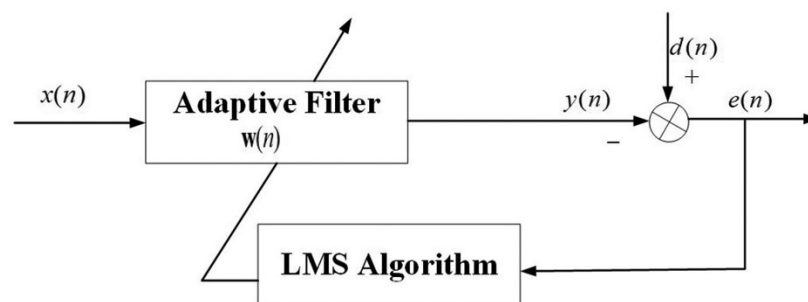


Figure 1. 7: LMS algorithm block diagram.

In the figure below:

- $x(n)$ is the input signal to a linear filter,
- $y(n)$ is the corresponding output signal,
- $d(n)$ is an additional input signal to the adaptive filter,

- $e(n)$ is the error signal that denotes the difference between $d(n)$ and $y(n)$.

Different linear filter types, such as finite impulse response (FIR) and infinite impulse response (IIR), are available. To reduce the power of $e(n)$, an adaptive algorithm iteratively modifies the linear filter's coefficients. Among other adaptive algorithms, the LMS method iteratively modifies the FIR filter coefficients. The LMS algorithm performs the following operations to update the coefficients of an adaptive FIR filter: The LMS algorithm performs the following operations to update the coefficients of an adaptive FIR filter:

- Calculates the FIR filter's output signal, $y(n)$:

$$y(n) = \vec{u}^T(n) * \vec{w}(n) \tag{1.16}$$

Where:

- $\vec{u}(n)$ is the filter input vector and

$$\vec{u}(n) = [x(n)x(n - 1) \dots x(n - N + 1)]^T \tag{1.17}$$

- $\vec{w}(n)$ is the filter coefficients vector and

$$\vec{w}(n) = [w_0(n)w_1(n) \dots w_{N-1}(n)]^T \tag{1.18}$$

- Calculates the error signal $e(n)$ by using the following equation:

$$e(n) = d(n) - y(n) \tag{1.19}$$

- Updates the filter coefficients by using the following equation:

$$\vec{w}(n + 1) = (1 - \mu)\vec{w}(n) + \mu * e(n) * \vec{u}(n) \tag{1.20}$$

where

- μ is the step size of the adaptive filter;
- $w(n)$ is the filter coefficients vector, weights;
- $u(n)$ is the filter input vector.

When evaluating the performance of the LMS algorithm, convergence and stability are crucial factors to consider.

Convergence refers to the behavior of the algorithm as it iteratively updates the weights towards the optimal solution. Stability, on the other hand, relates to the behavior of the algorithm in the presence of perturbations or noise. A stable algorithm makes sure that minor changes in the learning process or the input data don't lead to abrupt, significant changes in the weight updates.

An important parameter to detect stability and convergence in the LMS algorithm is the step size, sometimes referred to as the learning rate or adaption parameter. To perform well, the selection of an adequate step size is crucial.

If the value of the step size, μ , is chosen to be large, the weights may vary by a significant amount, which could cause a gradient that was initially negative to turn positive. This is because the weights' amount of change is very dependent on the gradient estimate. And because of the negative gradient, the weight may shift significantly in the other way at the second moment, continuing to oscillate with a wide variance around the ideal weights [13].

On the other hand, if μ is chosen to be too small, time to converge to the optimal weights will be too large.

Consequently, an upper bound on μ is required, and it is given as

$$0 < \mu < \frac{2}{\lambda_{max}} \tag{1.21}$$

where λ_{max} is the greatest value of the R, where

$$R = E(u(n)u^T(n)) \tag{1.22}$$

is the autocorrelation matrix of the input signal. Maximum convergence speed is

achieved when:

$$\mu = \frac{2}{\lambda_{max} + \lambda_{min}} \quad (1.23)$$

where λ_{min} is the smallest eigenvalue of \mathbf{R} . If μ is less than or equal to this optimum, then λ_{min} determines the rate of convergence, with a bigger value indicating a quicker rate of convergence. This means that faster convergence can be achieved when λ_{max} is close to λ_{min} , that is, the maximum achievable convergence speed depends on the eigenvalue spread of \mathbf{R} [14].

1.4.2 Normalized Least Mean Square (NLMS) Algorithm

The Normalized Least Mean Squares filter (NLMS) is a variant of the LMS algorithm that solves the problem of the stability and convergence speed of the algorithm by normalizing the learning rate in relation with the power of the input. The step size is replaced by learning rate $\Omega(k)$ normalized with every new sample according to input power as follows:

$$\Omega(k) = \frac{\mu}{\epsilon + \|x(k)\|^2} \quad (1.24)$$

where $\|x(k)\|^2$ is norm of input vector and ϵ is a small positive constant. To maintain stability when the input is close to zero, this constant is introduced. With this, more robust and reliable implementation of NLMS algorithm is obtained.

The stability of the NLMS filter is given by:

$$0 \leq \mu \leq 2 + \frac{2\epsilon}{\|x(k)\|^2} \quad (1.25)$$

The following example highlights the difference in convergence speed between the LMS and NLMS algorithms when using various parameters, which will be further specified. Using LMS and NLMS algorithms, extract the desired signal from a noise-corrupted signal by filtering out the noise. During the simulation filters of the 6-th order are used (6 adaptive coefficients). In fact, In Figure 1.3, sinusoids resulting from each filter—Wiener, LMS, and NLMS adaptive filters—are displayed to compare the

performance of these various techniques. This comparison is of significant scientific interest as it provides crucial insights into the effectiveness and robustness of different adaptive filters in the context of noise cancellation. One key aspect to consider is the adaptive filters' ability to reduce noise while preserving the desired signal. This can be evaluated by analyzing the percentage of noise reduction achieved by each filter relative to the original signal. Additionally, assessing the quality of the cleaned signal, including the presence of any artifacts or distortions introduced by the filtering process, is essential. Another important metric is the convergence speed of the filters—i.e., the time required for the filter to reach its optimal configuration and begin producing effective results. Rapid convergence is desirable for real-time applications, where changes in the acoustic environment need to be swiftly and efficiently managed. Furthermore, it's crucial to consider the adaptive filters' robustness to variations in the acoustic environment. This can be evaluated by examining how the filters respond to sudden or long-term changes in noise characteristics, such as variations in intensity or frequency.

Lastly, the analysis should also consider the computational resources required by each adaptive filter. Computational complexity is a significant consideration, particularly for real-time applications, where striking a balance between performance and computational efficiency is essential.

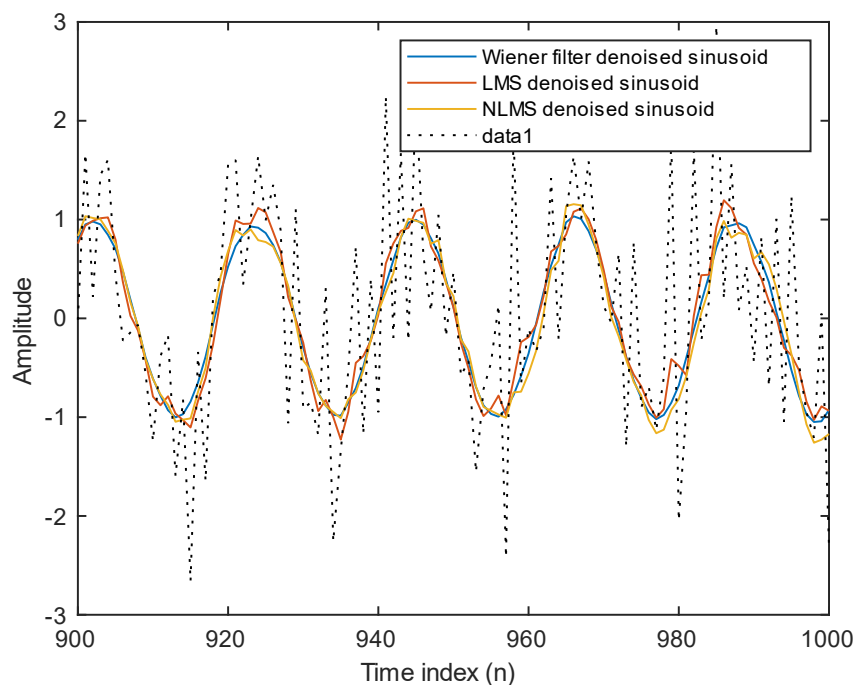


Figure 1. 8: Resulting denoised sinusoid for each filter.

During signal processing, calculating the Mean Square Error (MSE) at regular intervals, such as every 10 samples as depicted in *Figure 1. 8*, can provide valuable insights into the performance of the signal processing algorithm. This approach allows for the efficient monitoring of the algorithm's convergence and its ability to accurately model and adapt to the underlying signal and noise characteristics.

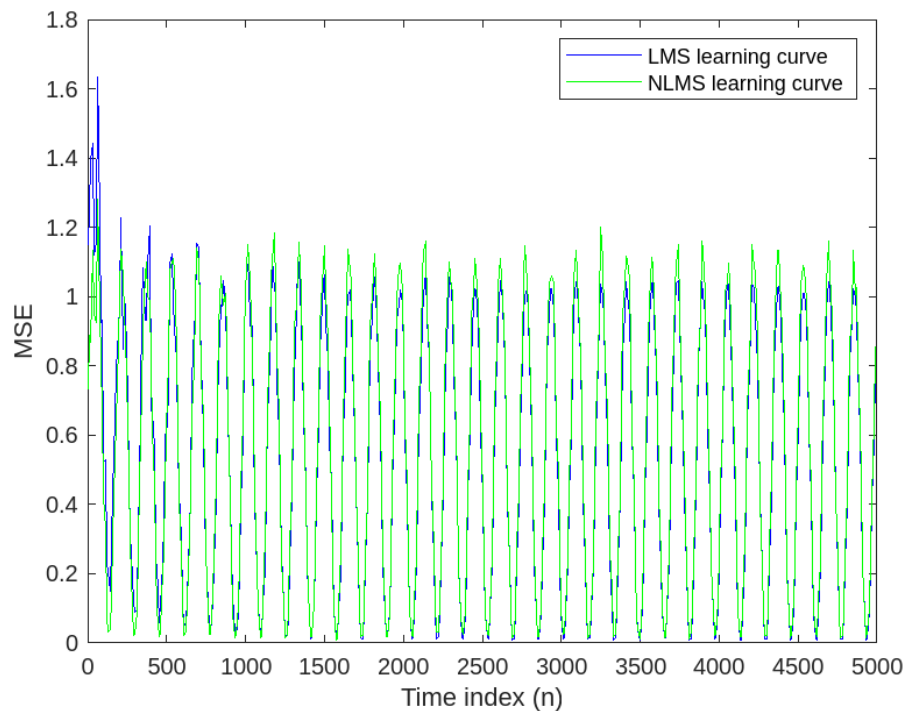


Figure 1. 9: Calculated learning curves for the LMS and NLMS adaptive filters.

Theoretical learning curves for the Least Mean Squares (LMS) and Normalized Least Mean Squares (NLMS) algorithms can be calculated in MATLAB software, as shown in *Figure 1. 9*. These learning curves provide insightful information on how the algorithms function and behave during the adaptation process. Calculating these learning curves is justified scientifically by the need to evaluate the algorithms' long-term convergence and stability. Plotting the MMSE (Minimum Mean Squared Error) and EMSE (Excess Mean Squared Error) *Figure 1. 10* across time or iterations allows researchers to see whether the algorithms show any indications of instability or divergence, as well as how quickly they converge to solutions.

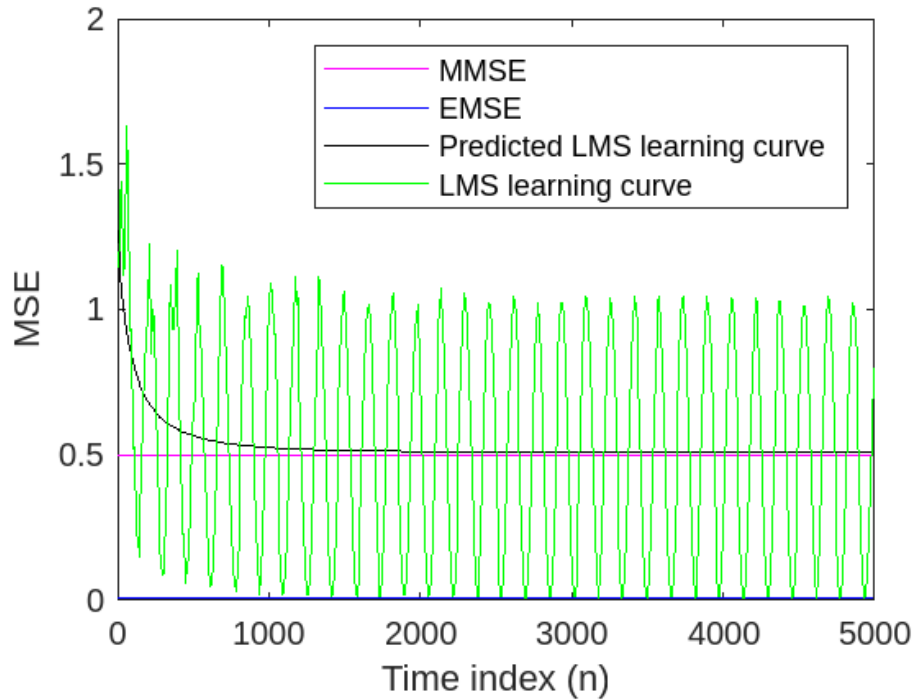


Figure 1.10: Predicted and actual LMS curves.

1.4.3 The Exponentially Weighted Recursive Least Square (RLS) Algorithm

The Recursive Least Squares (RLS) algorithm is an adaptive filter algorithm that iteratively determines the coefficients by minimizing a weighted linear least squares cost function associated with the input signals. This differs from other algorithms like the Least Mean Squares (LMS) algorithm, which aims to minimize the mean square error. While the LMS and other comparable algorithms treat the input signals as stochastic, the Recursive Least Squares (RLS) algorithm treats them as deterministic. In contrast to many rival algorithms, the RLS method exhibits very quick convergence [15]. It is more computationally intensive due to the higher computational complexity that comes with this benefit.

By carefully choosing the filter coefficients W_n and updating the filters as new data is received, RLS filters aim to minimize a cost function C . The negative feedback diagram below, *Figure 1.11*, defines the erroneous signal $e(n)$ and desired signal $d(n)$:

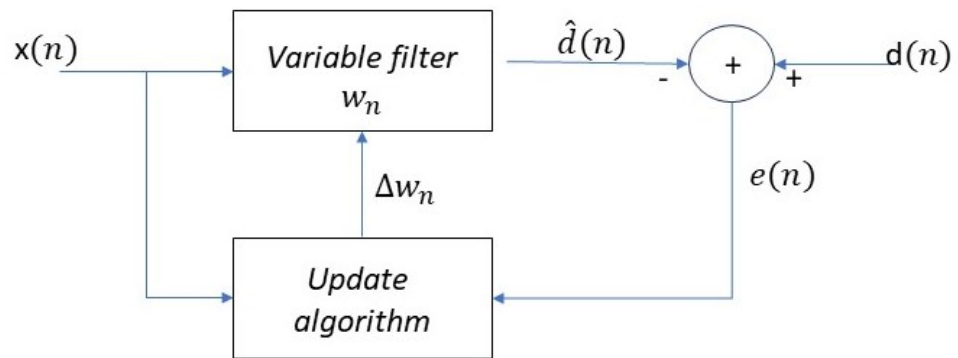


Figure 1. 11: Negative feedback diagram RLS.

Through the estimate $\hat{d}(n)$, the error is implicitly dependent on the filter coefficients:

$$e(n) = d(n) - \hat{d}(n) \quad (1. 26)$$

The weighted least squares error function C -the cost function we desire to minimize- being a function of $e(n)$ is therefore also dependent on the filter coefficients:

$$C(w_n) = \sum_{i=0}^n \lambda^{n-i} e^2(i) \quad (1. 27)$$

where $0 < \lambda \leq 1$ is the “forgetting factor” which gives exponentially less weight to older error samples [16].

1.4.4 Filtered-x Least Mean Square (FxLMS) Algorithm

The weights of the control filter are frequently updated in ANC systems using the filtered-x least mean-square (FxLMS) algorithm, although the complexity of the FxLMS technique rises linearly with the length of the filter. The control filter can number in the thousands in some situations. The FxLMS algorithm is a simple LMS variation, which is why it was chosen based on the criteria for minimization of mean square error. In a textbook, Haykin has offered a comprehensive analysis of this adaptive method [17].

The diagram of the FxLMS algorithm is presented in *Figure 1.12*. The following figure is formed by:

- $P(z)$: represents the primary path.
- $S(z)$ represents the secondary path (as will be illustrated in the upcoming sections).
- $W(z)$ represents the weight vector.
- $x(n)$ is the reference signal picked up by a reference microphone.
- $y(n)$ is the filtered cancelling signal driven by a secondary loudspeaker.
- $d(n)$ is the disturbance signal at the error microphone.

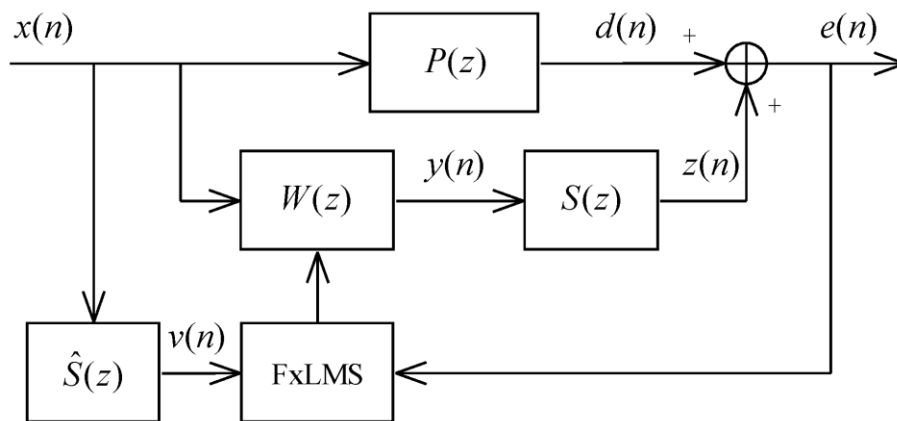


Figure 1.12: Fx-LMS Algorithm.

The block $W(z)$ of the control filter at the time index n is formed by the equation $\mathbf{w}(n) = [w_0(n), w_1(n), \dots, w_{N_w-1}(n)]^T$ with a length of N_w .

$$y(n) = \mathbf{x}^T(n) \mathbf{w}(n) \quad (1.28)$$

where $\mathbf{x}(n) = [x(n), x(n-1), \dots, x(n-N_w+1)]^T$ is the reference signal vector. The cancelling signal $y(n)$ is then filtered by secondary path $S(z)$ to obtain the control signal $z(n)$ at the location of the error microphone:

$$z(n) = \bar{\mathbf{y}}^T(n) \mathbf{s} \quad (1.29)$$

where $\bar{\mathbf{y}}(n) = [y(n), y(n-1), \dots, y(n-N_s+1)]^T$ and $\mathbf{s} = [s_0, s_1, \dots, s_{N_s-1}]^T$ is the weight vector of the secondary path with a length of N_s .

The residual error signal picked up by the error microphone is:

$$e(n) = d(n) + z(n) \quad (1.30)$$

The primary objective of the FxLMS method is to update the weight vector [18].

The following equation represents the weight vector in relation to step size μ and filtered reference signal vector $\mathbf{V}(n) = [v(n), v(n-1), \dots, v(n-N_w+1)]^T$:

$$\mathbf{w}(n+1) = \mathbf{w}(n) - \mu \mathbf{v}(n)e(n) \quad (1.31)$$

and

$$v(n) = \mathbf{x}_s^T(n) \hat{\mathbf{s}} \quad (1.32)$$

where both variables, $\mathbf{x}_s(n)$ and $\hat{\mathbf{s}}$ are the estimate of the actual weight vector of the secondary path.

$$\mathbf{x}_s(n) = [x(n), x(n-1), \dots, x(n-N_s+1)]^T \quad (1.33)$$

$$\hat{\mathbf{s}} = [\hat{s}_0, \hat{s}_1, \dots, \hat{s}_{N_s-1}]^T \quad (1.34)$$

The Fx-LMS needs a precise estimate of the secondary path, which may be obtained using either an offline model or an online model [19]. The multiplications are necessary for the Fx-LMS algorithm. The weight vector's length could exceed a thousand taps in some circumstances. As a result, real-time systems are very concerned about computational complexity.

Mean Square Error (MSE) is determined to assess the Fx-LMS algorithm's efficacy in reducing noise. This parameter shows the average of the squared errors between the intended signal, such as a clear signal free of noise, and the filtered signal obtained by using the Fx-LMS algorithm to reduce the noise.

Using MATLAB software, the MSE value, in *Figure 1.13*, is calculated such as the length of the adaptive filter to 32 taps, step size to 0.008, and the decimation factor for analysis and simulation to 5.

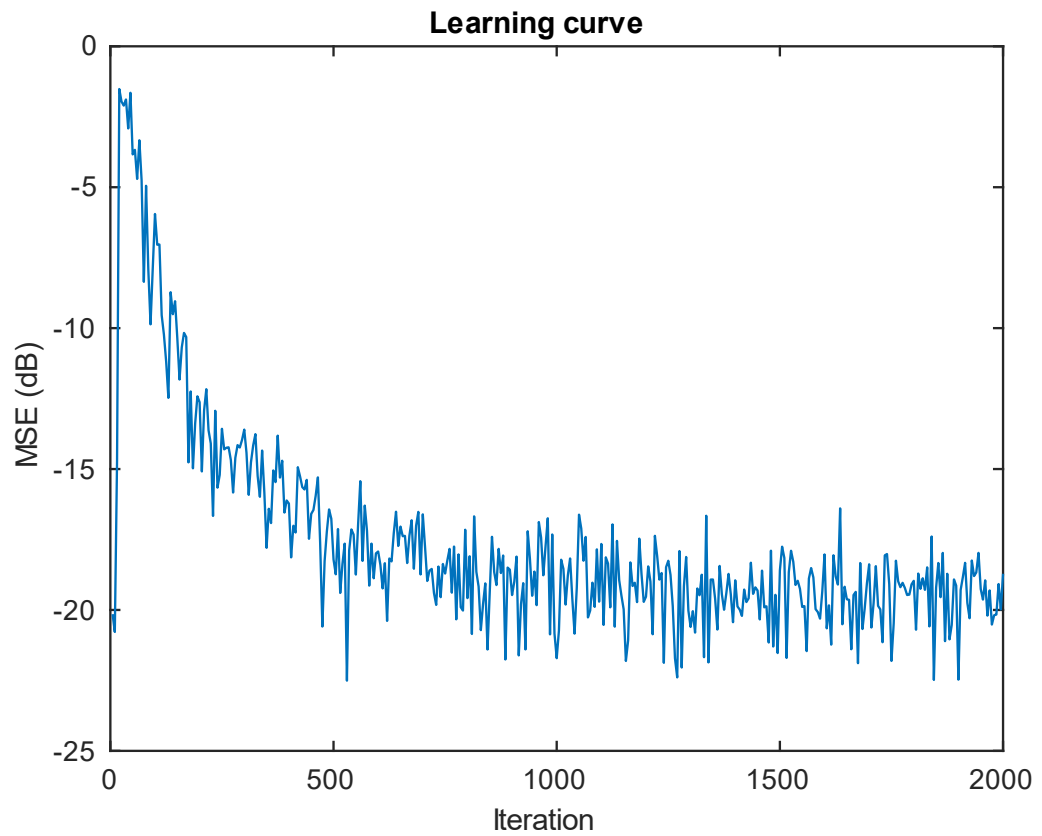


Figure 1. 13: MSE behavior of the Fx-LMS.

A low MSE signifies that there is little difference between the target signal and the filtered signal, which suggests that the Fx-LMS algorithm has a good ability to decrease noise. A high MSE score, on the other hand, denotes a lower level of noise reduction efficacy.

Finally, the following table I represents a comparison of the algorithms discussed above.

Algorithm	Strengths	Weaknesses
LMS	Low computational complexity, Stable	Slow speed of convergence and less robust
NLMS	Fast speed of convergence, stable	More computational complexity than LMS and less robust than RLS
RLS	Fast speed of convergence, More robust	Very high computational complexity and Unstable
Fx-LMS	Less computational complexity, Simple real time realization	Slow speed of convergence

Table 1. Comparison of the algorithms discussed.

1.4.5 Feedforward Active Noise Control Systems

Feedforward Active Noise Control (ANC) systems are a type of noise reduction system that aims to cancel out unwanted noise by generating an anti-noise signal. These systems are designed to attenuate noise before it reaches a desired location, such as a listener's ears or a specific area in a room. A reference microphone, a control algorithm, an adaptive filter, and a secondary loudspeaker are the main elements of a feedforward ANC system. The adaptive filter estimates the noise signal based on the reference input while the reference microphone records the undesirable noise signal [20],[21]. To maximize the cancellation of the noise signal, the control algorithm modifies the adaptive filter's coefficients.

Creating an anti-noise signal that is out of phase with the incoming noise is the core

tenet of feedforward ANC [22]. Destructive interference results from adding the anti-noise signal to the noise signal, which lowers the overall noise level. Based on the error signal, which is the difference between the reference microphone input and the filtered output, the adaptive filter continuously modifies its coefficients [23],[24].

In *Figure 1. 14* is represents a schematic of a basic feedforward ANC system.

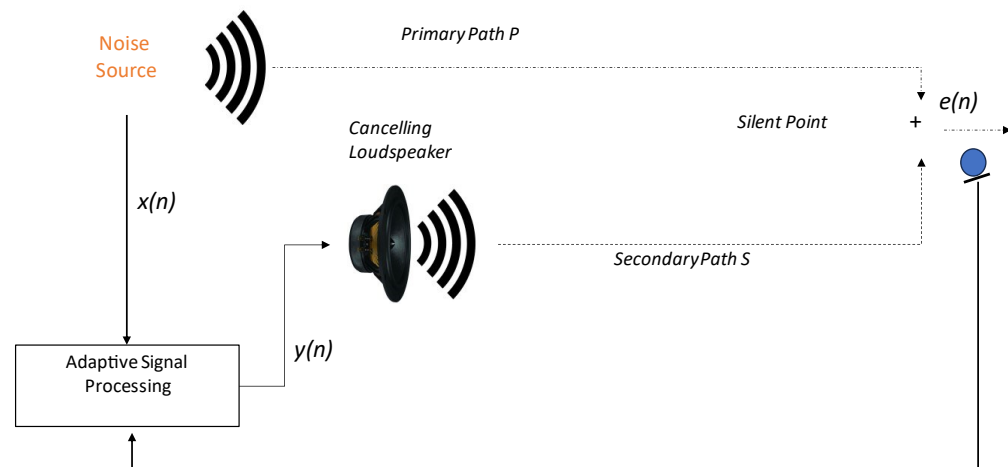


Figure 1. 14: Feed-forward configuration of single channel ANC system.

The noise control filter and the reference signal collected by the reference microphone combine to create the anti-noise in the feedforward ANC system. The undesired noise is then canceled by the anti-noise that is radiated by the secondary source. The undesirable noise should not get to the error microphone before the anti-noise does. The reference path, the noise controller, and the secondary path should all have a smaller overall delay than the primary path. The feedforward ANC system is unable to eliminate the undesired noise if the causality constraint is breached, which happens when this criterion is not met [25].

The causality constraint can be represented by:

$$D_p > D_r + D_c + D_s \tag{1.35}$$

- D_p is the propagation delay from the noise source to the error microphone
- D_r is the propagation delay from the noise source and reference microphone
- D_c is the processing lag caused by the calculations to produce the anti-noise
- D_s is the sum of the reaction times of the analog-to-digital converter, digital-to-analog converter, analog low-pass filters, secondary loudspeaker, secondary loudspeaker propagation time, and error microphone propagation time.

The inequality can be rewritten as:

$$D_p - D_r > D_c + D_s \tag{1.36}$$

The TDOA (Time Difference of Arrival) between the reference microphone and the error microphone is shown on the left side of the inequality [26].

The complete Acoustic Feedforward Active Noise Control system using the filtered-x least-mean-square (Fx-LMS) algorithm is pitched in Figure 1. 7 in the precedent paragraph.

The Fx-LMS method is implemented in this straightforward simulation for a single channel feedforward active noise control system. To prevent destructive interference from occurring at the sensor point, the controller generates an "anti-noise" signal in this case. The goal is to reduce the noise leftover.

Two jobs make up the process: "off-line" identification of the secondary propagation path that remains between the actuator and sensor, and "on-line" control, which involves modifying the controller's parameters.

Most methodologies for online modeling of the secondary path rely on using random white noise as a training signal to obtain an accurate estimation of the path itself, namely its transfer function. Typically, a preference is given to white noise with higher amplitude and low variance, as this promotes greater precision and faster convergence, covering a broader range of frequencies [27].

In *Figure 1. 15* the results of the product of the coefficients of the secondary path is presented, during its estimate, with generation of a white noise signal and applying least mean square algorithm.

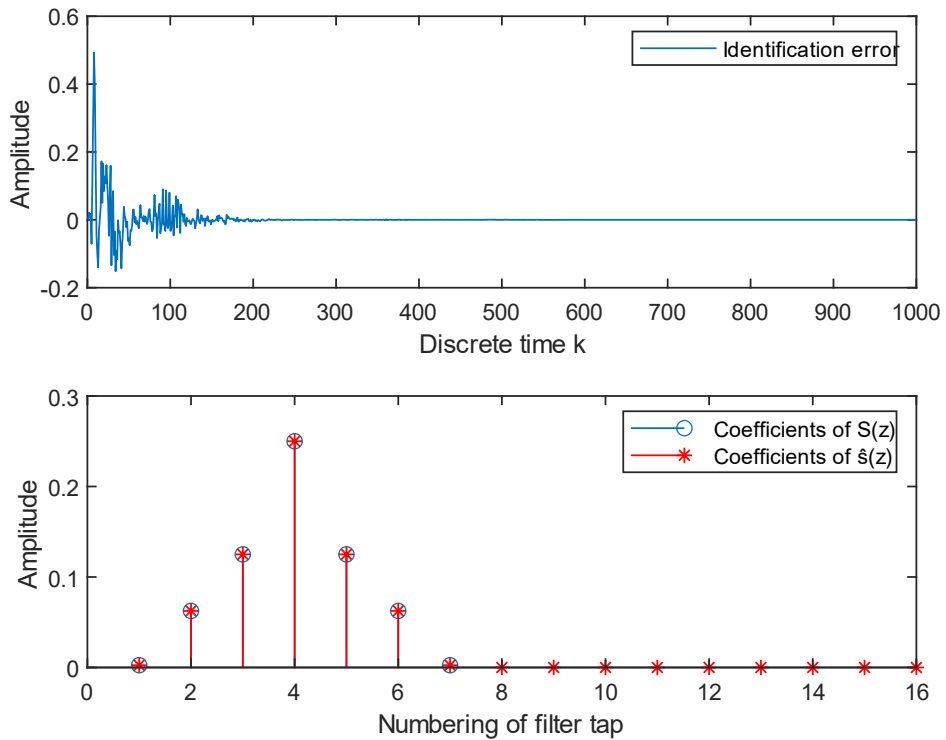


Figure 1. 15: The results of the coefficients when apply Least Mean Square algorithm.

In the *Figure 1. 16* the active control is turned on with generation of a noise and, measuring the arriving noise at the sensor position, plot the report of the results of the Noise residue, noise signal and control signal in discrete time with amplitude, applying the Fx-LMS algorithm.

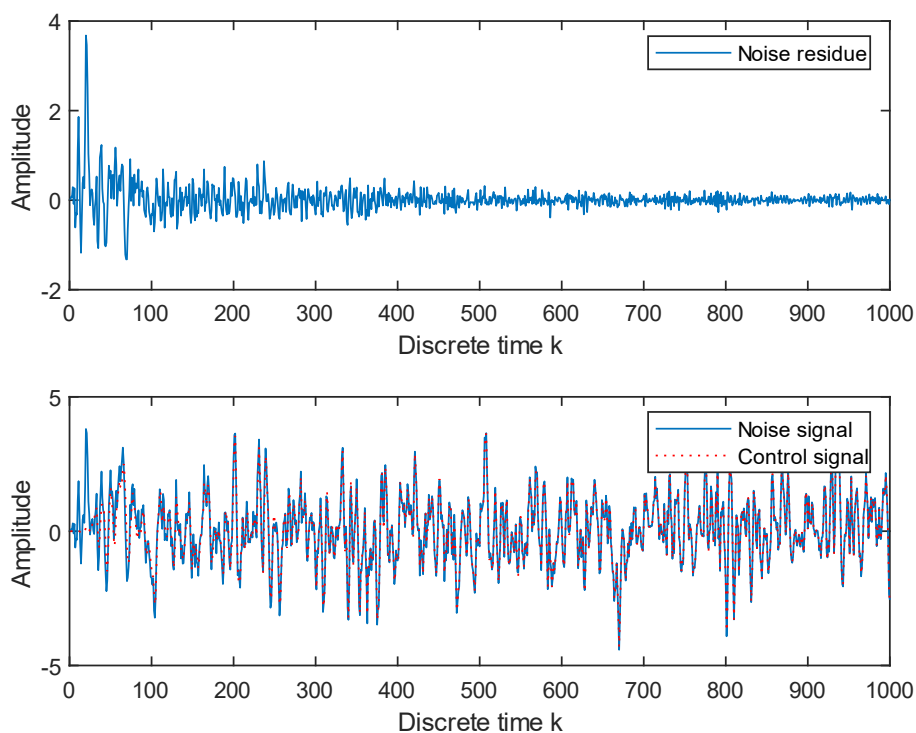


Figure 1. 16: Report the results of Noise Residue, Noise Signal and Control Signal of the feedforward ANC system.

1.4.6 Feedback Active Noise Control Systems

A feedforward system requires a reference sensor to produce a time-advanced reference signal of the primary noise, while a feedback active noise control (ANC) system does not. Instead, it estimates and cancels the principal noise using the error signal, which is the difference between the expected signal and the actual output [28],[29],[30]. A control algorithm, an adaptive filter, a second speaker, and a microphone to record the error signal are the main elements of a feedback ANC system. To reduce the difference between the desired signal and the actual output, the control algorithm modifies the adaptive filter's coefficients based on the error signal. In instances where it is challenging or impractical to directly detect or collect a reference signal of the source noise, feedback ANC systems are frequently used.

This could be because there are too many primary noise sources to affordably gather reference signals from each one, the primary noise is inaccessible, or real-time noise cancellation is required because there are too many primary noise sources [31].

In *Figure 1. 17* is represents a schematic of a basic feedback ANC system.

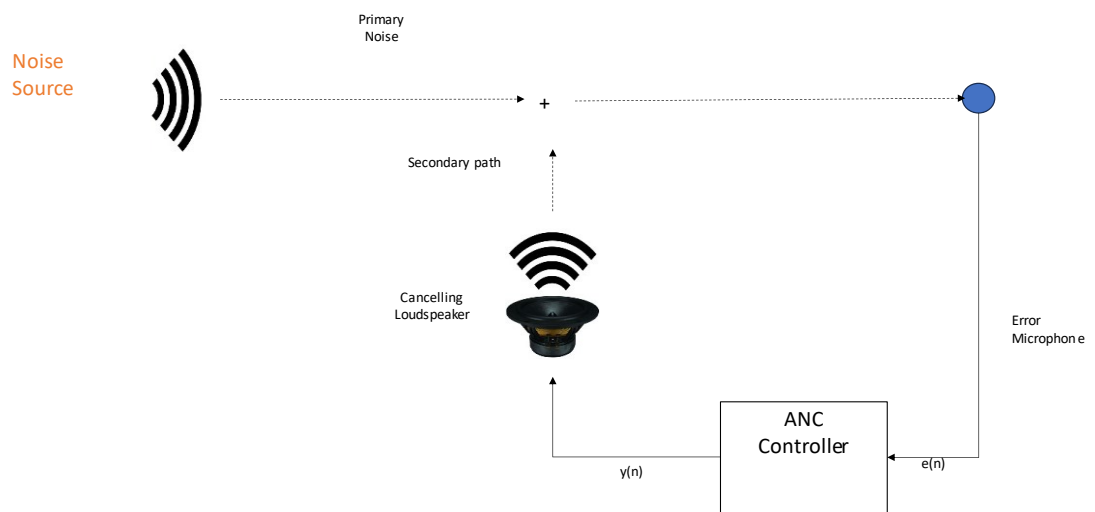


Figure 1. 17: Feed-back configuration of single channel ANC system.

The complete Acoustic Feedback Active Noise Control system using the filtered-x least-mean-square (Fx-LMS) algorithm is pitched in *Figure 1. 18*.

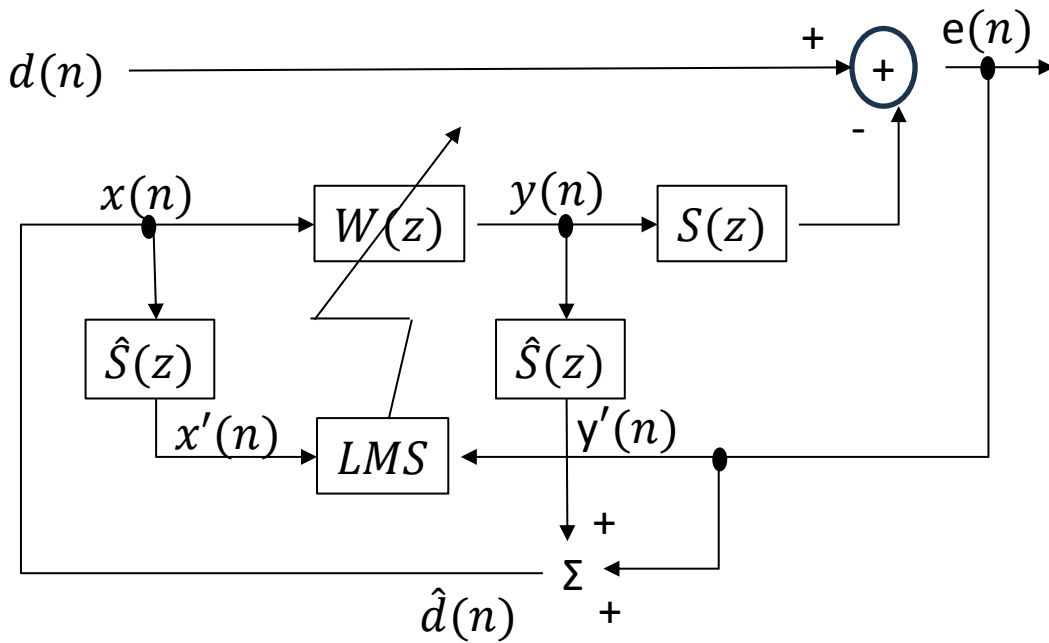


Figure 1. 18: Adaptive feedback ANC system block diagram.

In *Figure 1. 18* the reference signal $x(n)$ is synthesized as an estimate of $d(n)$, which is expressed as

$$x(n) \equiv \hat{d}(n) = e(n) + \sum_{m=0}^{M-1} \hat{s}_m y(n-m) \quad (1.37)$$

where $\hat{s}_m, m = 0, 1, \dots, M-1$ are the coefficients of the M th order FIR filter $\hat{S}(z)$ used to estimate the secondary path.

The secondary signal $y(n)$ is generated as:

$$y(n) = \sum_{l=0}^{L-1} w_l(n)x(n-l)$$

(1.38)

where $w_l(n), l = 0, 1, \dots, L-1$ are the coefficients of $W(z)$ at time n , and $L-1$ is the order of the FIR filter $W(z)$. The FXLMS method updates the filter's [31] coefficients as shown in the following expression:

$$w_l(n+1) = w_l(n) + \mu x'(n-l)e(n), \quad l = 0, 1, \dots, L-1$$

(1.39)

where μ is the step size, and

$$x'(n) \equiv \sum_{m=0}^{M-1} \widehat{s}_m x(n-m)$$

(1.40)

is the filtered reference signal.

The adaptive feedback active noise control algorithm represents in the previous equations, is incredibly efficient and small because it doesn't need a reference sensor on the outside of the headset. Large variations in noise levels, however, occasionally cause the algorithm to become unstable.

An effective solution is to employ the normalized Fx-LMS algorithm as follows:

$$w_l(n+1) = w_l(n) + \frac{\mu}{\widehat{P}_x(n) + c} x'(n-l)e(n),$$

(1.41)

for $l = 0, 1, \dots, L-1$, where the power estimate

$$\widehat{P}_x(n) = (1 - \alpha)\widehat{P}_x(n-1) + \alpha x^2(n)$$

(1.42)

is based on the first-order recursive with $\alpha = 0.99$, and c is a small constant to prevent using a large step size [32].

The Fx-LMS method is implemented in this straightforward simulation for a single channel feed-forward active noise control system, using MATLAB software. To prevent destructive interference from occurring at the sensor point, the controller generates an "anti-noise" signal in this case. The goal is to reduce the noise leftover.

Two jobs make up the process: "off-line" identification of the secondary propagation path that remains between the actuator and sensor, and "on-line" control, which involves modifying the controller's parameters. In *Figure 1. 19* is pitched the results of the product of the coefficients of the secondary path, during its estimate, with generation of a white noise signal and applying least mean square algorithm.

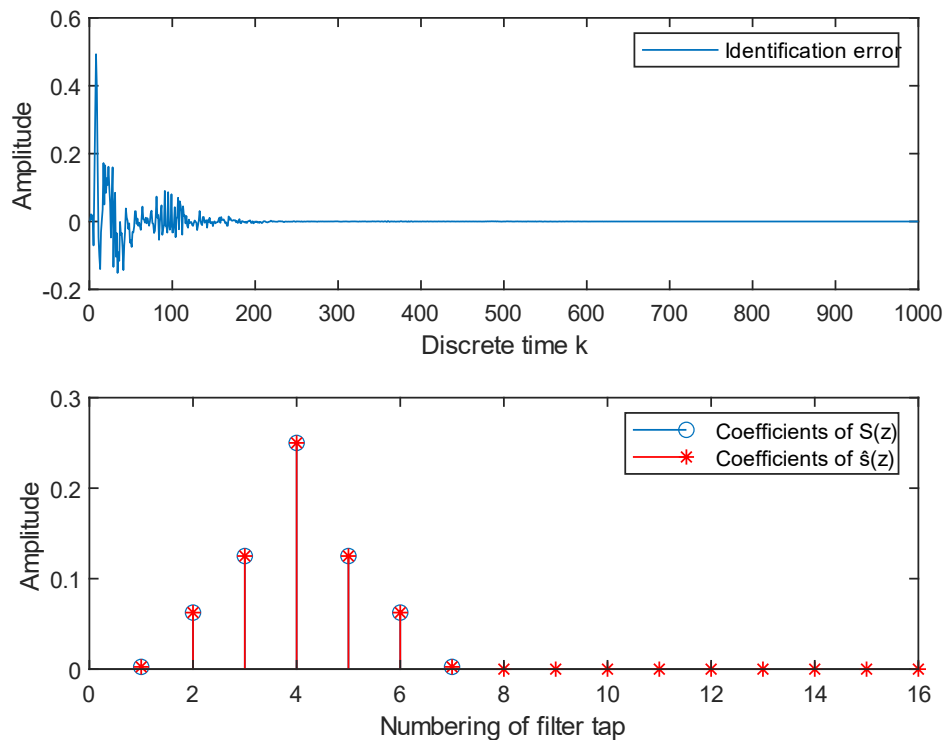


Figure 1. 19: The results of the coefficients when apply Least Mean Square algorithm.

Narrowband active noise control effectively manages low-frequency periodic noise, ensuring precise control. This entails capturing detailed frequency information of the primary periodic noise, including the count and specific values of its frequency components, to generate reference signals.

In broadband noise control applications, the feedforward ANC structure—which consists of reference and error microphones—is frequently employed. On the other hand, there is no reference microphone in the feedback mechanism. Rather, the error signal is used to internally synthesize the reference signal. It is better to use the feedback structure while handling narrowband noise. Analog or digital filters can be

used in an ANC system to generate anti-noise sound. For convenience, pre-trained control filters are used in noise-canceling headphones. Nonetheless, adaptive filtering algorithms provide benefits for adjusting to changes in the surrounding environment. The first adaptive ANC technique, Filtered-x Least Mean Squares (FxLMS), adjusts the control filter coefficients iteratively. The FxLMS algorithm is designed to minimize the power of the error signal, thereby positioning the control point at the error microphone [33].

In the *Figure 1. 20* the active control is turned on with generation of a narrow-band noise and, measuring the arriving noise at the sensor position, plot the report of the results of the Noise residue, noise signal and control signal in discrete time with amplitude.

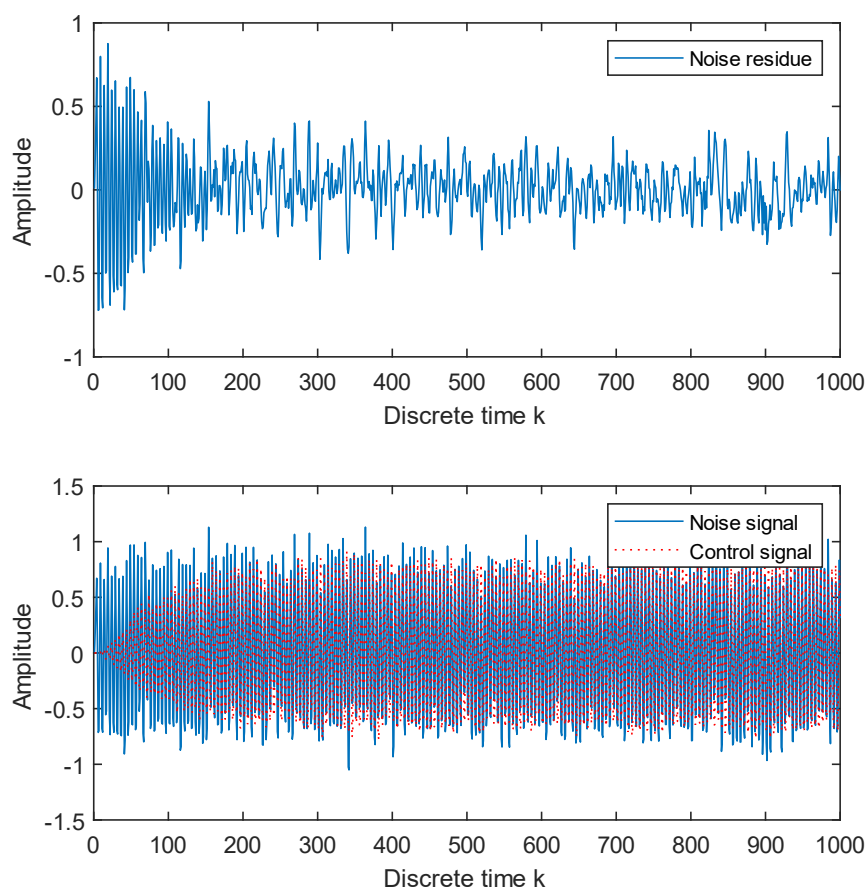


Figure 1. 20: Report the results of Noise Residue, Noise Signal and Control Signal of the feedback ANC system.

1.4.7 Secondary Path Estimation

The description above makes it clear that the adaptive noise controller's performance could depend on the real time estimation of the secondary path. The knowledge of the secondary path would increase the performance of the ANC system. Only a portion of this transfer function can be estimated because it is unknown and cannot be analyzed [34].

The secondary path cannot always be constant or calculated in a spatial ANC system that operates in the real environment. Consequently, it may be necessary to continually model the secondary path while also doing noise reduction. Using auxiliary noise, which is an internally created noise added to the loudspeaker output, to identify the secondary paths is one of the most used secondary path modeling techniques [35]. This idea is commonly referred to as Eriksson's method. A theoretical examination of the convergence characteristics for the single channel case was made in [36]. The approach was modified and given in [37] with a faster convergence rate at the expense of additional computations. Several scheduling plans have been put out to change the adaptive SPM filter's step size and auxiliary noise level while it is in operation. When the secondary route estimate is near to the true value, it is preferred to keep the step size large and the auxiliary noise low [38], [39]. A couple of these proposals [40], [41] have a particular focus on multichannel systems.

Eriksson et al. proposed to use additional random noise for estimating the secondary path filter. *Figure 1. 21* shows the Eriksson model.

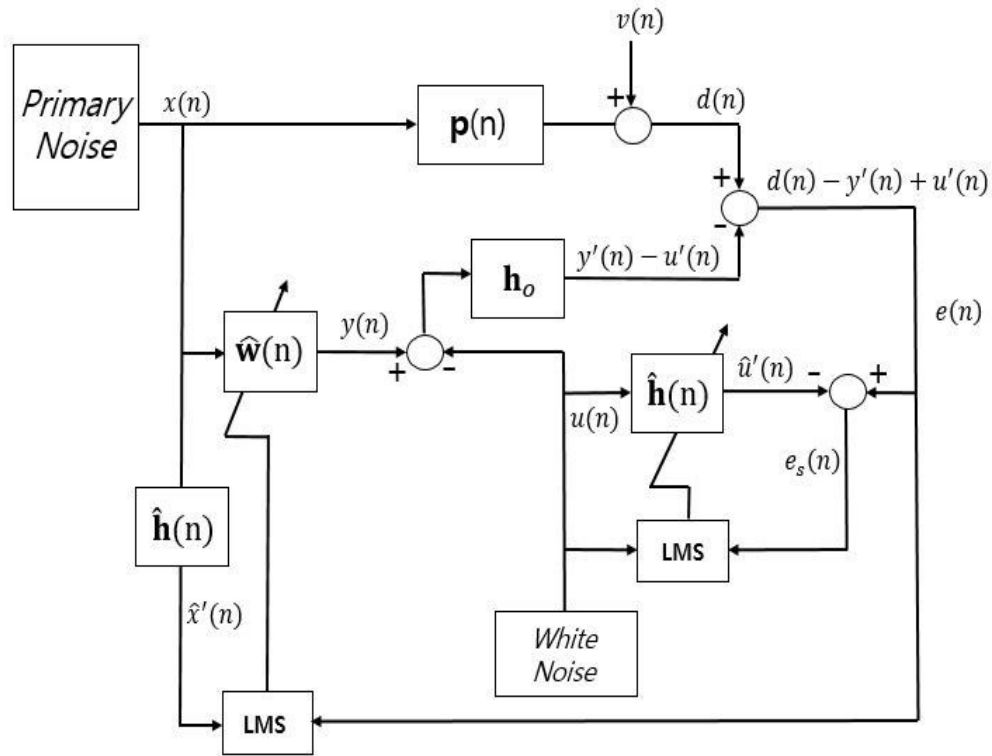


Figure 1. 21: ANC system with secondary path modeling (Eriksson's method).

The estimated primary path filter and the estimated secondary path filter are two adaptive filters in the ANC system. The error microphone is picking up two signals: the ANC system's residual noise and the auxiliary noise signal produced by secondary path estimation. The estimation of the primary path filter and the secondary path filter are both disturbed by the two signals. As a result, the Eriksson model's system exhibits gradual convergence and minimal steady state error. Bao, Kuo, and Zhang use the third adaptive filter to address this issue. By removing the remaining noise from the secondary path filter's error signal, the approaches increased the convergence speed and steady state error of secondary path estimation, but the algorithm's complexity is very high. More recently, the ANC system was introduced with increased performance with two filters [42].

The anti-noise travels along the second propagation channel from the output loudspeaker to the error microphone inside the silent zone.

The following simulation and figures, *Figure 1. 22* and *Figure 1. 23*, using MATLAB software, generates a loudspeaker-to-error microphone impulse response that is bandlimited to the range 160 - 2000 Hz and with a filter length of 0.1 seconds at sampling

frequency of 8000 Hz.

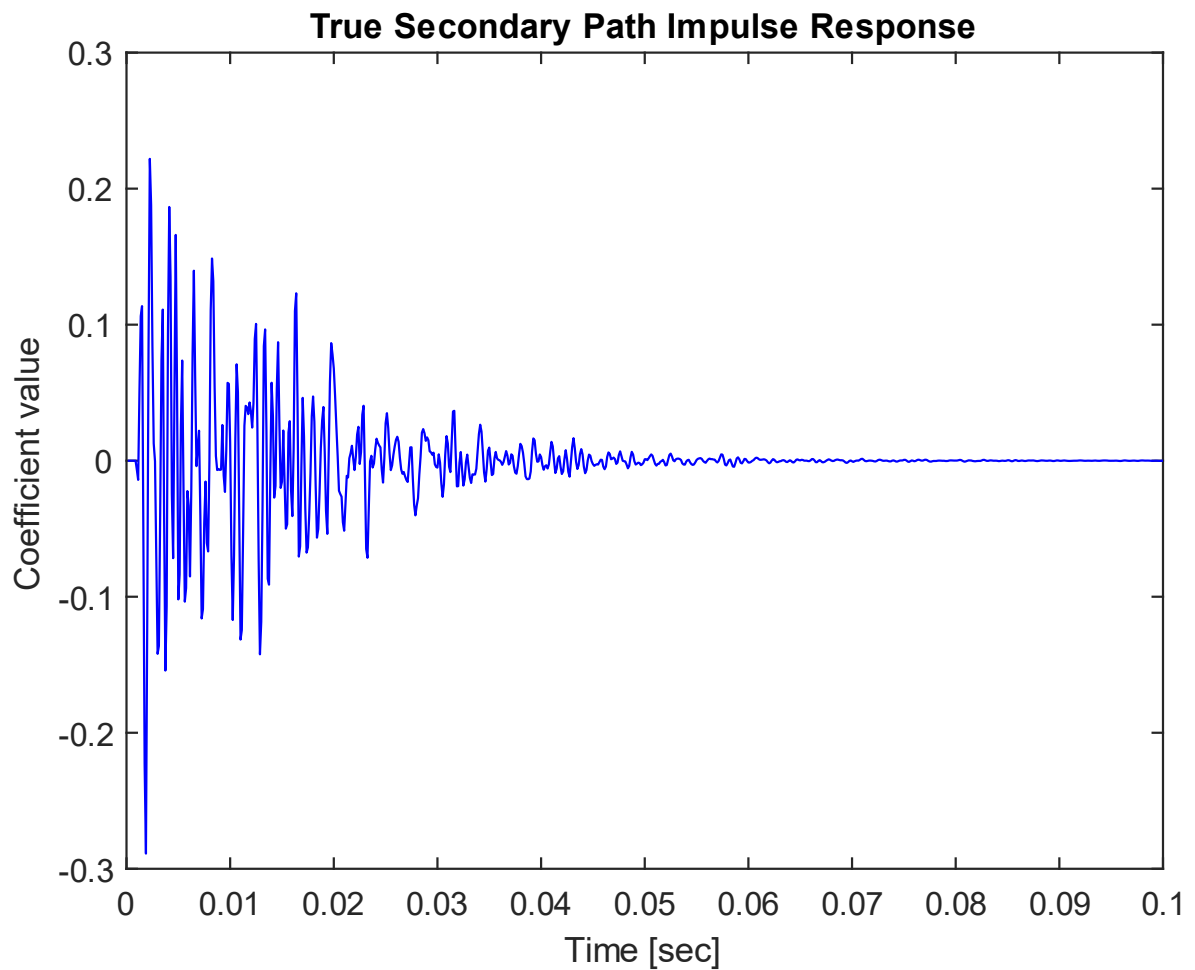


Figure 1. 22: Using filter noise to generate impulse response, true secondary path impulse response.

The coefficients for the true and estimated paths are displayed in *Figure 1. 23*. The genuine impulse response's tail is the only part that cannot be approximated precisely. The active noise control system's performance while doing the selected task is not considerably harmed by this residual error.

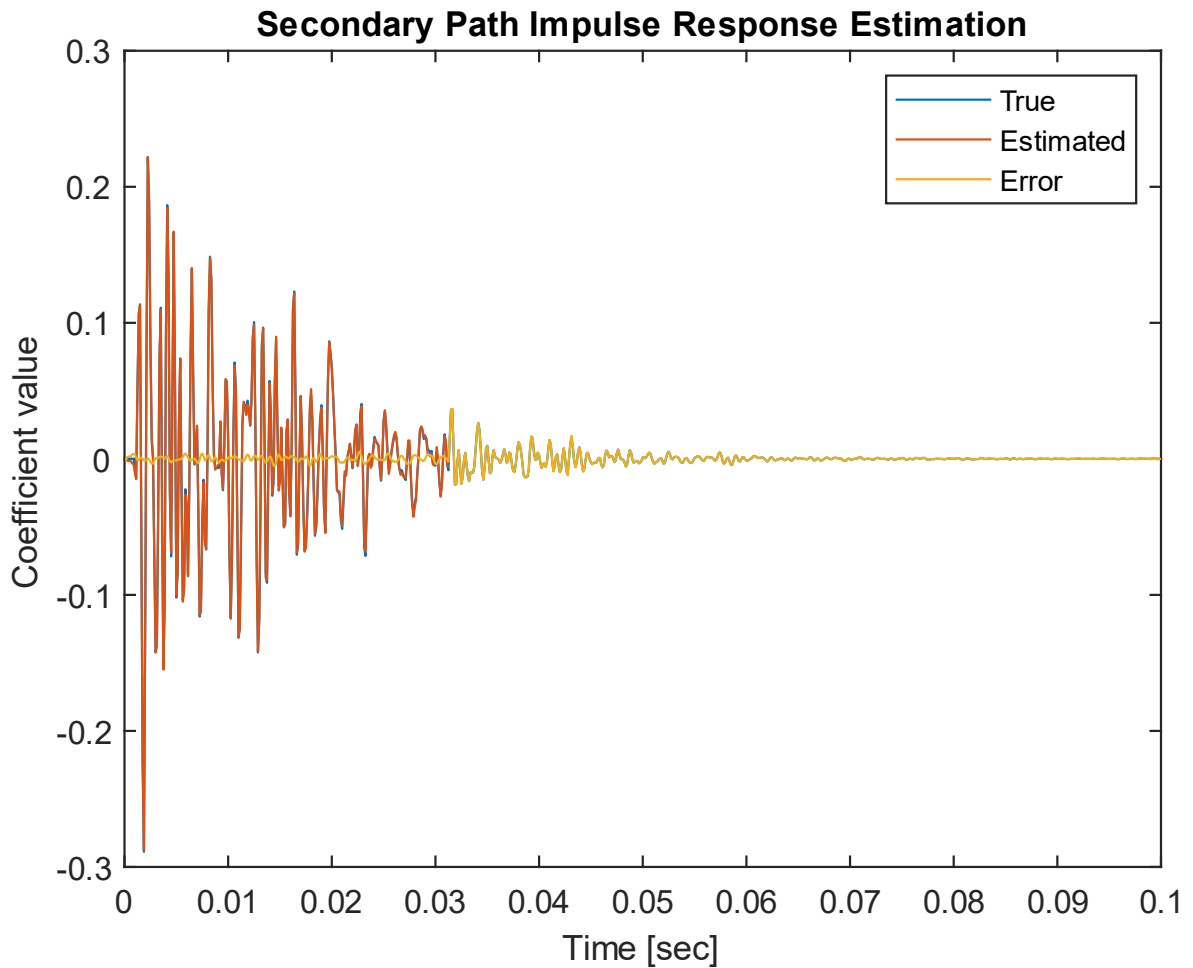


Figure 1. 23: Secondary Path Impulse Response Estimation.

1.4.8 Acoustic Feedback Estimation

Reflections of the sound produced by the speakers may travel upstream in feedforward ANC systems and be picked up by the reference microphone. Acoustic feedback from the secondary source to the reference microphone is what is causing this unwanted detection. The system becomes unstable due to this unwanted auditory feedback.

In *Figure 1. 24* is shown a block diagram of a single channel feedforward active noise control system. From the figure, as can be seen, the ANC system uses the reference microphone to pick up the reference noise and is the feedback path from the canceling loudspeaker to the reference microphone. Unfortunately, plane waves from a loudspeaker mounted on a duct wall will travel both upstream and downstream. The outcome is a distorted reference signal $x(n)$ since the anti-noise output to the loudspeaker not only suppresses noise downstream but also radiates

upstream to the reference microphone. This coupling of acoustic waves from the secondary loudspeaker to the reference microphone is called acoustic feedback [43],[44],[45].

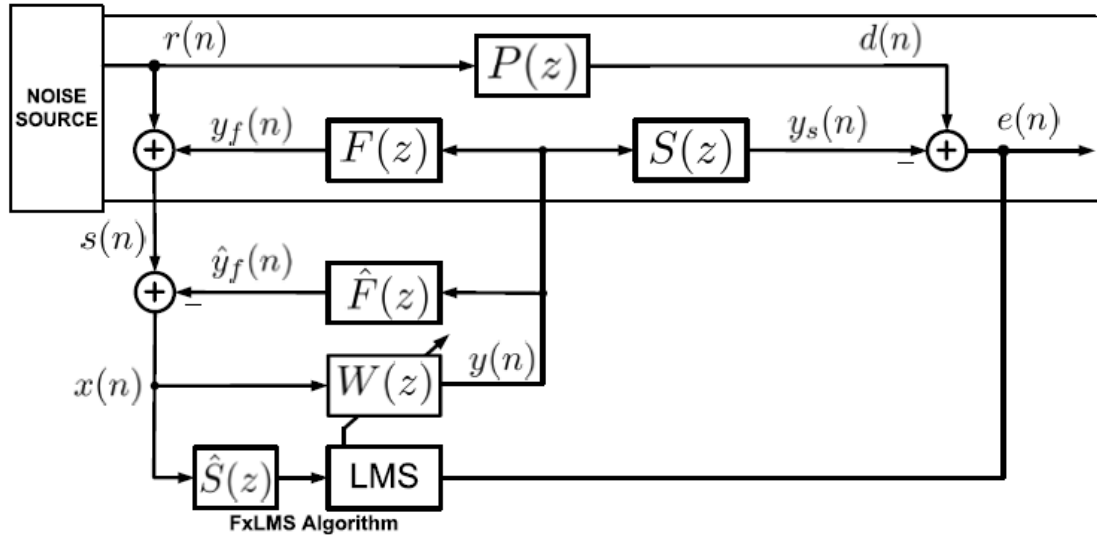


Figure 1. 24: Block diagram of single-channel ANC system with

1.4.9 Hybrid Active Noise Control Systems

When a reference signal is not available for all of the primary noises detected at the error microphone, hybrid ANC methods are employed. Space-incoherent turbulent noise, multi-source noise, noise from various propagation channels, and generated resonance are examples of situations that arise when it is not possible to sense or internally generate a totally coherent reference signal. Hybrid ANC is frequently employed in these circumstances to make up for the occasional disruptions. The fixed step size parameters used in the algorithms in Hybrid ANC limit how quickly these methods can converge. In [46], empirical formulas for step size variation are published. These formulas also incorporate other adjustable factors. According to [47] the variable step size method is based on minimizing the mis-alignment vector of the adaptive filters, which necessitates an estimation of the disturbance signal variance. For time-varying disturbances, offline estimation is useless because the variance of the disturbance signal is not directly accessible.

The feedback ANC system shown in *Figure 1. 25* comprises only an error microphone

and secondary loudspeaker, and there is no reference signal available for the primary disturbance. The output of the feedback ANC passes through to generate the residual error signal:

$$e(n) = d(n) - S(z) * y(n) \quad (1.43)$$

The Fx-LMS method is adjusted for $W(z)$ using the residual error signal $e(n)$, which is captured by the error microphone. Internally, the reference signal for $W(z)$ is created by passing $y(n)$ through a secondary path model $\hat{S}(z)$ and adding it to the residual error signal $e(n)$ as follows:

$$x(n) = e(n) + y'(n) \quad (1.44)$$

Consider the hybrid ANC system depicted in Figure 1. 21 that combines the feedforward ANC $W_1(z)$ and the feedback ANC $W_2(z)$.

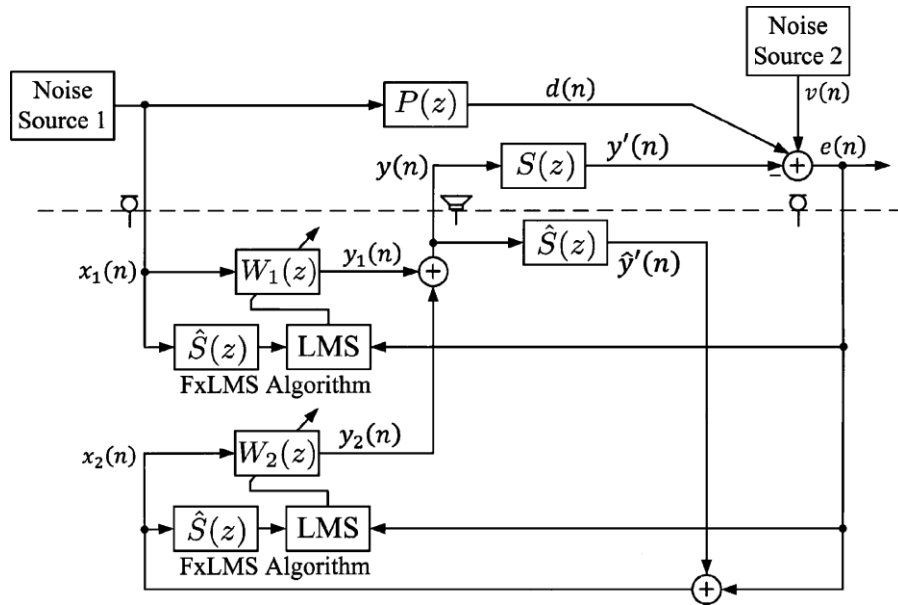


Figure 1. 25: Block diagram of hybrid ANC system with combination of feedback ANC and feedforward ANC.

The principal disturbances, $d(n)$ and $v(n)$, are assumed to be independent of one another by presuming that the signals $x_1(n)$ and $v(n)$ from two noise sources are. The feedforward ANC $W_1(z)$ receives the reference signal from the reference

microphone, $x_1(n)$, which is correlated with $d(n)$. The outputs of $W_1(z)$ and $W_2(z)$ are added to create the cancelling signal $y(n)$, which is then sent through $S(z)$ to produce the residual error signal $e(n)$:

$$e(n) = [d(n) + v(n)] - y'(n) = [d(n) - y'_1(n)] + [v(n) - y'_2(n)] \quad (1.45)$$

The Fx-LMS method employs this error signal for both $W_1(z)$ and $W_2(z)$. Thus, both ANC filters $W_1(z)$ and $W_2(z)$, are adapted using inappropriate error signals and therefore may converge slowly [48].

1.4.10 Multi Channels ANC systems

Using a single-channel feedforward ANC system to minimize various noise sources dispersed over a large area is challenging. In this scenario, an ANC system with many channels is employed to eliminate the undesired noises. In general, a multichannel feedforward ANC system has multiple reference microphones, secondary sources, and error microphones. A multichannel feedforward ANC system's construction and block diagram are depicted in *Figure 1. 26* and *Figure 1. 27*, respectively.

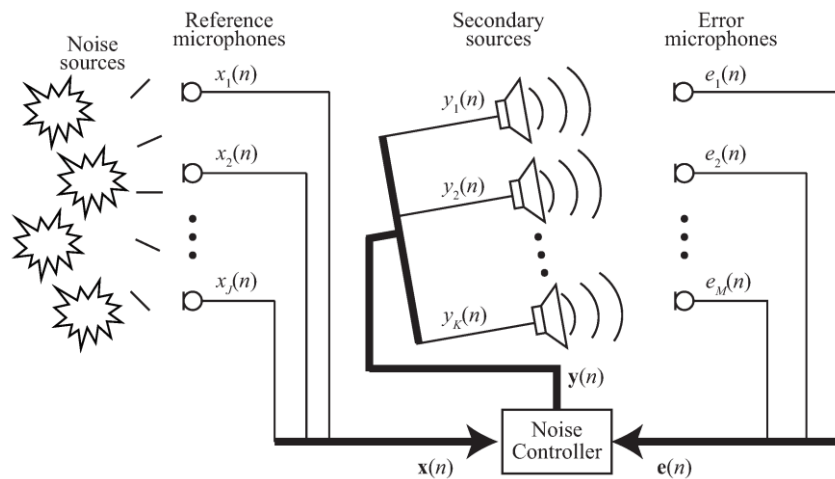


Figure 1. 26: J reference microphones, K secondary sources and M error microphones make up the structure of a multichannel feedforward ANC system.

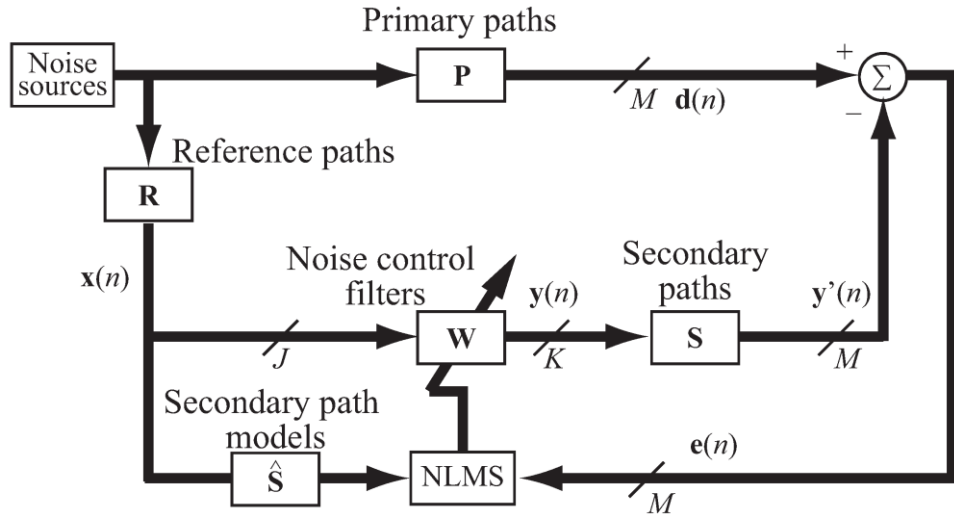


Figure 1. 27: Block diagram of multichannel ANC system with J reference microphones, K secondary sources and M error microphones.

J , K , and M in Figure 1. 26 and Figure 1. 27 stands for the quantities of reference, secondary, and error microphones, respectively.

The system in question is referred to as a case (J, K, M) ANC system. In a genuine situation, there are feedback paths from the secondary sources to the reference microphones; however, for the sake of simplicity, the feedback paths are disregarded. The unpleasant noise's overall direction is uncertain. The placement of the reference microphones close to the noise control point is one approach to solving this issue [49].

However, due to the exponential rise in computational complexity, the practicality diminishes as the number of channels rises.

A multichannel active noise control (MCANC) system with J reference microphones, K secondary sources, and M error microphones is shown in block diagram form in Figure 1. 28. $w_{kj}(n)$ denotes the k j th control filter that processes the j th reference signal and generates the output signal $y_{jk}(n)$, s_{mk} denotes the impulse response of the secondary path from k th secondary source to m th error microphone [50].

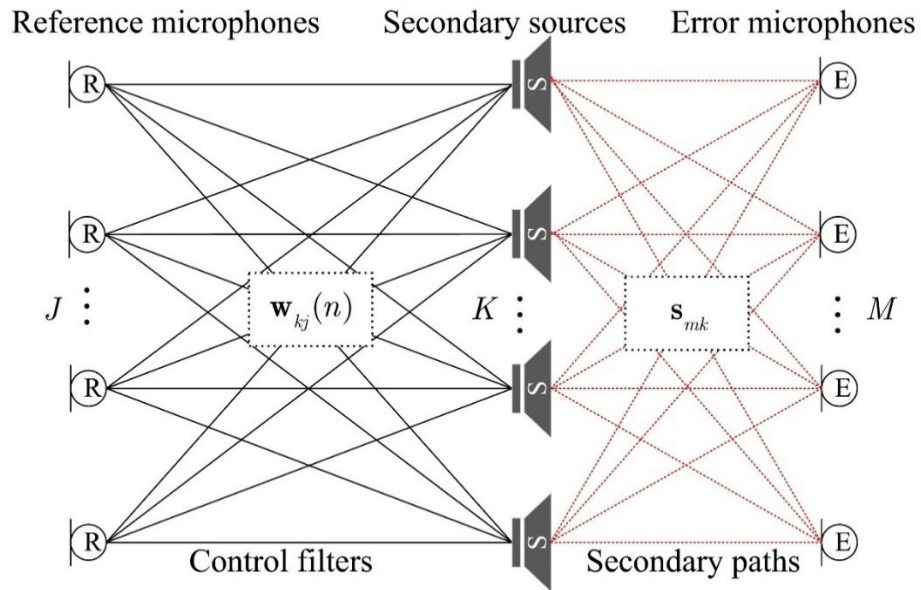


Figure 1. 28: Block diagram of the multichannel active noise control system with J reference microphones, K secondary sources and M error microphones.

1.4.11 Deep Learning for Single-Multi Channels ANC systems

Adaptive signal processing, with the least mean square (LMS) algorithm as its cornerstone, is the basis of conventional single-channel and multi-channel active noise reduction (ANC) techniques; this traditional ANC methods has need to estimate the secondary path and adaptive filter individually.

In recent years, scientific research has been exploring the use of neural networks and deep learning¹ for active noise control, focusing on the study of recursive functions². The main difference compared to traditional methods lies in the memory-based processing of sensitive data, which is essential for both secondary path estimation and signal attenuation in various types of environments and signals, whether stationary or not.

Deep ANC uses supervised learning and trains a deep neural network to directly approximate the optimal controller of the transfer function like to relationship between primary and secondary path in order to minimize the error signal under different situations. A diagram of deep ANC is shown in *Figure 1. 29* where:

¹ Are subfields of artificial intelligence inspired by the functioning of the human brain. Neural networks are composed of interconnected units ("artificial neurons") that process information similarly to how biological neurons process stimuli. Deep Learning is a type of neural network with a multi-layered structure that allows it to learn from large amounts of complex data.

² The output of a recursive function depends not only on the current input, but also on what the function has "computed" previously.

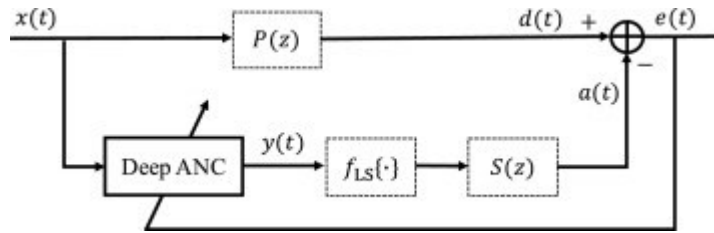


Figure 1. 29: Single channel diagram of the deep ANC approach.

- $F_{LS}\{\cdot\}$ denotes the function of the canceling loudspeaker;
- $y(t)$ the canceling signal (output of deep ANC).

The reference signal is used as input and set the ideal anti-noise as the training target. The optimal anti-noise should be the same as the primary noise to accomplish total noise cancellation. The deep ANC output is handled as a "intermediate product" during training, and the estimate of the anti-noise is produced by running the deep ANC output via the secondary path and the loudspeaker. The error signal is used to calculate the loss function. The reference signal divided into frames and short time Fourier transform (STFT) is applied to each time frame to produce the real and imaginary spectrograms which are denoted as $X_r(m, c)$ and $X_i(m, c)$, respectively, within a T-F unit at time m and frequency c .

The Convolutional Recurrent Network (CRN) is shown in Figure 1. 30.

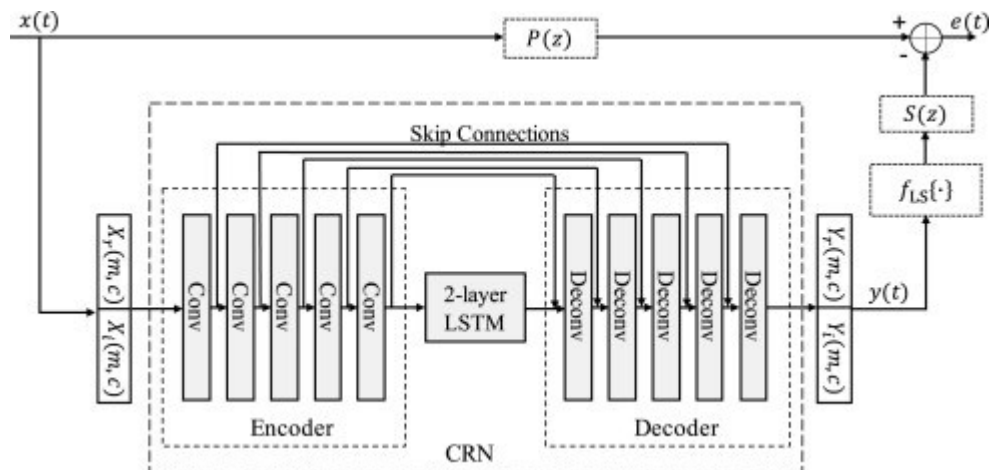


Figure 1. 30: Single channel diagram of CRN based deep ANC.

In this figure **Conv** blocks denote convolutional layers, **Deconv** blocks denote deconvolutional layers. Skip connections connect layers at the same level. The inputs and outputs of *CRN* are defined in the complex *STFT* domain.

The CRN is trained to map from the real and imaginary spectrograms of the reference signal to those of the canceling signal, $Y_r(m, c)$ and $Y_i(m, c)$. This is different from the methods that estimate only the magnitude spectrogram and use the phase spectrogram of the input signal to generate the estimated waveform output. The complex spectrogram of the canceling signal goes through the inverse Fourier transform to derive a waveform signal $y(t)$. The anti-noise, which can be regarded as an estimate of the training target, is then generated by passing the canceling signal through the loudspeaker and secondary path [51].

Like single-channel settings, deep learning for active control in multichannel systems uses recursive function computation and loss functions differently as well as integration systems. Integrating signals from several channels may present extra synchronization and information fusion difficulties in multichannel systems. Furthermore, modifications may be needed to the computation of recursive functions to appropriately manage the additional complexity of multichannel signals. Finally, it is necessary to create loss functions that consider the interplay of several channels when evaluating the efficacy of noise suppression. In the Figure 1. 31 is represent of the diagram of deep multi-channels ANC and CRN based deep multi channels ANC.

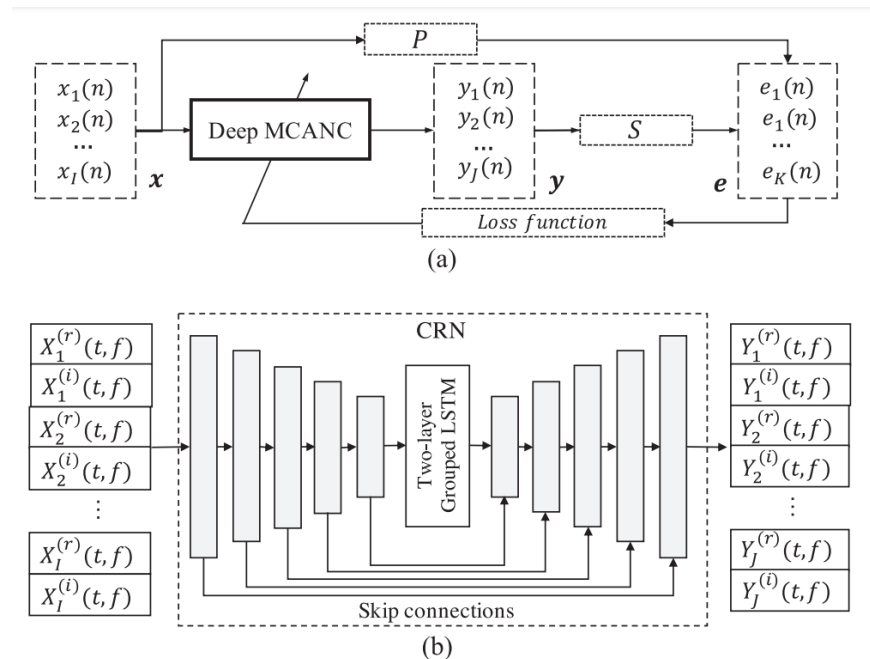


Figure 1. 31: Diagram of (a) deep MCANC approach, and (b) CRN based deep MCANC. P and S denoted primary and secondary paths. Superscripts (r) and (i) denote real and imaginary parts of signals, respectively.

The aim of deep Multiple Channel Active Noise Control (MCANC) is to produce

cancellation signals that effectively minimize the error signals detected by all error microphones.

CRN block, for model training, has an encoder-decoder architecture, where five convolutional layers make up the encoder and five deconvolutional layers make up the decoder, respectively.

The deep MCANC method has the capability to attenuate noise at multiple spatial points corresponding to the positions of error microphones. Furthermore, it can be trained to achieve ANC within a spatial zone using one or multiple canceling loudspeakers and multiple error microphones. The objective is to reduce noise in a target region. To accomplish this goal, the deep MCANC controller is trained on a variety of room impulse responses (RIRs) sampled within a spatial zone during training independently from the RIRs [52].

1.5 Motivation

Numerous investigations completed over the past ten years were taken into consideration when conducting the current research study. The different ANC (Active Noise Control) system configurations that have been created so far differ in how well they perform on different performance criteria, such as convergence speed, steady state error, computational complexity, tracking ability, and customizable parameters. Utilizing effective algorithms can help reduce the amount of processing needed for ANC applications, which will lower energy usage and the need for processing resources. To lower computational costs, several techniques for single-channel and multi-channel feedforward ANC systems have been developed. However, these algorithms perform poorly for signals like those examined in this research work. Therefore, it is necessary to use adaptive algorithms that quickly approach a modest steady state error without incurring additional computational expenses and tuning difficulties. This research study's contribution to this type of algorithm. Stable operation in the presence of disturbances of any kind is another addition. In the field of active noise cancellation, algorithms that can function in the presence of disturbances and attenuate these disturbances if they are associated are important. Adaptive algorithms are updated even after achieving convergence in the various control configurations described in the literature review, which is not helpful. A logical advancement is the creation of proactive algorithms that update frequently during the transition phase and infrequently during the stable state. The algorithms will be made to perform better without requiring more computations, making them appropriate for higher-order systems for both stationary and non-stationary signals. The thesis focuses on developing control algorithms that can

follow changes in non-stationary signal features and achieve tiny steady state errors in less time and with less computational work.

1.6 Contributions

For a variety of ANC system configurations, adaptive algorithms have been developed that provide the best performance in terms of steady state noise reduction level, convergence speed, computational complexity, tracking, and tunability. The contributions of this research are focused on “a priori known complex signals” and “stationary noise signals produced by large industrial machineries”. The main contributions are summarized as follow:

- The exploration of the potential application of ANC algorithms to reduce the ambulance siren noise.
- The analysis of the ANC techniques including adaptive signal processing and digital signal processing.
- The implementation of a feedforward ANC system using Fx-NLMS algorithms.
- The development of the Fx-NLMS algorithm in MATLAB Simulink and their execution on Speedgoat target HardWare;
- Study of limitations of the convergence speed, tracking and stability convergence of the step-size;
 - Development and publication of methods for selectively reducing the harmonic content of an ambulance siren using Reference Synthesis technique and Switching FxNLMS;
 - Reference Synthesis: allows the ANC system to cancel the noise without the need for reference microphones or direct connection to the noise source. Instead, the reference signal is generated by the canceling hardware itself, assuming that the noise to be canceled is perfectly known. This approach simplifies the setup and implementation of the ANC system, making it more efficient and versatile.
 - Switching Fx-NLMS: involves the implementation of separate banks of adaptive filters to individually cancel two alternating components of a bitonal siren. By applying this technique, the ANC system can selectively target and cancel

specific harmonic components of the siren noise, leading to a more precise and effective noise reduction.

- Analyzing various configurations of secondary sources distributed across the reactor's surface, with the intention of creating a virtual secondary source.
- To achieve a substantial reduction of electromagnetically induced noise in the far field. This reduction is at least 20 meters from the noise source.

1.7 Thesis outline

The thesis is structured as follows.

Chapter 2 presents an analysis of possible Algorithms for Active Noise Control of Siren Noise into an Ambulance. For the study and development of the signal associated to the ambulance system, there are numerous algorithms available. Depending on the study's goals, these algorithms differ from one another. Using spectral analysis techniques to pinpoint the distinctive siren components, one algorithm can be created specifically for the purpose of detecting ambulance sirens.

Chapter 3 presents the analysis of Active Noise Control (ANC) algorithms leading to the development of the Fx-LMS algorithm for active control of ambulance siren noise reduction. Additionally, the implementation process of this algorithm on real-time hardware, such as the Speedgoat system, is presented, highlighting the behaviors and differentiations at different frequencies.

Chapter 4 presents the method for selectively reducing the harmonic content of an ambulance siren. Based on the Fx-LMS feedforward algorithm, two developments are presented: 1) Reference Synthesis, for cases when the noise to be canceled is perfectly known, the reference signal is generated by the canceling hardware, without employing reference microphones nor connecting to the noise source; 2) Switching Fx-LMS, the implementation of separate banks of adaptive filters to individually cancel two alternating components of a bitonal siren.

Chapter 5 introduces the study of magnetostriction in electrical reactors, specifically examining how the reactor emits vibrations that result in 100 Hz noises. Furthermore, it suggests the potential use of active control along with Fx-NLMS algorithms. The tests carried out involve real-time experiments using dedicated software and hardware.

Chapter 6 provides an overview of potential areas for improvement, along with suggestions for methods to achieve optimal performance. This section of the document identifies the areas that require further interventions to achieve better results and presents various strategies and approaches that can be implemented to maximize overall performance.

Chapter 2

Analysis of possible Algorithms for Active Noise Control of Siren Noise into an Ambulance

Using a variety of secondary sources, like speakers, to create a "anti-noise" wave that cancels out the noise from a primary source is the fundamental idea behind Active Noise Control (ANC). This method is based on the idea of wave superposition, which states that undesired noise can be successfully cancelled out by using an equal-amplitude and opposite-phase wave.

For ANC to be effective, signal processing methods that are customized to the unique properties of the noise coming from the primary source that needs to be cancelled must be used. This could entail creating appropriate control algorithms, identifying propagation patterns, and performing spectral analysis on the noise. The primary signal is recorded by control microphones, which also give the ANC system feedback in real time. This enables the system to produce an appropriate anti-noise signal to reduce noise in the target area while dynamically adapting to variations in the primary noise. ANC, or active noise cancellation, has uses in consumer electronics, aviation, the automobile industry, and noise cancellation in both home and office settings.

Statement of Authorship

Title of Paper	Analysis of possible Algorithms for Active Noise Control of Siren Noise into an Ambulance
Publication Status	Published
Publication Details	Buttarazzi, M.G., Bartalucci, C., Borchì, F., Carfagni, M., Paolucci, L. (2022). Analysis of Possible Algorithms for Active Noise Control of Siren Noise into an Ambulance. In: Rizzi, C., Campana, F., Bici, M., Gherardini, F., Ingrassia, T., Cicconi, P. (eds) Design Tools and Methods in Industrial Engineering II. ADM 2021. Lecture Notes in Mechanical Engineering. Springer, Cham. https://doi.org/10.1007/978-3-030-91234-5_63

Principal Author

Name of Principal Author (Candidate)	Buttarazzi Massimo Generoso
Contribution to the Paper	Designed the core idea and performed analysis on the concept, interpreted data, wrote manuscript and acted as corresponding author
Certification:	This paper reports on original research I conducted during the period of my Higher Degree by Research candidature and is not subject to any obligations or contractual agreements with a third party that would constrain its inclusion in this thesis. I am the primary author of this paper.

Co-Author Contributions

By signing the Statement of Authorship, each author certifies that:

- The candidate's stated contribution to the publication is accurate (as detailed above)
- Permission is granted for the candidate to include the publication in the thesis; and
- The sum of all co-author contributions is equal to 100% less the candidate's stated contribution.

Name of Co-Authors	Paolucci Libero, Bartalucci Chiara, Borchì Francesco, Carfagni Monica
Contribution to the Paper	Supervised development of work, helped in refining core concept and manuscript evaluation.

Position in Appendix A-1

Chapter 3

An active noise control system for reducing siren noise inside the ambulance.

For both patients and ambulance staff, siren noise can be an annoying and dangerous problem. In the past, research has suggested simulated ways to lessen ambulance siren noise inside utilizing Active Noise Control (ANC). This paper presents the implementation of a feedforward ANC system based on the well-known FxLMS algorithm. The system is tested in a laboratory setting using real-time hardware to assess its effectiveness. The algorithms are developed in MATLAB Simulink and executed on Speedgoat Target hardware.

Statement of Authorship

Title of Paper	An active noise control system for reducing siren noise inside the ambulance.
Publication Status	Published
Publication Details	Design Tools and Methods in Industrial Engineering II. ADM 2023. Lecture Notes in Mechanical Engineering. Springer, Cham.

Principal Author

Name of Principal Author (Candidate)	Buttarazzi Massimo Generoso
Contribution to the Paper	Designed the core idea and performed analysis on the concept, interpreted data, wrote manuscript and acted as corresponding author
Certification:	This paper reports on original research I conducted during the period of my Higher Degree by Research candidature and is not subject to any obligations or contractual agreements with a third party that would constrain its inclusion in this thesis. I am the primary author of this paper.

Co-Author Contributions

By signing the Statement of Authorship, each author certifies that:

- The candidate's stated contribution to the publication is accurate (as detailed above)
- Permission is granted for the candidate to include the publication in the thesis; and
- The sum of all co-author contributions is equal to 100% less the candidate's stated contribution.

Name of Co-Authors	Borchi Francesco, Mambelli Alessandro, Carfagni Monica, Puggelli Luca, Governi Lapo
Contribution to the Paper	Supervised development of work, helped in refining core concept and manuscript evaluation.

Position in Appendix A-2

Chapter 4

Ambulance Siren Active Noise Cancellation: Reference Synthesis and Switching FxLMS on Real-Time Target Hardware

This research has eloquently demonstrated the efficacy of the operational principles of the Active Noise Control (ANC) method through a series of painstakingly planned and executed tests in a rigorously controlled laboratory environment, employing sophisticated target hardware mounted on a headrest and a faithful replica of a sound source representative of the noise emitted by a real ambulance siren. It is clear from a detailed examination of the data that there is a great deal of promise for the successful cancellation of the noise signal when real-time hardware, active control algorithms, and signal synthesis approaches are combined. As a result, this research has made a substantial contribution to our understanding of and ability to use ANC as a practical method of reducing noise inside ambulances. It has also laid a strong scientific basis for future studies and technology advancements in this area.

Statement of Authorship

Title of Paper	Ambulance Siren Active Noise Cancellation: Reference Synthesis and Switching FxLMS on Real-Time Target Hardware
Publication Status	Under review
Publication Details	ADM-Springer International Publishing

Principal Author

Name of Principal Author (Candidate)	Buttarazzi Massimo Generoso
Contribution to the Paper	Designed the core idea and performed analysis on the concept, interpreted data, wrote manuscript and acted as corresponding author
Certification:	This paper reports on original research I conducted during the period of my Higher Degree by Research candidature and is not subject to any obligations or contractual agreements with a third party that would constrain its inclusion in this thesis. I am the primary author of this paper.

Co-Author Contributions

By signing the Statement of Authorship, each author certifies that:

- The candidate's stated contribution to the publication is accurate (as detailed above)
- Permission is granted for the candidate to include the publication in the thesis; and
- The sum of all co-author contributions is equal to 100% less the candidate's stated contribution.

Name of Co-Authors	Borchi Francesco, Mambelli Alessandro, Carfagni Monica, Puggelli Luca, Governi Lapo
Contribution to the Paper	Supervised development of work, helped in refining core concept and manuscript evaluation.

Position in Appendix A-3

Chapter 5

Acoustic Source Array for Noise Reduction in Power Stations - an Active Noise Control Application

Active control techniques represent a promising strategy for managing noise and vibrations generated by large-scale machinery, such as power station reactors. In this regard, a preliminary study has been conducted using simulations to assess the acoustic field generated by the reactor and investigate the application of an active control system. This analysis involved examining various configurations of secondary speaker arrays and evaluating the optimal placement of error microphones. The primary objective was to identify the most effective solutions for reducing noise and vibrations, thereby contributing to improving the working environment within power stations and ensuring the well-being of operators. Operators, but mainly to also reduce the acoustic pollution perceived by residents of areas neighbouring the electric station. The findings of this study provide a solid foundation for the development and implementation of large-scale active control systems, promoting efficiency and safety in industrial infrastructure.

5.1 Introduction to Electromagnetically Induced Acoustic Noise

Reactor units play an essential and fundamental role in an electrical power system. Their basic operation relies on the generation of rotating magnetic fields, [53] which, in turn, produce vibrations, sometimes extremely hazardous. To ensure stable and secure operations, it is crucial to install safety systems around reactors.

Vibrations not only pose a concrete threat to the operational safety of the reactors, but also contribute to significant acoustic pollution, which is the central focus of this chapter.

Noise generated by reactors is due to the phenomenon known as Magnetostriction, which will be described in detail in the following section. Magnetostriction can cause substantial deformations in materials due to expansion and contraction induced by the presence of a magnetic field.

Therefore, it is of paramount importance to mitigate and control reactor vibrations to preserve operational efficiency, ensure stability in electrical energy transfer, and - as is the focus of our study - also reduce the adverse impact on the surrounding acoustic environment [53].

Studying reactors' vibration reduction therefore has significant practical implications. Now, vibration isolation and noise shielding are the main reduction methods employed. The addition of steel springs, rubber gaskets, or other elastic materials between the reactor body and the base is known as vibration isolation. To reduce noise, placing concrete shields close to reactors is a possible way. However, shields don't offer any real answers to the noise issue due to the low frequency emission of reactors focused at 100 Hz.

In the context of noise pollution, there is a still unmet need of mitigating the sound produced by the vibrating core, which is the principal aim of our studies and activities.

5.1.1 The Magnetostriction Phenomenon

When exposed to a magnetic field, ferromagnetic materials are subject to this phenomenon called magnetostriction that modifies their geometrical dimensions [54]. This occurs because the microscopic magnetic domains that make up these ferromagnetic materials all have different magnetic orientations, locations, and sizes.

When there is no magnetic field traveling through the ferromagnetic material, magnetic orientation is often random [55]. Figure 5. 1, 1a, shows a magnetic orientation where there is no magnetic field passing through. The color coding corresponds to a correlation with an upward direction.

Nevertheless, the material's magnetic domains respond to an external magnetic field by partially rearranging their sizes and orientation; altering the magnetic orientation of the materials on their individual surfaces causes the domains that have magnetic orientation that matches the external magnetic field to increase the resultant magnetic field. As a result, magnetic domains, each pointing in a different magnetic orientation decreasing in opposition to the external magnetic field, show in Figure 5. 1. The areas color coded in grey, represent the fractions of the non-aligning magnetic domains with the external magnetic field. These gray areas will then connect to their more aligned neighboring magnetic domains, Figure 5. 1[56].

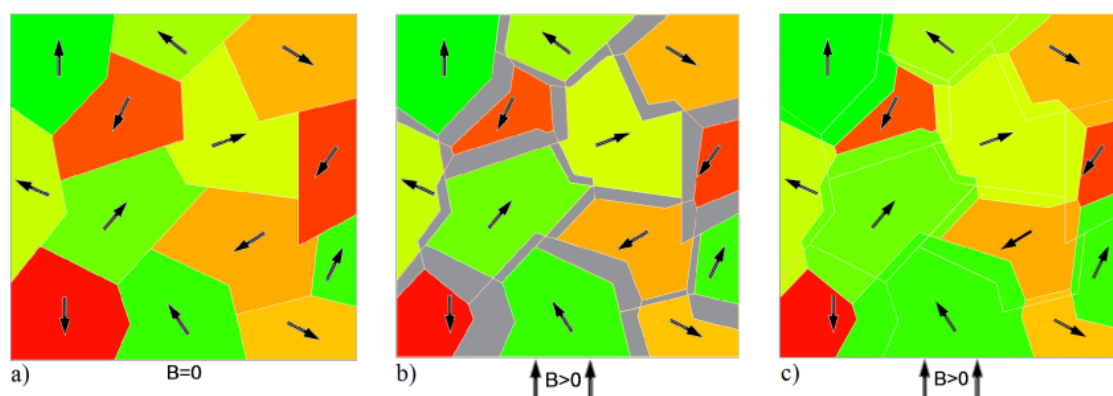


Figure 5. 1: a) ferromagnetic material magnetic domain individual orientation with no external magnetic field; b) magnetostriction process in ferromagnetic material domains; c) resulting outcome of magnetostriction process in ferromagnetic material domains [56].

The molecules within a domain are arranged so that their dipoles face the same way. As a result, the domain develops a north and south pole or sections that are negatively and positively charged. Any number of domains in a material is acceptable as long as it reduces the internal energy of the structure (Figure 5. 2). Bloch walls are the lines that divide these areas in bulk materials. A thin layer of molecules that have had their molecular dipoles gradually rotated to line up with their neighboring domains makes up a block wall, illustrated in Figure 5. 3.

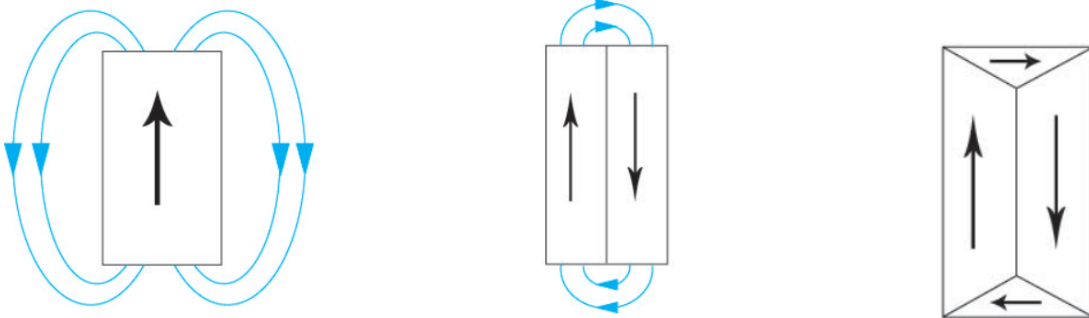


Figure 5. 2: Diagram illustrating how increasing the number of domains can lower the external demagnetizing field and hence lower the magnetostatic energy.

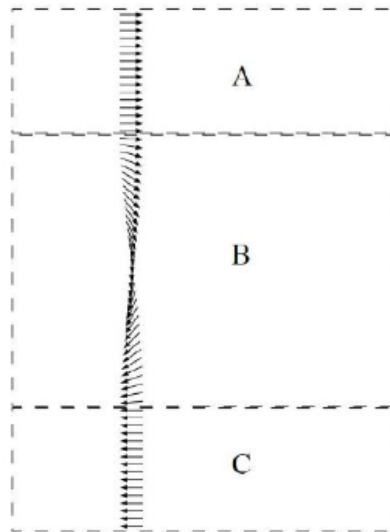


Figure 5. 3: Gradual tilt of molecular dipoles in a Bloch wall (B) to satisfy adjacent domains (A) and (C).

A Bloch wall's orientation is determined by the magnetic anisotropy of the crystal structure and the directions of the applied magnetic field. The molecular dipoles of ferromagnetic materials are pushed to align with the magnetic field when a magnetic field is applied to the material.

5.1.2 An Active Noise Control solution applied to an Electric Reactor

To reduce reactor noise emissions, placing concrete shields close to reactors is a possible way. However, noise barriers don't offer any real answers to the noise issue due to the low frequency emission of reactors focused at 100 Hz. In fact, noise barriers could offer a significant noise reduction of diffracted sound wave at higher frequencies.

At the same time the ANC technique could be very effective in the low frequency range where noise barriers are not effective.

In the past, an approach that combine ANC system and noise barriers were investigated. Anyway, also this approach demonstrated to be ineffective [57],[58] and [59].

In this research a new promising approach to noise cancellation through active control no longer focuses on managing the noise generated by diffraction at the edges of barriers placed near the source. Instead, the idea behind this new approach was to create a virtual secondary source using an array of speakers employed to generate an anti-noise field that would be accurately overlaid onto the acoustic field produced by the primary noise source. To define the virtual secondary source array new systematic investigations have been carried out regarding the emissions from the primary source. These investigations were conducted through simulations that examined various configurations of secondary sources distributed across the entire surface of the reactor. The ultimate objective of this study was to achieve a significant reduction of the electromagnetically induced noise in the far field, at a distance of at least 20 meters from the noise source [60],[61].

5.1.3 Design Assumptions for the Canceling Acoustic Field to be generated.

The underlying hypothesis of these studies assumes a cylindrical emission pattern from the reactor, which can be reconstructed by placing a series of secondary sources as close as possible to the primary source and with a controlled distance between them. These secondary sources are intended to define a virtual secondary source that closely mimics the primary source, and it will be appropriately phase-shifted and amplitude-adjusted by the control algorithm. Achieving this overlapping condition in the near field is indeed challenging, unless many secondary speakers are used. However, in the far field, as demonstrated through acoustic simulations, this outcome is achievable even with a limited number of speakers, and the global cancellation in the far field cancellation is the primary goal of this endeavor, as this is where the receivers are likely to be located. Therefore, this does not impose a limitation on the proposed solution.

Another assumption concerns the acoustic field generated by the virtual secondary source, which is subject to the same variations due to irregularities and obstacles in the acoustic field as those affecting the primary source. Consequently, once the feasibility of recreating a cylindrical source with an array of secondary speakers is demonstrated, it is presumed that the desired noise reduction can be achieved as long as the secondary sources are positioned as close to the reactor as possible. To validate these hypotheses, simulations were conducted to assess the feasibility of this approach.

The assumption of cylindrical emission mentioned above arises from both the geometric shape of the reactor and the presence of the following conditions:

The dimensions of the reactor are at least comparable to or larger than the wavelength of the emitted signal (a 100 Hz sine wave, with a wavelength of approximately 3.44 meters). Therefore, the shape of the reactor can influence the directionality of the emission even at 100Hz.

The materials and closure thickness of the reactor are effective in attenuating the signal propagated through the air. As a result, the emission primarily occurs through surface vibration. Given that the surface has a cylindrical shape, this generates a cylindrical acoustic field.

5.2 Proposed Solution: Distributed Secondary Sources Used for Antinoise Generation (virtual modelling)

During this research, Finite Element Analysis (FEM) within the Comsol Multiphysics package was employed to conduct a detailed study on the reconstruction of acoustic fields. FEM is an advanced numerical technique widely used to solve engineering problems involving partial differential equations, such as those governing acoustics and vibrations.

In the context of this research, realistic three-dimensional geometries of power station reactor systems were created within the Comsol modeling environment. These geometries included accurate details of the reactor components and surrounding structures, necessary for an accurate representation of the acoustic field. Subsequently, appropriate boundary conditions were applied to model the propagation of noise and anti-noise within the simulated environment. This involved defining noise sources, such as the reactor itself, as well as the position and characteristics of transducers used to generate the anti-noise signal. The analysis was performed iteratively, using various configurations of error microphones to identify optimal placement points that maximize the effectiveness of the active noise control system. During this process, detailed numerical simulations were conducted to assess the effectiveness of the proposed configurations and optimize the overall performance of the system. The use of FEM within the Comsol Multiphysics software enabled a thorough and detailed analysis of acoustic fields in power station reactor systems, providing valuable insights for the development and optimization of active noise control systems.

5.2.1 Simulations for Analyzing Acoustic Fields

A 3D model of the reactor was built (Figure 5. 4) of the individual reactor constructed using structural dimensions taken from the technical drawings of a real system where our field test will be conducted. A ring of secondary acoustic sources was positioned close to the surface of the reactor as shown in Figure 5. 5.

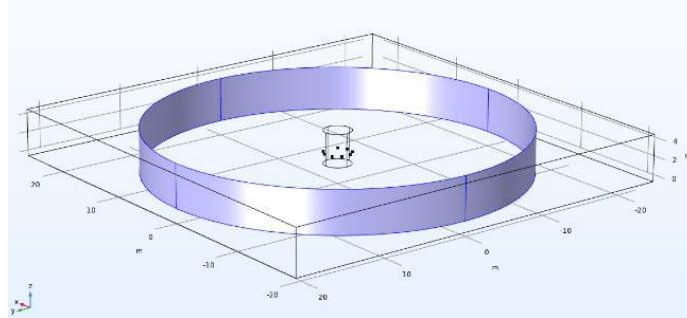


Figure 5. 4: Primary source and control surface at 20 meters (note a series of secondary sources located near the reactor, represented by the black dots around the reactor).

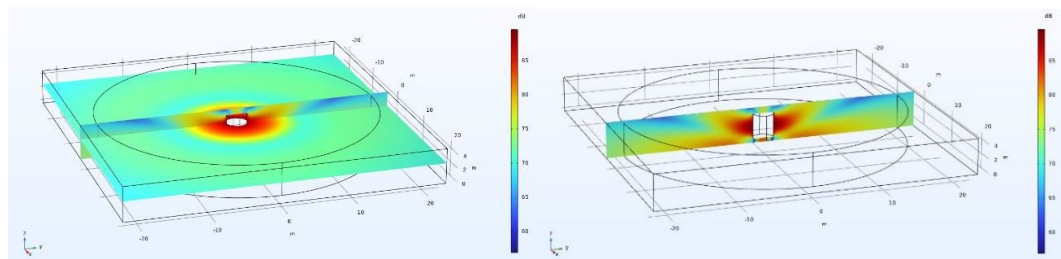


Figure 5. 5: a) Emission from the primary source b) Detail of the emission on the "vertical" plane.

The simulation results were analyzed in terms of sound pressure levels on a control surface located at 20 meters (also visible in figure 5.5) from the reactor. However, the pressure values were calculated over the entire field to provide a more comprehensive view of the emission model's quality.

The chosen simulation configurations (position and number of secondary sources) were selected considering the following constraints:

- To recreate a cylindrical emission, secondary sources must be positioned at a distance less than $\lambda/2$, relative to the frequency of the disturbance to be attenuated [62] and [63].
- To faithfully recreate a source that closely overlaps with the noise field of the (single) reactance, it is necessary to position the secondary sources as close as possible to the emitting surface of the reactor itself [63], [64] and [65].

The goal of this simulation activity is to minimize the overall number of secondary sources to simplify and make the system more cost-effective to implement. The number of secondary sources has therefore been optimized, based on the constraints mentioned above, through FEM simulations, resulting in two interesting configurations:

- One circle with 9 control speakers positioned at half height of the reactor's height (as shown in **Figure 5. 6** and **Figure 5. 10**).
- Two circles, each with 6 control speakers. The first circle is positioned at 1/3 of the reactor's height, and the second circle is placed at 2/3 of the reactor's height (as depicted in **Figure 5. 7** and **Figure 5. 11**).

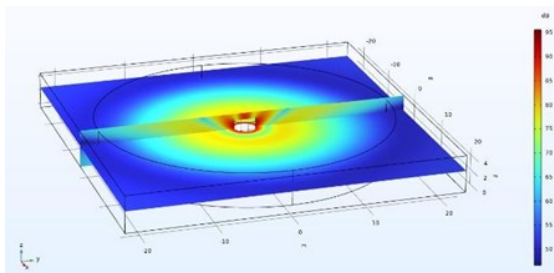
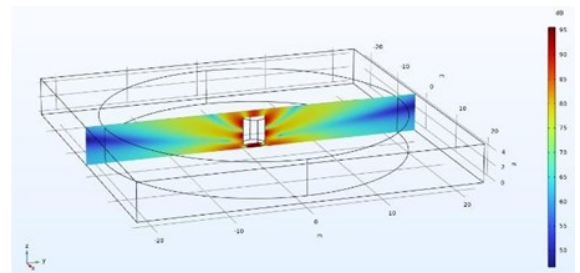


Figure 5. 6: a) Emission with Active Control 9x1



b) Detail of Vertical Plane Control

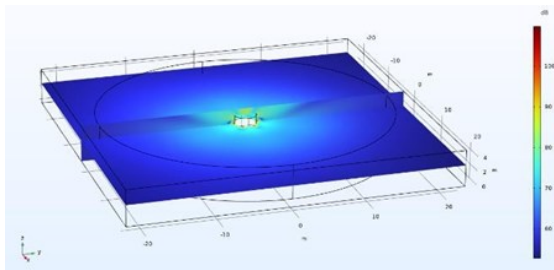
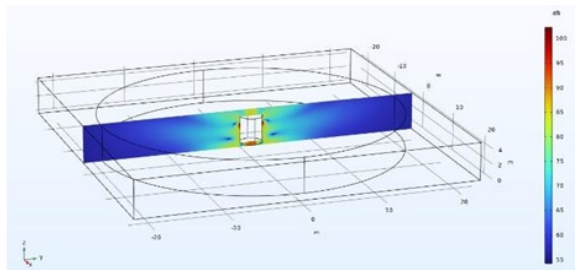


Figure 5. 7: a) Emission with Active Control 6x2



b) Detail of Vertical Plane Control

The model has been enhanced with the addition of two firewalls (Figure 9), and the same simulations have been conducted (**Figure 5. 9**, **Figure 5. 10** and **Figure 5. 11**) with substantially similar results.

These results are highly promising, as they demonstrate that:

- The overlap of the noise field emitted by a cylindrical structure can be overlaid with a field emitted by distributed sources appropriately positioned, emitting a signal that is suitably modulated in phase and amplitude.

- The configurations require the use of a limited number of control sources and associated electronics.

At least two possible configurations have been determined for testing, with similar results in terms of attenuation values. However, when compared to each other, they exhibit qualitative differences that can be significant.

On this last point, further investigation was also conducted by comparing the fields generated by the two solutions, 9x1 and 6x2 (**Figure 5. 6** and **Figure 5. 7**). Using 9 loudspeakers on a single circumference (**Figure 5. 7**) involves fewer control sources, but this results in a satisfactory level of attenuation at greater distances from the primary source compared to the configuration with 2 lines of loudspeakers (**Figure 5. 7**). This may not be a significant issue because the numerical values of average attenuation on the reference surface at 20 meters are very close (the calculated values from the simulation are 57.7 dB for the 9x1 configuration, compared to 56.6 dB for the 6x2 configuration, with all other parameters being equal); at the same time, if you consider the values of sound pressure in the vertical plane, the configuration with more control sources, and therefore a higher cost, appears to promise a more uniform attenuation in space.

Looking at the values of the same configurations once the firewalls are included, as shown in **Figure 5. 10** and **Figure 5. 11**, consistent results are observed, with average attenuation values at 20 meters of 56.9 dB and 56.3 dB, respectively, along with similar considerations about the uniformity of attenuation in the vertical plane.

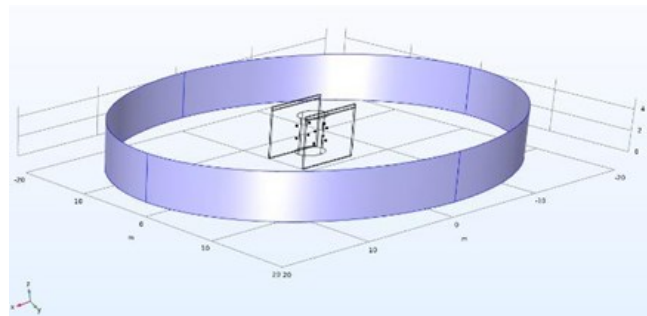


Figure 5. 8: Primary source and control surface at 20m with firewalls.

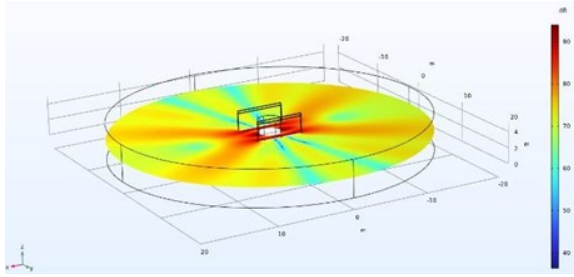
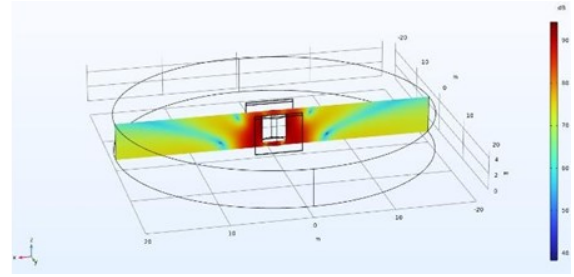


Figure 5. 9: a) Primary source emission



b) Detail of Vertical Plane Control

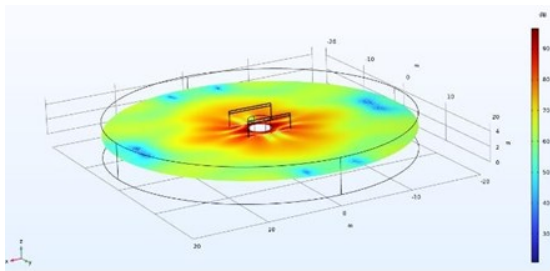
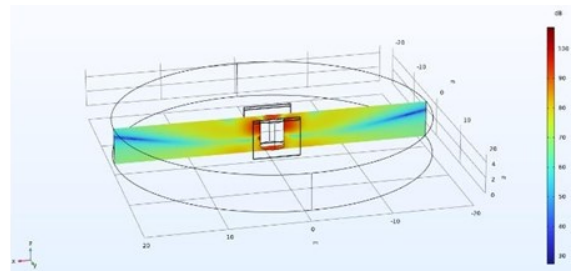


Figure 5. 10: a) Emission with Active Control 9x1



b) Detail of Vertical Plane Control

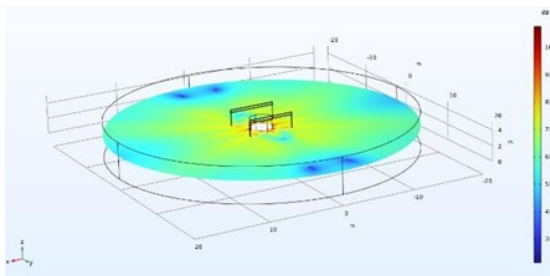
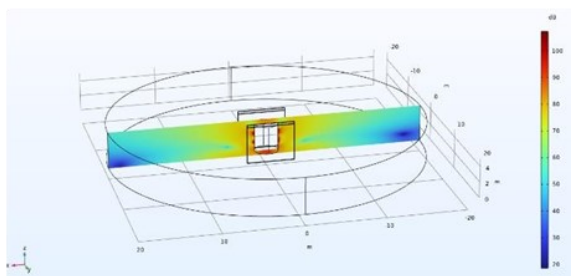


Figure 5. 11 a) Emission with Active Control 6x2



b) Detail of Vertical Plane Control

5.2.2 Identifying the optimal placement points for error microphones

During the simulation phase, another investigation was conducted regarding the optimal placement of error microphones. To define the optimal position for error microphone the following assumptions are considered:

- in the error microphone position only the contribution of one reactor should be significant.
- in the error microphone the reduction level ANC_off vs ANC_on should be significant.

Based on these presumptions, two acoustic fields—one for the ANC_off scenario and

the other for the ANC_on scenario—were created in order to evaluate which position was the best performer. Specifically, the configuration mirrored the real world, with three electrical reactors and four firewalls. Then, simulations were run on this model, as **Figure 5. 12** illustrates.

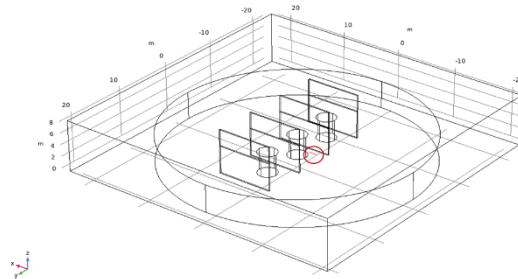


Figure 5. 12: Full implant model. ANC microphones assumed area highlighted in red.

In **Figure 5. 13** and **Figure 5. 14**, the simulation depicted the behavior of the cylindrical emissions from the reactor. The simulations were conducted with active control turned off and on, respectively.

The evaluation of the most performing position was done on a segment positioned in a horizontal plane placed at 1.5 meters over the ground, analyzing different points placed closed to each reactor between 0.5 meters and 2 meters from the central reactor, **Figure 5. 15**. It is worth noting that during this type of simulation, error microphones were not directly incorporated into the simulation.

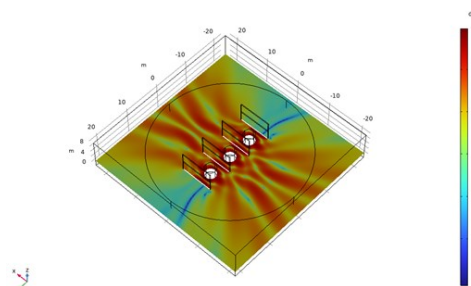


Figure 5. 13: ANC off.

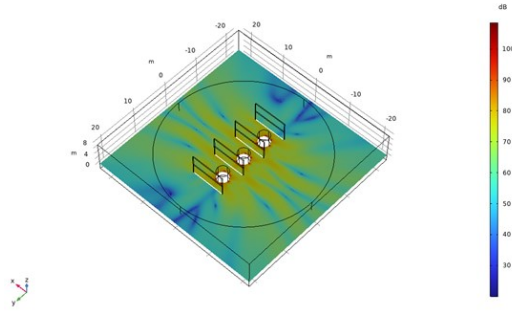


Figure 5. 14: ANC on.

From these data, we determine the optimal position for the error microphones, which is highlighted in the following graphs. By comparing the results, we can establish that the best location to place the error microphones is at approximately 1.5 meters from the central reactor. In **Figure 5. 15** and **Figure 5. 16**, the most notable difference in SPL is the one considered optimal for the microphone placement.

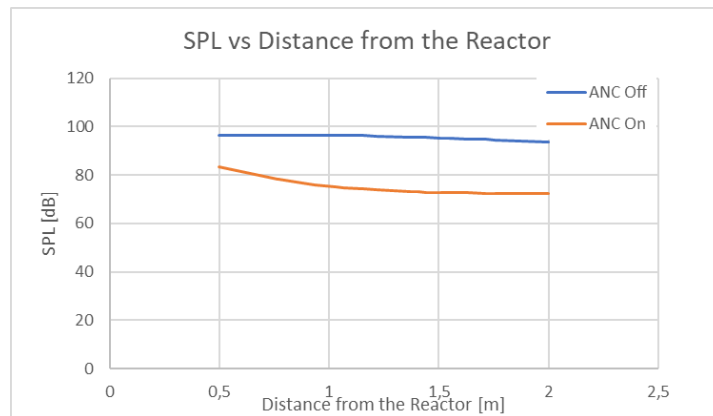


Figure 5. 15: SPL vs Distance from the Reactor.

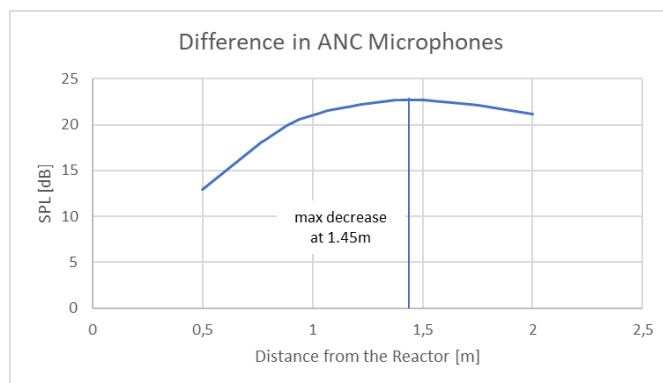


Figure 5. 16: Graph of SPL along the segment where the placement of ANC microphones was assumed between the ANC On and ANC Off.

5.3 Creation of Antinoise Field with an ANC algorithm

The choice of the adaptive algorithm in this type of application is highly relevant to the application presented in the Smart Ambulance article (the latest article). The type of algorithm chosen is the Fx-NLMS algorithm, with the substantial difference lying in the management of the cylindrical emission of the reactor based on three independent channels³ and 36 secondary speakers (each channel drives 12 secondary speakers placed in parallel). This setup is managed by an array of power amplifiers in such a way as not to decrease the power of the loudspeakers but rather to consolidate it into a single channel. Therefore, as far as the algorithm is concerned, the control hardware consists of three channels with three error microphones and three groups of secondary speakers in parallel.

5.3.1 Feedforward FxNLMS with Reference Synthesis System

The canceling system in question is based on Simulink Real Time (SLRT) executed on a Speed goat multichannel platform, with the distinction of using three separate channels and secondary.

We employed a feedforward Fx-NLMS algorithm, with Reference Synthesis, an algorithmic variation of the Fx-NLMS described in our second paper on the "Smart Ambulance" project (please refer to that publication for further details).

In **Figure 5. 17** and **Figure 5. 18**, we can observe the active control monitoring system, involving the acquisition of signals emitted by the reactor through three distinct and separate channels. Furthermore, the microphone is positioned at a maximum distance of 1.5 meter at height.

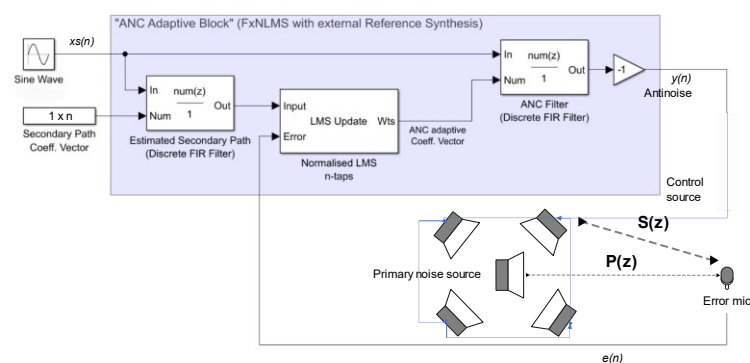


Figure 5. 17: Basic building block to generate a synthetic reference signal, $x_s(n)$, for a sine tone at 100Hz.

³ By channel, we mean a combination of a 'control speakers' and an 'error microphone.'

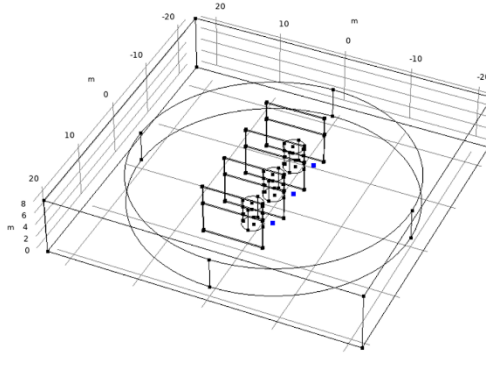


Figure 5. 18: Schematic representation of the system with 3 reactors and 3 error microphones, each paired with respective secondary acoustic speakers.

This approach enables exceptional precision in the detection and control of signals emitted by the reactor, thanks to the use of three distinct channels and the strategic placement of the microphones. Additionally, the use of secondary loudspeakers arranged in parallel, with a dedicated channel for each speaker.

5.4 Field tests results

This section presents a thorough explanation and clarification of the findings from the experiments carried out in our lab as well as at the power plant where the reactors are situated. It's important to remember that the reactor in the station was not the same as the type used in the laboratory testing. Important information and conclusions have surfaced from our analysis of the data, and these will be covered in more detail in the section that follows.

5.4.1 Field pre-tests results

In this phase of the project, a practical test was conducted to evaluate the application of results obtained through prior simulations. The test environment closely resembled that of the electrical station housing the three reactors under study. **Figure 5. 19** and **Figure 5. 20** illustrates the system's configuration and provides measurements of a tonal signal at 100 Hz, along with its corresponding attenuation margin. The primary objective of this test was to assess how effectively the simulation results could be applied in real-world scenarios. Specifically, the focus was on verifying the signal attenuation when employing a configuration with secondary speakers placed in parallel.



Figure 5. 19: Attempts to Replicate Attenuation System.



Figure 5. 20: Attempts to Reproduce the Cylindrical Noise Source (Tried with Control Boxes Both Outside and Inside the Cylinder of Figure 5.19).

In the visual representation of **Figure 5. 21**, we can observe a simplified scenario involving a single channel for a single reactor. The term "ZoS," which stands for "Zone of Silence," denotes a specific region where a reduction in the intensity of the signal emitted by the electrical reactor occurs, with a frequency of 100 Hz, on a global scale.

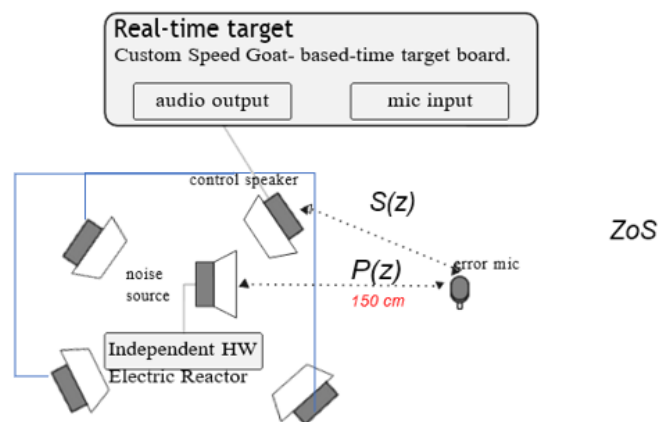


Figure 5. 21: A laboratory configuration is shown, where the noise source is connected to the real-time target audio output. This setup emphasizes the primary and secondary acoustic paths, represented as $P(z)$ and $S(z)$, along with the highlighted "zone of silence."

In **Figure 5. 22**, a reduction in the respective 100 Hz frequency is evident, which corresponds to the operating frequency of the electrical reactor. At a frequency of 100Hz, test results have highlighted a significant reduction in sound and a uniform sound emission in all directions. This means that at 100Hz, the sound appears to be well distributed in the surrounding environment without significant directional deviations.

However, as we move to higher frequencies, the secondary speakers begin to exhibit a different behavior. Specifically, they start emitting sound in a more directional manner, indicating that the sound tends to be focused in a specific direction rather than spreading uniformly. Furthermore, at these higher frequencies, there is a slight overall instability in the sound emission pattern. This implies that the sound may vary slightly in intensity or direction, introducing greater variability in the overall auditory experience.

In summary, at 100Hz, there is a uniform sound distribution, but at higher frequencies, a directional emission pattern with some instability is observed, signifying a significant change in the behavior of the secondary speakers with changing frequency.

However, further analysis revealed that the signal emission was not perfectly cylindrical, as observed in the simulated electrical reactor case, but rather displayed a slight radial distribution. This finding holds significance in the overall assessment of the effectiveness of the secondary speakers placed in parallel, as it influences the actual attenuation of the 100 Hz signal in a real-world used scenario.

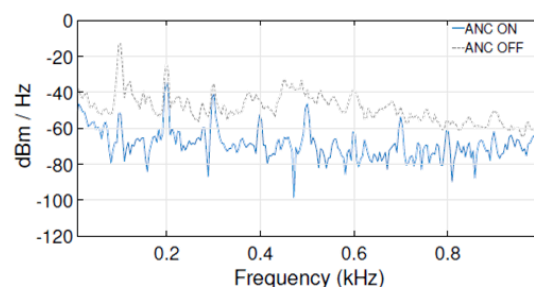


Figure 5. 22: Configuration with sinusoidal tone at 100 Hz.

5.4.2 Experimental results

Currently, field tests have not been conducted yet, and, as a result, the associated conclusions are under development. The outcomes of these tests will be pivotal in further enhancing the conclusions and validating the new active control application.

5.5 Conclusions

The study's experimental component encountered difficulties, necessitating additional research and a follow-up session planned for May 2024. The contents of this phase could not be incorporated into the existing thesis due to these unanticipated challenges.

With this research work new Active Noise Control (ANC) approaches for noise reduction have been presented. In particular, the objectives of the research have been focused on two main noise signals and applications, the first one related to a priori known time-varying signals (chapter 3-4) and the second one related to stationary noise produced by large industrial machinery (chapter 5).

The performance of the developed systems has been evaluated in terms of signal reduction, algorithm robustness, convergence speed, and memory usage with respect to computational cost.

Signal reduction, robustness and convergence rate, memory use and computational requirements have been evaluated for each ANC application. As results, signal reduction, robustness and convergence rate are directly related to the efficiency of the ANC systems, whereas memory use and computational requirements are connected to the implementation domain.

A summary of the thesis' results is provided in this chapter along with directions for future research work.

6.1 Thesis' Results

Main results obtained referring to the a priori known time-varying signals.

In this research, Active Noise Control (ANC) algorithms are examined to reduce the noise of the ambulance's siren as perceived by driver inside the vehicle.

Our DSP implementations are all based on a feedforward ANC architecture, using the classic Fx-NLMS algorithm, running it on a real-time hardware platform to test the efficacy of the cancelling solution in a laboratory environment. These algorithms are developed using MATLAB Simulink environment and ran on Speedgoat target hardware; with such a setup our system achieves:

- Synthesis of references signal for known noises, providing cancellation selectivity and simplifying hardware requirements. ⁴
- By decomposing complex time-varying signals into their constituent's stationary sound patterns, we could implement the adaptive filtering for each such patterns, rather than having the system to track a rapidly changing signal; This allows for more stable and faster performances, and it is achieved by implementing Switching FxNLMS.²

Main results obtained referring to the stationary noise produced by large industrial machinery.

In this case the main challenge is not the complexity of the noise signal, since a pure tone was a good model of the real primary noise source, but the physical application of the canceling hardware to optimally obtain a significant global attenuation. The results of research and activities demonstrated the possibility to obtain approximately 5dB of global attenuation around the complex primary noise source, rather than the classic cancellation focused on the error microphones.

⁴ The implementations were carried out in real-world scenarios, rather than relying on simulations, which are more commonly encountered.

6.2 Future work

The directions for future works are the following ones:

- Referring to the siren noise reduction application, it is expected to implement the noise canceling system aboard an actual ambulance. To achieve this, several further developments and improvements are foreseen. One essential step is to enhance the control board by incorporating two dedicated microcontrollers, one for each channel/Zone of Silence (ZoS) close to each ear:
 - The Reference Synthesis technique will be subject to further investigation to optimize the creation of the reference signal. The aim is to reduce the number of adaptive filters required, making the system more efficient while targeting 5-6 harmonics per pulse wave for successful noise cancellation.
 - To ensure the ANC system's practical implementation, considerations must be made for the system's expansion, especially in the vicinity of the error microphone. Physical microphones near the driver's ear are not feasible for safety and comfort reasons, requiring the implementation of virtual microphone solutions within the headrest. An array of virtual microphones might help address the expansion of the Zone of Silence (ZoS) and improve performance.
 - To optimize the algorithm's execution on the target hardware, lower-level programming languages should be considered, potentially further enhancing cancellation performance.
- The current results obtained for reactors can be extended to more complex and multifrequency electrical machinery, such as transformers, where in addition to the main 100Hz frequency associated with the phenomenon of magnetostriction, it is essential to consider other frequencies related to the noise generated by cooling devices like air thermals. However, according to successfully results obtained on reactors it is expected that ANC techniques developed and tested on reactors can be easily adapted to reduce the noise emissions of transformers.

References

- [1] "Fundamentals of Acoustics" by Lawrence E. Kinsler, Austin R. Frey, Alan B. Coppens, and James V. Sanders, John Wiley & Sons, 12 gen 2000.
- [2] "Introduction to Sound: Acoustics for the Hearing and Speech Sciences" by Charles E. Speaks. Charles E. Speaks, 2018.
- [3] Pulkki, Ville & Pöntynen, Henri & Santala, Olli. (2019). Spatial Perception of Sound Source Distribution in the Median Plane. *Journal of the Audio Engineering Society*. 67. 855-870. 10.17743/jaes.2019.0033.
- [4] Nelson, P.A.; Elliott, S.J.: *Active Control of Sound*, Academic Press, San Diego, 1992.
- [5] Kuo, S.M.; Morgan, D.R.: *Active Noise Control Systems–Algorithms and DSP Implementations*, Wiley, New York, 1996.
- [6] Fuller, C.R.; Elliott, S.J.; Nelson, P.A.: *Active Control of Vibration*, Academic Press, San Diego, 1996.
- [7] Elliott, S.J.: *Signal Processing for Active Control*, Academic Press, San Diego, 2001.
- [8] Lizhe Tan, Jean Jiang, *Adaptive Filters and Applications*, Academic Press, 2019.
- [9] B. Widrow and S. D. Stearns, *Adaptive noise cancelling: Principles and applications*, Practise-Hall Signal Processing Series, New Jourcy, 1985.
- [10] Macchi, O. "The Theory of Adaptive Filtering in a Random Time-Varying Environment.", *Digital Signal Processing in Telecommunications*. Springer, London, 1996.
- [11] Anthony Zaknich. *Principles of Adaptive Filters and Self-learning Systems*. Springer Science & Business Media, 2005.
- [12] Widrow, B., and Hoff, M.E., , *Adaptive switching circuits: IRE WESCON Conv. Rec.*, 1960.
- [13] Widrow, B., and Stearns, S., *Adaptive Signal Processing: Prentice-Hall*, New York, 1985.
- [14] Simon S. Haykin, Bernard Widrow, *Least-Mean-Square Adaptive Filters*, 2003.
- [15] Bernard Widrow, Samuel D. Stearns: *Adaptive Signal Processing*, Prentice Hall, 1985.
- [16] D. T. Slock and T. Kailath, "Numerically stable fast transversal filters for recursive least-squares adaptive filtering," in *Numerical Linear Algebra, Digital Signal Processing and Parallel Algorithms*. Springer, 1991.

-
- [17] S. Haykin, "Adaptive Filter Theory, 3rd-ed," Printice Hall, 1996.
- [18] Kuo, S.; Morgan, D. Active Noise Control Systems–Algorithms and DSP Implementations; Springer: New York, NY, USA, 1996.
- [19] Kajikawa, Y.; Gan, W.S.; Kuo, S.M. Recent advances on active noise control: Open issues and innovative applications. *APSIPA Trans. Signal Inf. Process.*, 1, 1–21, 2012.
- [20] A. Schüeli. *Digitale Signalverarbeitung*. HSR, 2002.
- [21] S. M. Kuo and D.R. Morgan. *Active Noise Control Systems*. John Wiley & Sons Inc., New York, 1996.
- [22] Swain, A. "Active Noise Control: Basic Understanding". Research Gate, 2013.
- [23] Das, D.P.; Panda, G.; Kuo, S.M. New block filtered x LMS algorithms for active noise control systems. *IET Signal Process.*, 1, 73–81, 2007.
- [24] Das, K.K.; Satapathy, J.K. Frequency-domain block filtered-X NLMS algorithm for multichannel ANC. In *Proceedings of the First International Conference on Emerging Trends in Engineering and Technology*, Nagpur, Maharashtra, India; pp. 1293–1297, 16–18 July 2008.
- [25] Kuo, S.M.; Morgan, D.R. Active noise control: A tutorial review. *Proc. IEEE*, 87, 943–973, 1999.
- [26] Widrow, B.; Stearns, S. *Adaptive Signal Processing*; Prentice Hall: Upper Saddle River, NJ, USA, 1985.
- [27] Kuo, Sen & Vijayan, D.. (1995). Optimized secondary path modeling technique for active noise control systems. 370 - 375. 10.1109/APCCAS.1994.514578.
- [28] Pawelczyk M. Analogue active noise control. *Appl Acoust*; 63:1193–213, 2002.
- [29] Chuang Shi, Mengjie Huang, Chunyu Liu, Huiyong Li. Active noise control with selective perceptual equalization to shape the residual sound, *Applied Acoustics*, Volume 208, 2023, 109376, ISSN 0003-682X.
- [30] Zhang L, Wu L, Qiu X. An intuitive approach for feedback active noise controller design. *Appl Acoust*; 74:160–8, 2013
- [31] Kaiser OE, Pietrzko SJ, Morari M. Feedback control of sound transmission through a double-glazed window. *J Sound Vib*; 263:775–95, 2003.
- [32] Lifu Wu, Xiaojun Qiu, Yecai Guo, A simplified adaptive feedback active noise control system, *Applied Acoustics*, Volume 81, Pages 40-46, 2014.
- [33] Gan, Woon-Seng & Mitra, Sohini & Kuo, Sen., Adaptive feedback active noise control headset: Implementation, evaluation and its extensions. *Consumer Electronics, IEEE Transactions on*. 51. 975 – 982, 2005.
- [34] SNYDER-S. D., AND HANSEN-C. H.. The effect of transfer function estimation

-
- errors on the filtered-x LMS algorithms, *IEEE Transactions on Signal Processing*, 42, pp. 950–953, 1994.
- [35] L. J. Eriksson and M. C. Allie, “Use of random noise for on-line transducer modeling in an adaptive active attenuation system,” *J. Acoust. Soc. Am.*, vol. 85, no. 2, pp. 797–802, June 1989.
- [36] S. Chan and Y. Chu, “Performance analysis and design of FxLMS algorithm in broadband ANC system with online secondary-path modeling,” *IEEE Trans. Audio, Speech, Lang. Process.*, vol. 20, no. 3, pp. 982–993, Mar. 2012.
- [37] Ming Zhang, Hui Lan, and Wee Ser, “Cross-updated active noise control system with online secondary path modeling,” *IEEE Trans. Speech Audio Process.*, vol. 9, no. 5, pp. 598–602, July 2001.
- [38] S. Ahmed, M. T. Akhtar, and X. Zhang, “Robust auxiliary-noise-power scheduling in active noise control systems with online secondary path modeling,” *IEEE Trans. Audio, Speech, Lang. Process.*, vol. 21, no. 4, pp. 749–761, Apr. 2013.
- [39] A. Carini and S. Malatini, “Optimal variable step-size NLMS algorithms with auxiliary noise power scheduling for feedforward active noise control,” *IEEE Trans. Audio, Speech, Lang. Process.*, vol. 16, no. 8, pp. 1383–1395, Nov. 2008.
- [40] M. T. Akhtar, M. Abe, M. Kawamata, and A. Nishihara, “Online secondary path modeling in multichannel active noise control systems using variable step size,” *Signal Process.*, vol. 88, no. 8, pp. 2019 – 2029, Aug. 2008.
- [41] P. Yuxue and S. Pengfei, “Online secondary path modeling method with auxiliary noise power scheduling strategy for multi-channel adaptive active noise control system,” *J. Low Freq. Noise, Vib. Act. Control*, vol. 38, no. 2, pp. 740–752, Feb. 2019.
- [42] D. W. Kim and P. Park, “Online secondary path estimation in active noise control systems using a scheduled step size algorithm,” *11th Asian Control Conference (ASCC)*, Gold Coast, QLD, Australia, pp. 801-806, 2017.
- [43] S. M. Kuo and J. Luan, “On-Line Modeling and Feedback Compensation for Multiple-Channel Active Noise Control Systems,” *Applied Signal Processing*, vol. 1, no. 2, pp. 64–75, 1994.
- [44] M. T. Akhtar, M. Abe, and M. Kawamata, “On Active Noise Control Systems with Online Acoustic Feedback Path Modeling,” *IEEE Trans. Audio Speech Language Processing*, vol. 15, no. 2, pp. 593–600, Feb. 2007.
- [45] S. M. Kuo, “Active Noise Control System and Method for On-Line Feedback Path Modeling,” *US Patent 6,418,227*, July 9, 2002.
- [46] L. Mokhtarpour and H. Hassanpour, “A self-tuning hybrid active noise control

-
- system," J. Franklin Inst., vol. 349, no. 5, pp. 1904–1914, 2012.
- [47] T. Padhi, M. Chandra, A. Kar, and M. N. S. Swamy, "Design and analysis of an improved hybrid active noise control system," *Appl. Acoust.*, vol. 127, pp. 260–269, Dec. 2017.
- [48] M. T. Akhtar and W. Mitsuhashi, "Improving Performance of Hybrid Active Noise Control Systems for Uncorrelated Narrowband Disturbances," in *IEEE Transactions on Audio, Speech, and Language Processing*, vol. 19, no. 7, pp. 2058-2066, Sept. 2011.
- [49] Iwai, K.; Hase, S.; Kajikawa, Y. Multichannel Feedforward Active Noise Control System with Optimal Reference Microphone SelectorBased on Time Difference of Arrival. *Appl. Sci.*,8, 2291, 2018.
- [50] Dongyuan Shi, Bhan Lam, Junwei Ji, Xiaoyi Shen, Chung Kwan Lai, Woon-Seng Gan, Computation-efficient solution for fully-connected active noise control window: Analysis and implementation of multichannel adjoint least mean square algorithm, *Mechanical Systems and Signal Processing*, Volume 199, 2023.
- [51] Hao Zhang, DeLiang Wang, Deep ANC: A deep learning approach to active noise control, *Neural Networks*, Volume 141, 2021, Pages 1-10, ISSN 0893-6080.
- [52] Hao Zhang, DeLiang Wang, Deep MCANC: A deep learning approach to multichannel active noise control, *Neural Networks*, Volume 158, 2023, Pages 318-327, ISSN 0893-6080.
- [53] Y. Gao, K. Muramatsu, K. Fujiwara, Y. Ishihara, S. Fukuchi, and T. Takahata, *IEEE Trans. Magn.* 45, 4789 (2009).
- [54] Schoenekess H., Ricken W., Becker W., Influences of Magnetostriction and Magnetisation State on Strain and Force Measurement with Eddy-Current SensorsApplied to Steel Reinforced Concrete, *Proceedings of International Symposium onNonDestructive Testing in Civil Engineering NDT-CE (16-19 September 2003,Berlin, Germany)*, DGZfP, 2003.
- [55] Asano S., Fujieda S., Hashi S., Ishiyama K., Fukuda T., Suzuki S., MagneticDomain Structure and Magnetostriction of Fe-Ga Single Crystal Grown by theCzochralski Method, *IEEE Magnetics Letters*, 2016.
- [56] Marks, Janis and Vitolina, Sandra. "Modelling of magnetostriction of transformer magnetic core for vibration analysis" *Open Physics*, vol. 15, no. 1, 2017, pp. 803-808.
- [57] M. Biagini, F. Borchì, M. Carfagni, L. Fibucchi, A. Lapini, F. Argenti, Active noise systems for reducing outdoor noise (2017) 24th International Congress on Sound and Vibration, ICSV 2017.

-
- [58] J. R. Glover, Jr., "Adaptive noise canceling applied to sinusoidal interferences," *IEEE Trans. Acoust., Speech, Signal Processing*, vol. ASSP-25, pp. 484–491, Dec. 1977.
- [59] Vikram Kumar, P.; Prabhu, K.; Das, D.: Block filtered-s least mean square algorithm for active control of nonlinear noise systems. *IET Signal Process.*, 4 (2) (2010), 168–180.
- [60] Borchi, F., Carfagni, M., Martelli, L., Turchi, A., Argenti, F.: Design and experimental tests of active control barriers for low-frequency stationary noise reduction in urban outdoor environment. *Applied Acoustics*, 114 (2016), 125–135.
- [61] Bartalucci, C., Borchi, F., Carfagni, M., Paolucci, L.: Analysis and development of an active noise control system for the cancellation of noise produced by the reactors of electric stations. *INTER-NOISE and NOISE-CON Congress and Conference Proceedings*, 10 (2020), 749–758.
- [62] Omoto, A., Fujiwara, K.: A study of an actively controlled noise barrier. *J Acoust Soc Am* 1993;94(4):2173–80.
- [63] P. Nelson and S. Elliott, The minimum power output of a pair of free field monopole sources, *J. Sound Vib.* 105 (1986) 173–178.
- [64] Lee, Hsiao Mun, Zhaomeng Wang, Kian Meng Lim, and Heow Pueh Lee. 'A Review of Active Noise Control Applications on Noise Barrier in Three-Dimensional/Open Space: Myths and Challenges'. *Fluctuation and Noise Letters* 18, no. 04 (December 2019): 1930002.
- [65] A. Montazeri, J. Poshtan and M. H. Kahaie, Application of genetic algorithms for overall optimization of an active noise control system in an enclosure, *Fluct. Noise Lett.* 8 (2008) L51–L64.

Appendix A

In this section, details of scientific publications relevant to the thesis's purpose will be provided.



Analysis of Possible Algorithms for Active Noise Control of Siren Noise into an Ambulance

Massimo Generoso Buttarazzi¹  , Chiara Bartalucci¹ , Francesco Borchi¹ ,
Monica Carfagni¹ , and Libero Paolucci² 

¹ Department of Industrial Engineering (DIEF) – Florence, University of Florence,
Via di Santa Marta 3, 50139 Firenze, Italy
{massimogeneroso.buttarazzi, chiara.bartalucci, francesco.borchi,
monica.carfagni}@unifi.it

² Department of Information Engineering (DINFO) – Florence, University of Florence,
Via di Santa Marta 3, 50139 Firenze, Italy
libero.paolucci@unifi.it

Abstract. This paper discusses a potential application of Active Noise Control (ANC) algorithms for the reduction of ambulance siren noise inside the vehicle. The study starts from the analysis of ANC techniques available in literature and currently used in industrial and consumer applications. The concept of ANC is based on the introduction of a canceling “antinoise” wave through a suitable speaker array known as secondary sources. These generators are managed through a specific signal-processing algorithm tailored according to the characteristics of the noise generated by the primary source that has to be cancelled. The primary signal is recorded by the control microphones and then processed by the ANC algorithm. An “antinoise” is then generated to reduce the primary source noise in a specific target zone. Based on the fundamental principles of wave superposition and wave cancellation, ANC technique is a very effective solution from a theoretical point of view; nevertheless, this technique faces numerous practical implementation problems and despite the wide number of available industrial and domestic applications, it is still poorly exploited. In this paper, the state of the art about most advanced ANC techniques and applications is analyzed. In particular, the implementation of adaptive signal processing algorithms and digital signal processing (DSP) in ANC systems is analyzed.

Keywords: Active Noise Control · Comfort zone · Feed-forward ANC · Virtual ANC · Acoustical · FIR · IIR · X-LMS · U-LMS · Genetic algorithms

1 Introduction

Active Noise Control (ANC) is an effective way to reduce noises that can otherwise be very difficult and expensive to control. It could be effective also when dealing with low frequency disturbances where physical barriers may fail. Lueg proposed the concept of acoustic ANC in 1936, using a microphone and an electronically driven loudspeaker to generate a canceling sound [1]. In general, the properties of the acoustic noise source

and the environment change over time; hence the frequency content, amplitude, phase, and sound velocity of the undesired noise are nonstationary. Consequently, it is not possible to operate an ANC with static algorithms. A possible solution is the use of adaptive filters [2–5] that adjust their coefficients to reduce an error signal. Finite impulse response (FIR), infinite impulse response (IIR), and transform-domain filters (TDF) can be used to realize these algorithms. In the following section four ANC strategies based on adaptive filters and a possible application to ambulance noise abatement is presented.

Section 2 describes the basic concept of active noise control techniques and discusses the Least Mean Square (LMS) and FxLMS algorithms. The third section delves into the idea of using active noise control in an ambulance.

2 Active Noise Control Architecture

Concerning the ambulance siren noise, it is a stationary signal characterized by a single tone at a medium-high frequency (2 or 3 kHz). Hence it is possible to estimate its spectral behavior, and the control concerns mainly the amplitude of the disturbance. In the following section a LabVIEW simulation tool is used to test the behavior of different ANC strategies and evaluate their response as a function of a certain noise type. Most of the ANC algorithms are based on the Least-Mean-Square (LMS) filter because of its simplicity of implementation and adaptability. The system is usually composed of a reference microphone which records the primary signal noise, one or more secondary sources that generate the “antisound”, one or more error microphones which record the resulting from the superposition of the primary and secondary sound and a processing unit. A general scheme of an ANC system is presented in Fig. 1. Most of these systems are based on digital controllers, as a result, signals from electroacoustic or electromechanical transducers are sampled and processed in real time using Digital Signal Processing (DSP) systems before being synthesized, amplified, and delivered to the loudspeakers. Clearly the entire process must be carried in real time, where the sound is generated and the moment it reaches the target zone which is the physical place where the primary noise must be reduced. Hence, especially in the past years, it has been necessary to achieve an optimal trade-off between processing time and algorithm complexity. In recent years the development of improved high-speed digital signal processing hardware allowed the implementation of complex ANC algorithms [6, 7]. However, the mathematical implementation of the cancellation algorithm has still to be optimized to take into account the causation principle and the convergence time.

The choice of the ANC algorithm type in general depends on the primary noise characteristics in terms of signal bandwidth and amplitude. The goal of adaptive algorithms is to keep filter coefficients up to date in order to achieve optimal noise cancellation. The optimization process of the filter coefficients can usually be stochastic or deterministic. LMS and Normalised-LMS (NLMS) algorithms use the stochastic approach. The deterministic approach, which is used with the RLS (Recursive Least Squares) algorithm, necessitates the calculation of the characteristics of many samples. The Filtered-x LMS (FxLMS) filter is a modified version of the LMS algorithm, and it is computationally simple where secondary path effects are also included, but its convergence speed is low. The fundamental issues in the afore mentioned approaches are inherent to stability

issues in IIR-based structures, increases in computational requirements, and numerical instability issues in RLS-based ANC systems. For these reasons, FxLMS is still a viable option for ANC applications [8].

The simulation scenario makes use of the single-channel duct-acoustic ANC system depicted in Fig. 1 with a single reference sensor, single secondary source, and single error sensor.

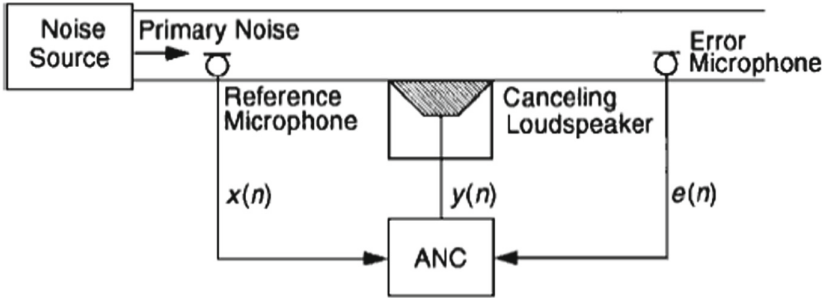


Fig. 1. A duct-based single-channel broad-band feedforward ANC system.

2.1 LMS Algorithm

In Fig. 2 a scheme of an LMS adaptive filter used in system identification applications is shown. The scheme highlights the behavior of the filter where $x(n)$ is the primary source signal, $d(n)$ is the disturbance in the target zone, $y(n)$ is the ‘antisound’ and $e(n)$ is the sum of $d(n)$ and $y(n)$. The Adaptive Filter in this case is an LMS adaptive filter which has to adapt to an unknown channel to minimize the resulting error $e(n)$. It represents an LMS adaptive filter block diagram where each iteration of LMS involves three steps: filter output $y(n)$, estimation error $e(n)$ and tap-weight adaptation $w(n + 1)$.

The frequency-domain analysis of the residual error signal $e(n)$ can be used to determine the performance of ANC. The $e(n)$ autopower spectrum is given by:

$$S_{ee}(\omega) = [1 - C_{dx}(\omega)]S_{dd}(\omega) \tag{1}$$

where $C_{dx}(\omega)$ is the magnitude-squared coherence function between two stationary random processes with wide-sense $d(n)$ and $x(n)$, while $S_{dd}(\omega)$ is the autopower spectrum of $d(n)$. The term $[1 - C_{dx}(\omega)]$ represents an ANC system’s noise reduction at frequency ω , but the maximum noise reduction in decibel is given by $-10\log_{10}[1 - C_{dx}(\omega)]$.

In Fig. 3 $S(z)$ is introduced in order to model the secondary path effects, representing the secondary path connecting the canceling loudspeaker and the error microphone.

The z-transform of the error signal is:

$$E(z) = [P(z) - S(z)W(z)]Xr(z) \tag{2}$$

where it is constrained by the coherence of the reference signal to obtain the residual error (ideally equal to zero), the optimal transfer function $W(z)$ must be defined:

$$W_o(z) = \frac{P(z)}{S(z)} \tag{3}$$

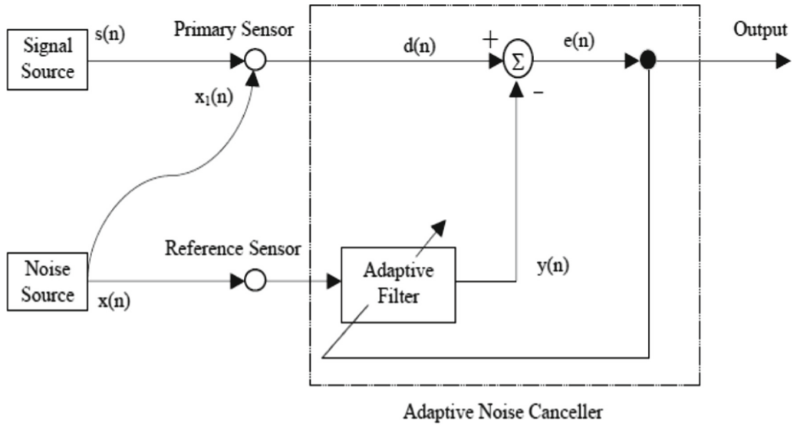


Fig. 2. LMS adaptive filter block diagram used in system identification applications.

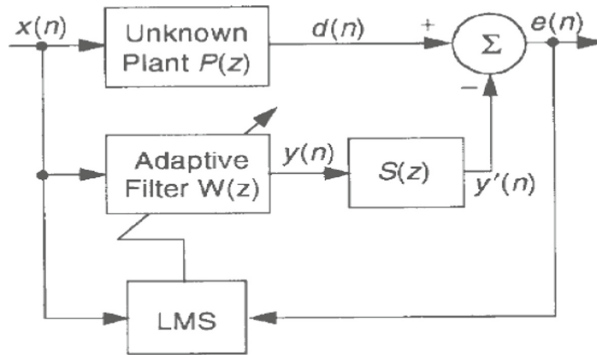


Fig. 3. LMS adaptive filter used with secondary path transfer function.

In other words, the adaptive filter $W(z)$ must model both $P(z)$ and $S(z)$ simultaneously. The expression of the filter output is the following:

$$y_s(j) = \sum_{i=0}^{N-1} x_r(j-i)w_i(j) = x_r^T(j)w(j) \tag{4}$$

Filter weights updating is performed according to Eqs. (5),

$$w(j+1) = w(j) + \mu e(j)x(j) \tag{5}$$

Where:

1. μ = convergence coefficient (step size)
2. $x(n)$ = reference signal
3. $p(n)$ = primary signal
4. $w(n)$ = filter coefficients

the condition for stability is:

$$0 < \mu < \frac{2}{\text{input signal power}} \quad (6)$$

With large values of the step-size, the filter increases its adaptation rate (faster convergence) and increases the residual mean-squared error. The major advantages of this filter are:

1. it is simple in implementation
2. it guarantees stable and robust performance against different signal condition a disadvantage is the slow convergence.

In Fig. 4 it is shown the variation of Mean Square Error (MSE) with different step-size.

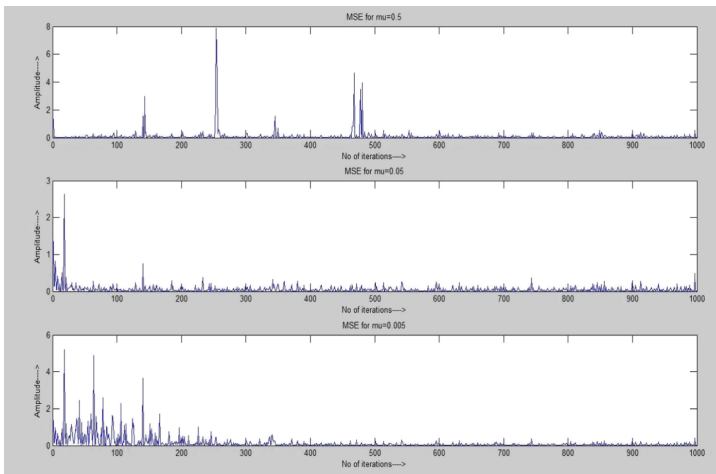


Fig. 4. Variation of MSE with different step-size.

In Fig. 5, instead, it is shown the response of the LMS filter to a broadband noise. It is possible to highlight that given a step size of 0.5 the system is not stable, and the error diverges.



Fig. 5. Instability LMS Algorithm.

2.2 FxLMS Algorithm

The integration of a secondary path model in the reference signal path was proposed by Widrow, Shur, and Shaffer (from the speaker to the error microphone). Figure 6 depicts a block diagram of the FXLMS algorithm, which Kuo and Morgan used to demonstrate how the noise reduction algorithm works.

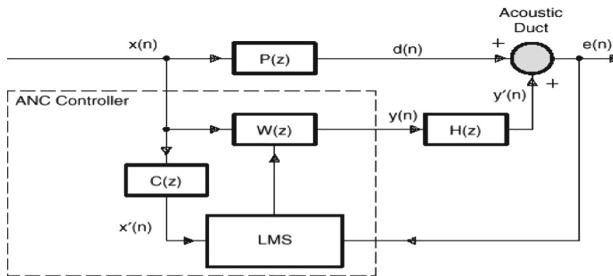


Fig. 6. FxLMS algorithm block diagram.

The FXLMS algorithm is a simple variation on the LMS algorithm [9]. The dashed box (Fig. 6) depicts the functional block diagram of a FxLMS algorithm adjusting an ANC controller, where $C(z)$ represents an estimated model of the secondary path. The reference signal is filtered by $C(z)$ before being used by the standard LMS algorithm, as shown. The reference signal can be determined in two ways: feedforward or feedback. An upstream microphone was used in the feedforward structure to provide information about the unwanted noise propagating down the system. The feedforward ANC algorithm

is depicted in Fig. 7. As shown in Fig. 7, a microphone, called ‘reference microphone’, is located at a position where the signal of the primary source is dominant and the influence of the anti-noise source is negligible.

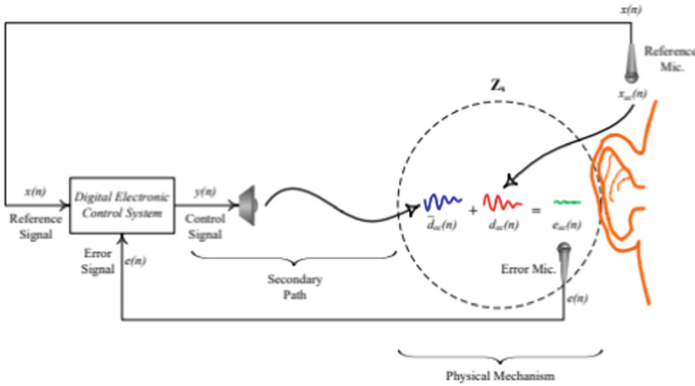


Fig. 7. General diagram for feedforward ANC.

Eriksson proposed ANC controllers with a feedback structure as an alternative to the feedforward structure in 1991. In the feedback structure the error microphone is directly used to evaluate the reference signal (Fig. 8) [10]. Because a reference microphone is not required in this structure, feedback ANC controllers are more compact and cost effective than feedforward ANC controllers.

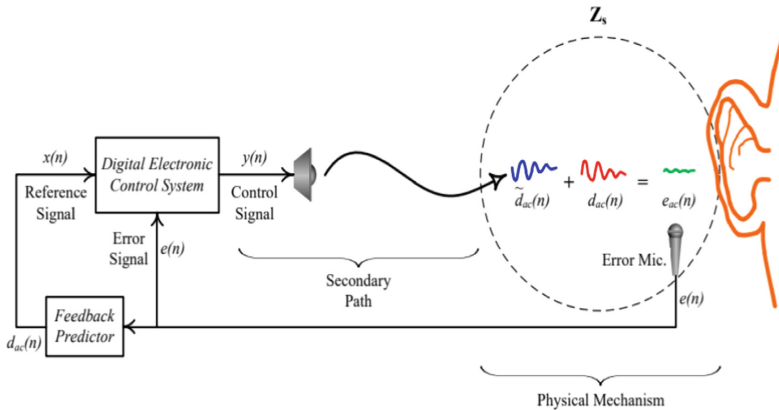


Fig. 8. General diagram for feedback ANC.

Aiming to test the effectiveness of the ANC system varying the step-size, authors have implemented into the Matlab-Simulink environment a single channel Adaptive Feedback ANC using a Filtered-X LMS [11]. Starting from this model of a Filtered-X LMS ANC system, it is possible when the error microphone signal is simulated as the

sum of the noise source filtered by the primary acoustic path and the ANC output filtered by the secondary acoustic path.

In Fig. 9 the output of the error microphone is shown referring to step-size 0.5, 0.05 and 0.005. It is possible to highlight that given a step size of 0.5 the system is not stable, and the error diverges, while for step-size of 0.05 and 0.005 the system is stable with a better convergence rate for the step-size of 0.05.

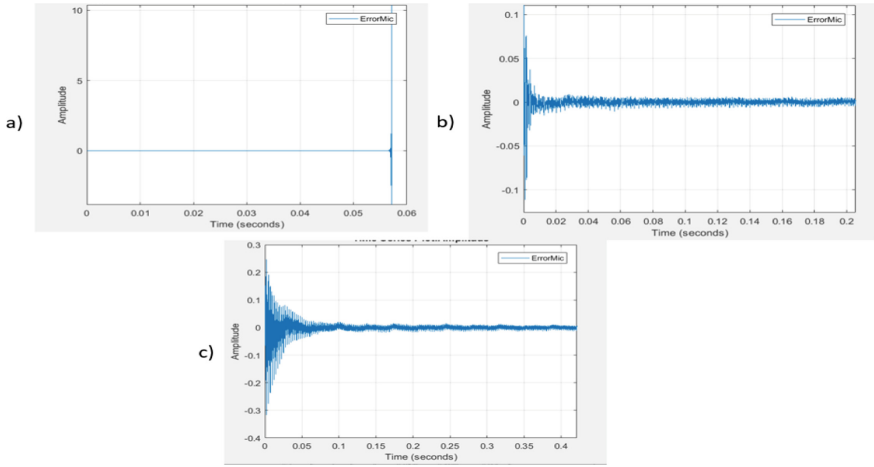


Fig. 9. Output of FXLMS Algorithm Simulation (Single channel - Broadband noise signal) utilizing various step sizes (a) Step size = 0.5, (b) Step size = 0.05, and (c) Step size = 0.005.

In Fig. 10 the results of the simulation, in terms of original noise signal and attenuated one, are shown considering the step-size 0.05.

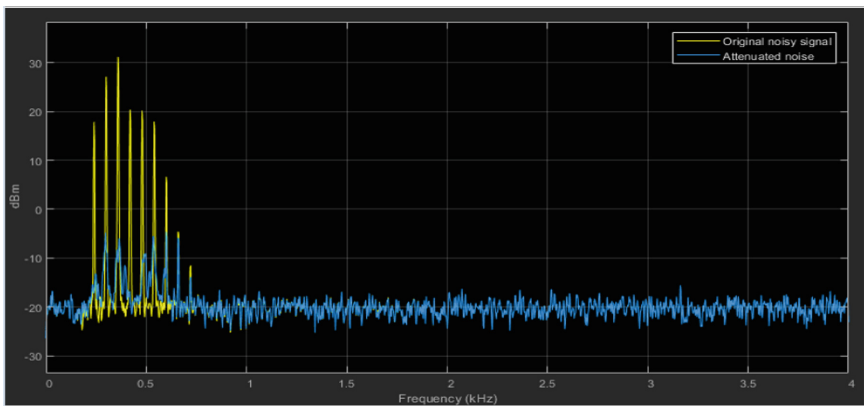


Fig. 10. Output of FxLMS algorithm simulation considering a broadband noise signal: original noise signal (yellow line) and attenuated signal (blue line).

3 Noise Control in Ambulance

Emergency vehicles often use high amplitude screeching sirens. The European normative only allows for the use of a high/low series of tones in emergency vehicles. The ambulance siren signal alternates between two tones at frequencies of 392 Hz (Sol natural) and 660 Hz (Mi natural). The sounds must be played in a continuous sequence with no breaks or noticeable overlap. The duration of the complete cycle is $3 \text{ s} \pm 0.5 \text{ s}$. Between a cycle and the next there may be a pause whose duration should not exceed 0.2 s [12].

Many estimates peg the noise level of a typical ambulance siren in the neighborhood of 120–130 decibels (dB) at roadside positions. The noise of an ambulance siren penetrates the ambulance doors and reaches the ears of the patient and staff. Inside the ambulance, sound pressure levels of about 87 dB(A) are common in the patient zone, while in the driver zone sound pressure levels up to 90 dB(A) are present [13].

Since exposure at these levels, over 80 dB(A), could be a problem of concentration for the driver, also due to the long exposure to siren noise during the same working day, according to the numerous trips with the siren switched on, and also for the patient [14]. In fact, the patient has a short time of exposure to the siren noise, which however could be sufficient to generate problems given the difficult health conditions he may have to face at that moment.

During the rescue operation the patient is already critically ill, and the noise produced can be reduced by passive measures like increasing sound insulation of the ambulance and installing sound absorbing material between doors. However, these interventions require several modifications reducing the free space into the ambulance and involving extra costs. Another possible solution can be that the patient put on ear muffs but based on his condition this solution is considered not feasible [15]. Also for the driver, the use of ear muffs that reduce the overall environmental noise is not considered beneficial, as safe driving conditions must be ensured.

The solution based on the active noise control (ANC) system can be used to solve the problem. It does not need physical modifications of the ambulance and does not affect the safe driving conditions for the driver. A local zone of silence is created around the heads of the staff and of the patient, leading to a significant noise reduction [16].

This solution creates a controller unit that consists of a filter and DSP with use of a fixed step-size, where the system's stability is jeopardized because the convergence rate is slow. The simulation and testing of the two-tones ambulance siren signal is performed for both LMS and FXLMS algorithm, by using Matlab and Simulink software, considering a fixed step-size. The noise signal used in the simulation consists of an ambulance siren signal (Fig. 11).

In Fig. 11 it is shown the examined signal has 51.2 kHz sample/s, 32 bit.

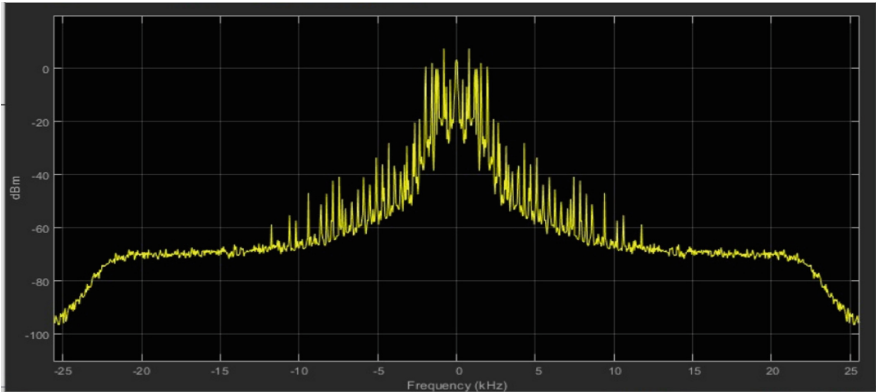


Fig. 11. Frequency spectrum of the ambulance siren signal.

From the preliminary analysis of the simulation results both algorithms lead to convergence. In particular, the FxLMS algorithm converges faster. In the future applications the algorithms will be experimentally tested.

4 Conclusions

In this paper a possible application of Active Noise Control (ANC) algorithms for the reduction of ambulance siren noise inside the vehicle is investigated. In particular, a general analysis of LMS and FxLMS is reported and a comparison of the two algorithms in reference to broadband noise and different fixed step-size is performed.

Furthermore, a preliminary analysis of the ambulance siren signal in reference to the two algorithms LMS and FxLMS is made and a possible preference for FxLMS is highlighted referring to the convergence speed.

On the basis of outcomes achieved in this paper, the ANC technique demonstrates to be a possible and promising application also in the reduction of noise due to the ambulance siren signal, potentially affecting the driver, the patient and the medical staff.

Next research activities will consist of the development of a prototype system for experimental tests to verify the algorithms and the optimal parameters for the siren case study. Moreover, in future steps the analysis of the applications with variable step-size will be tested to improve the FxLMS algorithm's convergence. However, authors consider that convergence could be a secondary problem when known signals have to be reduced as in the case of the ambulance siren noise.

References

1. Lueg, P.: "Process of silencing sound oscillations," U.S. Patent 2 043 416, June 9 (1936)
2. Goodwin, G.C., Sin, K.S.: Adaptive Filtering Prediction and Control. Prentice-Hall, Englewood Cliffs (1984)
3. Davisson, L.D., Longo, G. (eds.): Adaptive Signal Processing. ICMS, vol. 324. Springer, Vienna (1991). <https://doi.org/10.1007/978-3-7091-2840-4>

4. Cowan, C.F.N., Grant, P.M.: *Adaptive Filters*. Prentice-Hall, Englewood Cliffs (1985)
5. Honig, M.L., Messerschmitt, D.G.: *Adaptive Filters: Structures, Algorithms, and Applications*. Kluwer, Boston (1986)
6. Borchi, F., Carfagni, M., Martelli, L., Turchi, A., Argenti, F.: An active noise barrier system optimized for reducing outdoor stationary noise. In: *Proceedings of the 22nd International Congress on Sound and Vibration*, Florence, Italy, 12–16 July (2015)
7. Lapini, A., Biagini, M., Borchi, F., Carfagni, M., Argenti, F.: Design of active noise control systems for pulse noise, advances on mechanics, design engineering and manufacturing. In: *Proceedings of the International Joint Conference on Mechanics, Design Engineering & Advanced Manufacturing*, Catania, Italy, 14–16 Sept (2016)
8. Sakshi, G., Gupta, V.K.: A review on filtered-X LMS algorithm. *Int. J. Signal Process. Syst.* **4**(2), 172–176 (2015). <https://doi.org/10.12720/ijpsps.4.2.172-176>
9. Ardekani, I.T., Abdulla W.: FxLMS-based active noise control: a quick review. In: *Proceedings of*, pp. 1–11 (2011)
10. Ardekani, I., Abdulla, W.: FxLMS-based active noise control: a quick review. In: *Proceedings of 2011 Asia Pacific Signal and Information Processing Association Annual (APSIPA) Summit and Conference*, Xi'an, China (2011)
11. Sachau, D., Jukkert, S.: Real-Time Implementation of the Frequency-Domain FxLMS Algorithm without Block Delay for an Adaptive Noise Blocker. Helmut-Schmidt-University, Germany (2014)
12. Meucci, F., Pierucci, L., Del Re, E., Lastrucci, L., Desii, P.: A real-time siren detector to improve safety of guides in traffic environments (2008)
13. Nataletti, P., Pieroni, A., Annesi, D., Di Giovanni, R., Morgia, F., Ruggeri, D.: Studio pilota dell'esposizione a rumore e vibrazioni degli addetti dei mezzi di soccorso del 118 e dei trasportati", *Atti del convegno dBA2008*, curato da e prodotto dal Dipartimento di Igiene del Lavoro, Laboratorio Agenti Fisici dell'Inail (ex Ispesl) (2008)
14. Weber, U., et al.: Emergency ambulance transport induces stress in patients with acute coronary syndrome. *Emerg. Med. J.* **26**(7), 524–528 (2009)
15. Sharma, M.K., Vig, R.: Ambulance siren noise reduction using LMS and FxLMS algorithms. *Indian J. Sci. Technol.* (2016). ISSN 0974-5645
16. Krishna, A., Ravinchandra, L., Fei, T.K., Yong, L.C.: Active noise reduction using LMS and FxLMS algorithms. *J. Phys.: Conf. Ser.* **1228**, 012064 (2019). <https://doi.org/10.1088/1742-6596/1228/1/012064>

An active noise control system for reducing siren noise inside the ambulance

Massimo G. Buttarazzi^[0000-0002-9819-3378], Francesco Borchi^[0000-0002-3569-313X], Alessandro Mambelli^[0009-0002-7938-677X], Monica Carfagni^[0000-0002-3393-7014], Lapo Governi^[0000-0002-7417-3487], and Luca Puggelli^[0000-0002-5352-9624]

Department of Industrial Engineering, University of Florence
via S. Marta, 3, Florence

Abstract. Siren noise constitutes a nuisance and could be harmful for ambulance personnel and patients. Several studies proposed simulated Active Noise Control (ANC) solutions to attenuate siren noise inside an ambulance. In this paper an implementation of a feedforward ANC system based on the classic FxLMS algorithm is presented, running it on a real-time hardware platform to test the efficacy of such solution in a laboratory environment. Algorithms are developed in MATLAB Simulink environment, and run on Speedgoat target hardware. The results of these experiments are presented, and while discussing our findings, the experienced limitations are described, and further work is suggested.

Keywords: Active Noise Control · FxLMS Algorithm · Feedforward ANC · Ambulance Siren Noise · Real-time Hardware Test

1 Introduction to Active Noise Control

Active Noise Control (ANC) is a technology that can be used to reduce unwanted sound in a given environment. Based on the superposition principle, ANC systems eliminate residual noise within a specific area called *zone-of-silence* (ZoS, or Z_s) by producing a secondary controlled noise with the same amplitude and opposite phase of the source noise, that creates the desired destructive interference with the primary noise at the right location. The basic working principle is depicted in figure 1.

Such systems employ acoustic sensors (speakers and microphones) and digital signal processors to generate the control signal. The control signal is usually shaped with the use of adaptive filters, since often the operational environment is non-stationary.

A variety of ANC systems have been studied ([1],[2]), based on different adaptive algorithms, depending on their application.

The first adaptive ANC system using the LMS algorithm was developed by B. Widrow in 1975 [3]. Dennis R. Morgan improved upon it [4] by adding

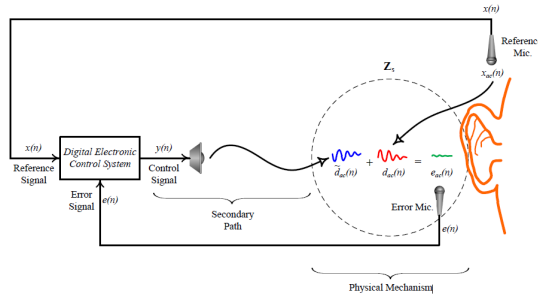


Fig. 1: Principle of noise cancellation, using a secondary noise source to generate a control signal $y(n)$ such as a desired destructive interference is obtained in Z_s , where noise $\tilde{d}_{ac}(n)$ is cancelled by antinoise $d_{ac}(n)$. Taken from [1].

an additional filter¹ to compensate for the effect of *secondary acoustic paths*² placed after the ANC adaptive filters, thus pioneering the so called *Filtered-x Least Mean Square Algorithm* (FxLMS), which is the one used in this study experiments too.

Several variations of the FxLMS algorithm can be found in [4]; for siren noise reduction, most systems seem based on variations of the LMS adaptive algorithm ([5] through [8]); In particular, a *Narrowband Feedforward ANC* structure (figure 2) seems to be the best solution to be applied because a reference signal $x(n)$ is available directly from the noise source, and the signal to be cancelled has a known limited-bandwidth spectrum, as described in detail in section 1.1.

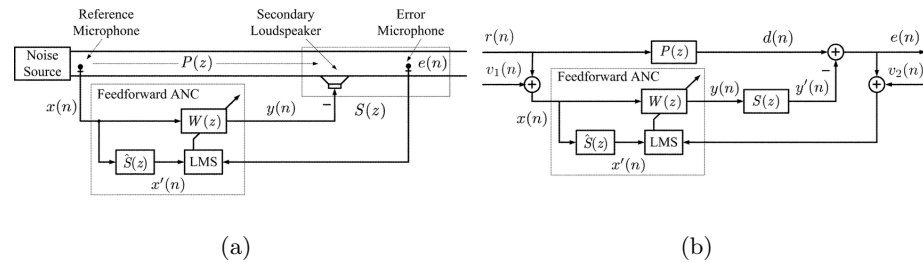


Fig. 2: FxLMS algorithm based single-channel feedforward ANC system. (a) Schematic and (b) block diagram. Figure taken from [9].

¹ In figure 2, please note $\hat{S}(z)$ is the aforementioned filter added by Dennis R. Morgan.

² The path the sounds travels between the secondary source, where the antinoise is produced, and the error microphone, where the cancellation has to be realised.

1.1 Characteristics of the siren’s signal

The siren noise presents non-trivial characteristics, in the context of ANC, as it is non-stationary, although periodic, and presents several high-frequency components in its spectral content. Also the siren sound is fast-changing between two different *pitch sounds*, which introduces challenges in and on itself when those switches occur.

Following the Italian regulations on the matter, therefore the siren in this study produces two distinct sounds by emitting two different *pulse waves*, one with a lower pitch at the fundamental frequency of 390Hz (figure 3a), and one with an higher pitch at 660Hz (figure 3b). Figure 3 shows the siren signal reconstructed by measuring the actual output of a typical siren marketed in Italy.

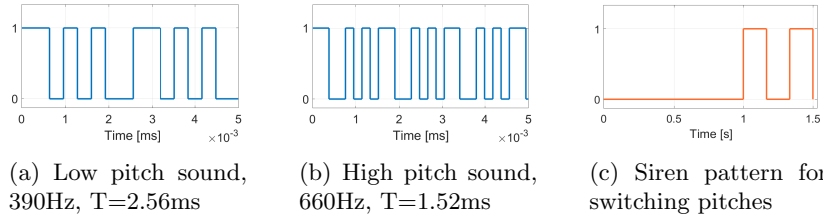


Fig. 3: Siren’s component pulse waves in the time domain.

These two pulse waves can each be generated with a series of 3 impulses, having periods of 2.56ms and 1.52ms respectively, with varying duty cycles and appropriate delays (the parameters for both pulse waves can be seen in table below). The siren then alternates between these pulse waves in a pattern described in figure 3c, where the low-level (or 0) is to be interpreted as the time when the siren is *playing* the low pitch sound, and high-level (or 1) when the high pitch is played instead. This pattern repeats periodically every 1.5s. Finally, the spectrum of both those individual pulse waves is shown in figure 4.

Table 1: Parameters to generate the 390Hz and 660Hz pulse waves

		f=390Hz: pulse1, pulse2, pulse3			f=660Hz: pulse1, pulse2, pulse3		
T	[ms]	2.56	2.56	2.56	1.52	1.52	1.52
delay	[ms]	0	0.96	1.6	0	0.76	1.14
d.c.	[%]	25	12.5	12.5	25	12.5	12.5

The most significant harmonics of the 390Hz pulse wave are 780, 1170, 1560, and 1950Hz. For the 660Hz pulse wave we have 1320, 1980, 2640, and 3300Hz.

2 Building blocks to reduce real siren noise

The intention with this study was to test cancelling algorithms in a laboratory setting, using a real-time target hardware to produce the adaptive control signal.

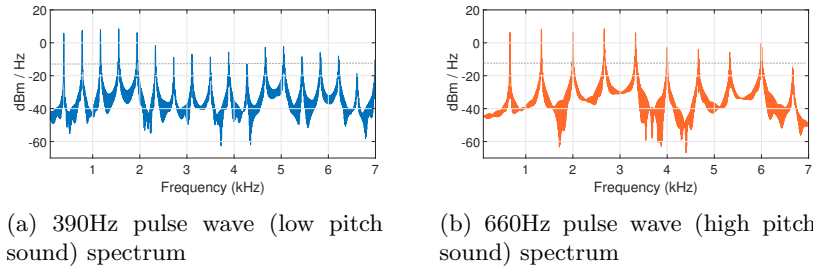


Fig. 4: Siren component signals in the frequency domain.

With a long-term goal of cancelling the siren inside a real ambulance, here the first steps towards the cancellation of a synthetic siren are presented; these are progressively achieving cancellation of: 1) Pure sinusoidal tones at increasing frequencies 2) Square waves at the same fundamental frequency as the siren pitches 3) Both pulse waves, components of the real siren as presented in section 1.1, individually tested.

This objective was chosen as the steps above are considered preliminary to then move toward the real scenario where the system will be optimised to cancel the real fast-changing siren signal.

3 Setting up the laboratory experiment

For our experiments, all noises were internally generated by the target computer and emitted via loudspeaker. The components of the systems under test: Speed-goat Performance Real-Time Target Machine, running Simulink Real-Time, PreSonus DIGIMAX FS, mic. amplifier, Behringer ECM8000 condenser microphones, custom-built audio amplifier and speakers, and Haztec 8-82414 EuroSmart siren³

Cancellation was tested on two different setups: *single channel*, where one control speaker generates the antinoise to cancel the noise from the primary source, and *dual channel*, where two control speakers⁴, are used (see figure 5).

A series of tests were conducted using different noise sources, starting with simple sinusoidal tones at increasingly high frequency, then using square waves, and finally the siren's individual pulse waves, which were synthesised⁵ to replicate the real siren sounds, and then emitted by a loudspeaker functioning as primary noise source, in place of the actual siren.

No reference microphone was placed in front of the primary source, but the noise signal was instead connected directly as an input into the target machine. Since this will be possible in the real ambulance scenario too, as the siren's

³ Used to study the siren signal, which was then synthesized.

⁴ Placed at the distance simulating the ambulance driver's headrest, with two error microphones placed in such a way to simulate the location of the driver's ears (the target area for our cancellation, *ZoS*)

⁵ Internally generated by our target computer.

electronic hardware can be accessed, this represents a promising *solution* for the future working system aboard the ambulance, saving on hardware, but moreover, highlighting that even though the sound is complex, we can have exact real-time information about the siren signal.

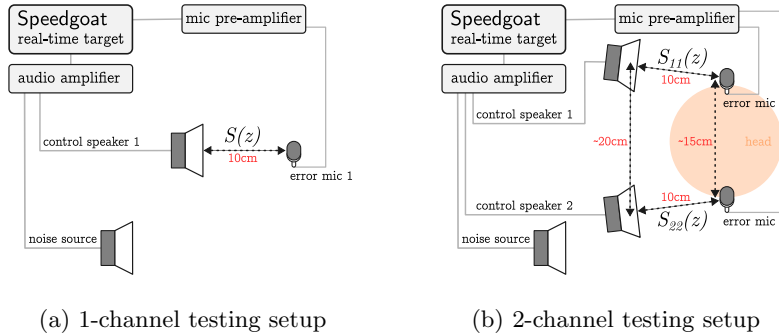


Fig. 5: Please note that the only distance that once chosen should remain fixed is the distance between error mics and control speakers (the secondary paths $S(z)$, $S_{11}(z)$, and $S_{22}(z)$). In figure 5b the secondary paths between speakers and the mic not directly in front of it (i.e. between speaker 1 and error mic 2) are not taken into account as their effect are negligible. The primary noise source can be freely placed a few meters from the ZoS .

Once all sensors were set in place, the secondary acoustic paths were estimated; this process generates a set of coefficients that will be then used to initialise an FIR filter $\hat{S}(z)$ ⁶ which approximates the transformation the sound undergoes by travelling through the air once emitted by the control speaker to the error microphone, $S(z)$.

4 Experimental results

Here the outcomes of our tests are presented, showing the spectra of the signals detected by the error microphones with and without the ANC system generating the antinoise (*ANC ON* and *OFF* respectively) for all the combinations of noise source under test configuration. In **figure 6** the 1-channel sine waves experiments are collected, in **figure 7** the 1-channel square wave ones, and in **figure 8** the 1-channel experiments with pulse waves. For the 2-channel configuration, only the results with sinusoidal tones are presented in **figure 9**, because no significant cancellation was obtained for the more complex signal with this setup.

In terms of individual frequencies, up to 3.6kHz noise cancellation was obtained with pure sinusoidal tones, which is within range of the five more significant harmonics of both siren’s pulse waves, hence the choice; consistent can-

⁶ As shown in figure 2 the additional filter is to be applied at the reference signal $x(n)$, coming directly from the siren in this case.

cellation between 36–86dB for all sine waves in the 1-channel setup (figures 6a to 6f), and similarly consistent cancellation between 31–70dB for the 2-channel setup (figure 9) was measured, which is considered to be very good performance for the system in exam.

When cancelling square waves, the system performed well for the 390Hz wave, cancelling the first three harmonics between 32–56dB (figure 7a), but with the 660Hz square wave the cancellation performance was more modest, in the range of 4–5dB (figure 7b), already showing signs of the limits of our system.

When the system was challenged with cancelling pulse waves, considering the first 6 harmonics, the 390Hz pulse wave saw a cancellation between 3–38dB (but most of it on the third harmonics only, see figure 8a), whereas the 660Hz pulse wave saw almost no cancellation (figure 8b).

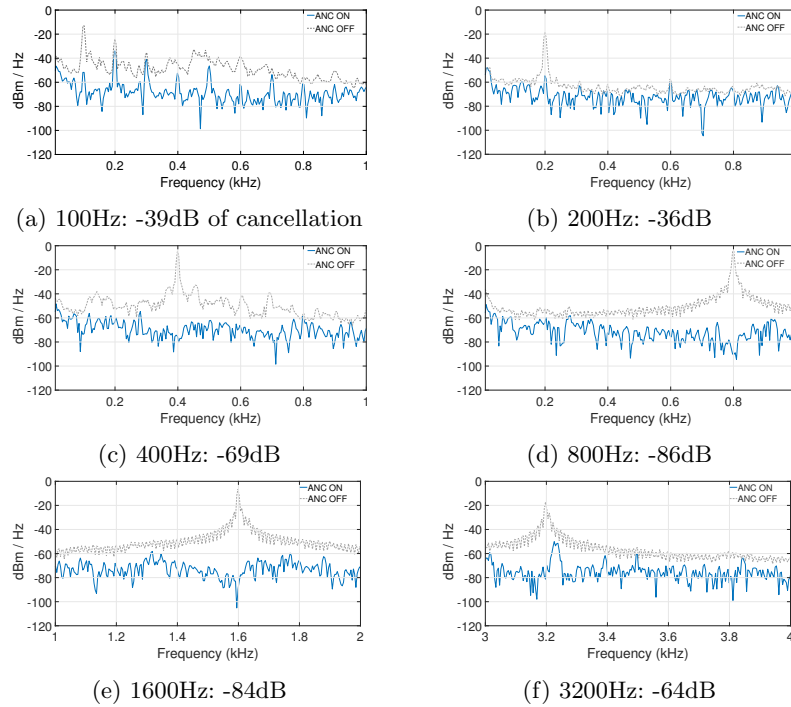


Fig. 6: 1-channel configuration with sinusoidal tones, or sine waves.

(Figures with experimental results continue at the end of section 5 *)

5 Conclusions

The use of the FxLMS algorithm is a well-established technique in active noise control applications, suited for reducing the sound of ambulance sirens. Such noise is proven challenging for the FxLMS algorithm. Therefore it seems that, overall, the feedforward ANC system based on the FxLMS algorithm variation presented here, is capable of cancelling signals that are *regularly changing with respect of time*, no matter how fast (within the ranges of our tests); but that same system cannot perform as well when signals behave in a less regular pattern in the time domain. Difficulties to latch onto the phase of the pulse and square waves is believed to be the cause of this system’s declining performance. This could be mitigated by upgrading the DSP component, devising a faster performing target hardware, custom-built to operate with the signals in question.

Finally, the ANC system had difficulties updating the cancellation adaptive filter in the short time allowed by the fast-switching siren⁷, but since we see promising results on the individual sounds of the siren, especially on the low-pitch one, and since we also believe that with the aforementioned hardware improvements we could obtain better performance for the high-pitch pulse wave as well, we believe it could be theoretically plausible to employ a set of individual ANC filters in parallel, each operating over a specific pulse wave/siren sound, and switch between them appropriately, to cancel the real siren, if the system would be able to correctly latch onto the phase of the siren’s signal.

(* continuing figures with experimental results)

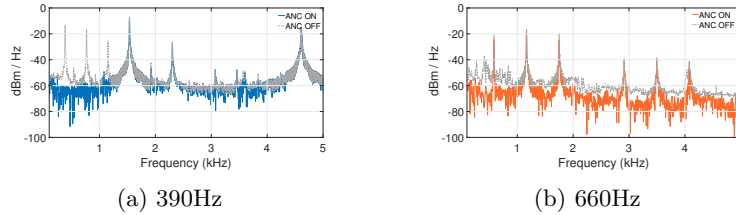


Fig. 7: 1-channel square w. harmonic canc. [Hz],[dB]. a: 390,-56, 769,-43, 1158,-32 1532,0 1921,-4 2305,0 ; b: 660,-4 1166,0 1749,-5 2911,0 3494,0 4077,-1

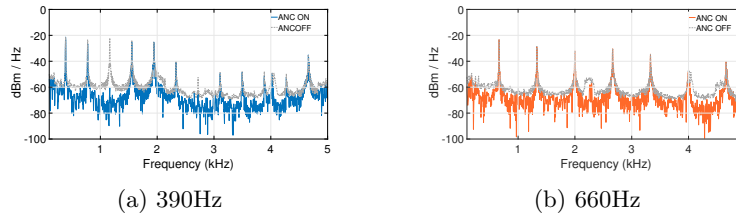


Fig. 8: 1-channel pulse w. harmonic canc. [Hz],[dB]. a: 390,0 775,-3 1166,-38 1554,-2, 1941,0, 2333,0 ; b: 660,0 1330,0 2000,0 2665,0 3330,0 3995,-2

⁷ bringing the overall behaviour towards instability

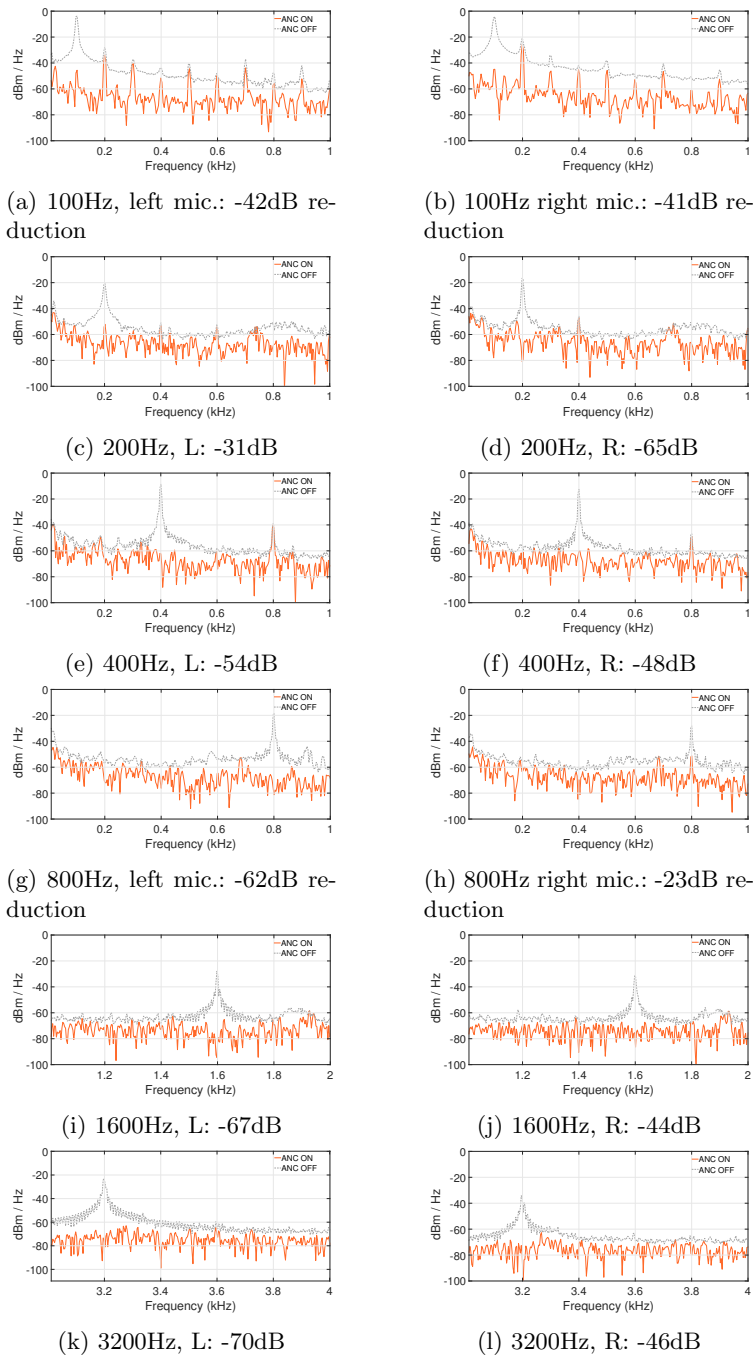


Fig. 9: 2-channel configuration with sinusoidal tones, or sine waves

Acknowledgement

The publication was made by a researcher with a research contract co-funded by the European Union - PON Research and Innovation 2014-2020 in accordance with Article 24, paragraph 3a), of Law No. 240 of December 30, 2010, as amended and Ministerial Decree No. 1062 of August 10, 2021.

References

1. Ardekani, I.T., Abdulla, W.H.: FxLMS-based active noise control: A quick review. In: Proceedings of Asia-Pacific Signal and Information Processing Association Annual Summit and Conference, vol. 1, pp. 1–11. Xi'an, China (2011)
2. Buttarazzi, M.G., Bartalucci, C., Borch, F., Carfagni, M., Paolucci, L.: Analysis of Possible Algorithms for Active Noise Control of Siren Noise into an Ambulance. In: International Conference on Design, Simulation, Manufacturing: The Innovation Exchange, pp. 630–640. Cham: Springer International Publishing, Rome, Italy (2021)
3. Widrow, B., Stearns, S.D.: Adaptive Signal Processing. Prentice-Hall Signal Processing Series, Upper Saddle River, New Jersey, USA (1985)
4. Kuo, S.M., Morgan, D.R.: Active Noise Control Systems Algorithms and DSP Implementations. Wiley, New York, USA (1996)
5. Singh, S., Sharma, M.K., Agrawal, S.: Ambulance siren noise reduction using psychoacoustic active noise control system with A-weighting filter. In: International Conference on Computing, Communication & Automation, pp. 990–993. Greater Noida, India (2015)
6. Pal, R., Sharma, M.K., Thangjam, S.: Ambulance Siren Noise Reduction Using Virtual Sensor based Feedforward ANC System. In: Proceedings 2nd International Conference on Advances in Computing and Communication Engineering, Dehradun, India (2015)
7. Gupta, P., Sharma, M.K., Thangjam, S.: Ambulance siren noise reduction using noise power scheduling based online secondary path modeling for ANC System. In: International Conference on Signal Processing, Computing and Control (ISPC), pp. 63–67. Wanknaghat, India (2015)
8. Sharma, M.K., Vig, R.: Ambulance Siren Noise Reduction using LMS and FXLMS Algorithms. Indian Journal of Science and Technology **9**(47), 1–6 (2016)
9. Akhtar, M.T., Abe, M., Kawamata, M.: Adaptive filtering with averaging-based algorithm for feedforward active noise control systems. In: IEEE Signal Processing Letters, vol. 11, no. 6, pp. 557–560 (2004)

Ambulance Siren’s Active Noise Cancellation: Reference Synthesis and Switching FxNLMS on Real-Time Target Hardware

Massimo G. Buttarazzi^[0000–0002–9819–3378], Francesco
Borchi^[0000–0002–3569–313X], Alessandro Mambelli^[0009–0002–7938–677X], Monica
Carfagni^[0000–0002–3393–7014], Lapo Governi^[0000–0002–7417–3487], and Luca
Puggelli^[0000–0002–5352–9624]

Department of Industrial Engineering, University of Florence
via S. Marta, 3, Florence

Abstract. An Active Noise Control method is presented for selectively reducing the harmonic content of an ambulance siren. Based on the FxNLMS feedforward algorithm, two developments are presented: 1) *Reference Synthesis*, for those cases where the noise to be cancelled is perfectly known, it is demonstrated that the reference signal can be generated by the cancelling hardware, without the need to employ reference microphones nor connecting to the noise source; 2) *Switching FxNLMS*, the implementation of separate banks of adaptive filters is presented to individually cancel two alternating components of a bitonal siren, as if they were two independent stationary noises. Demonstrations of the working principles are presented through tests carried out with a synthesised version of the real siren as a noise source, and real-time target hardware mounted on a headrest, in laboratory environment. Results and performance of these combined techniques for cancelling a complex but perfectly known noise signal are presented, and in conclusion further studies, improvements and potential applications are discussed.

Keywords: Active Noise Control ANC · Feedforward FxNLMS Algorithm · Ambulance Siren Noise · Reference Synthesis · Switching FxNLMS · Real-time Hardware Test

1 Introduction

The work in this paper represents the direct continuation of [1], in which a *feed-forward, normalised, Filtered-x Least Mean Square Algorithm* (FxNLMS, section 1.1) Active Noise Control (ANC) system had been implemented on a real-time target machine, and tested against a series of noise signals of increased *complexity*, with the ultimate goal of reducing the noise of a real ambulance’s siren. A signal is considered complex if it posses one or both of the following characteristics: in the time domain, if it switches rapidly between two or more distinct noise

patterns; in the frequency domain, if it has a wide spectrum with significant mid frequency components¹ that need to be reduced.

In that previous study, tests ranged from evaluating the cancellation of pure sinusoidal tones, until finally it was attempted to cancel the two alternating *stationary* signals that constitute the siren of an Italian ambulance (more on this in section 3). By the results obtained it was concluded that the complexity of the signal was the limiting factor for the cancellation performance, because the same FxNLMS algorithm, running on the same hardware, was successful in effectively reducing simpler noises, but was failing to do so with the ambulance's siren. Based on those conclusions, the improvements that are the subject of this work were identified, and will be introduced in section 2, 4 and 5.

1.1 Background on Feedforward FxNLMS

The basic principle of ANC is predicated on the adaptive generation of a so called *antinoise* having opposite phase and appropriate amplitude with respect to the noise signal that needs cancelling, done in such a way that the two signals will interfere with one another in a destructive manner, creating an attenuation to the sound levels in a specific area of interest, called *zone-of-silence* (ZoS), where noise reduction can be experienced. The fundamental theory of ANC can be retraced from [2] and [3], and was also previously summarised in [1].

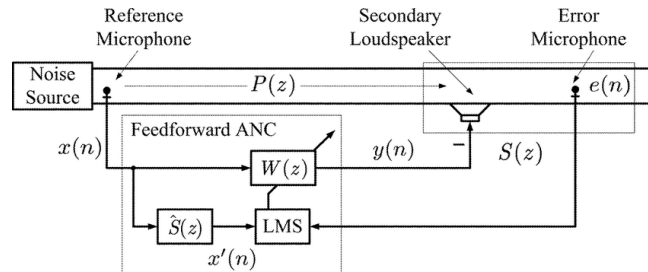


Fig. 1: FxLMS algorithm for a single-channel feedforward ANC system. Figure taken from [10].

In figure 1 the fundamental signals and ANC components are defined: $P(z)$, primary acoustic path between the noise source and *ZoS*; $S(z)$, secondary acoustic path, between the control source producing the antinoise and *ZoS*; $e(n)$, residual error to be cancelled, captured by an error microphone; $\hat{S}(z)$, the digital FIR filter² that replicates the transformation occurring to the control antinoise as it

¹ In this context, between 500–2000Hz.

² Usually the coefficient for this filter are estimated once, then provided that the relative position between control speaker and error microphone doesn't change, this filter is not modified.

travels between the control source and the error microphone; $W(z)$ the ANC filter, also implemented with a digital FIR filter, whose coefficients are adapted in real time in order to minimise $e(n)$.

FxLMS is a well suited technique for an ANC system that deals with siren noises, as proven by [4] and [5]; in particular, the feedforward variation was chosen because a reference signal³ is available directly from the noise source and also because the siren has a limited-bandwidth spectrum, as demonstrated also by [6] through [9].

As mentioned before, for this study the implemented algorithms are of the normalised variant, *FxNLMS*, which means that the step size parameter, μ used to regulate the speed of convergence of the LMS update adaptive filter $W(z)$ is made to dynamically and proportionally adjust to the energy of the reference signal, to mitigate adverse effects on the algorithm convergence due to large fluctuations of the energy levels of the reference signal itself.

In summary, from a practical standpoint, noise cancellation with FxLMS-type algorithms is essentially based on defining two digital FIR filters, $\hat{S}(z)$ that recreates the secondary acoustic path $S(z)$, whose coefficients are calculated once and unless the error microphone is moved will stay the same, and the ANC FIR digital filter $W(z)$, whose coefficients are constantly adapted in real time during the LMS optimisation process, with the objective to minimise the sound pressure at the error microphone.

2 Contribution proposed

Two directions for improvement over the previous FxNLMS implementation in [1] were identified and have been implemented and tested in this paper: first, an attempt to reduce the complexity of the reference signal, second, an attempt to improve hardware's capacity to work with fast-changing *known* signals.

Simplified reference signals tested against real noise

For complexity reduction, it was attempted to cut the spectral components of the reference signal that the ANC system would have to work with. The rationale being attempting to provide an input signal to the adaptive ANC block⁴ that, because of the reduced harmonic content at high frequency, would be smoother to track, giving the hardware more time to compute the adaptation necessary for cancellation (i.e. the cancellation coefficient for the $W(z)$ FIR filter).

At first it was attempted to use digital low-pass filters, but it proved to be computationally burdensome, impeding on the expected gains, so it was decided

³ Signal that is necessary for the adaptive cancelling system to track what noise it needs to cancel.

⁴ Block meaning the combination of the LMS adaptive update block and its following cancellation FIR filter, as well as the secondary path's FIR filter through which the reference signal passes before being input to the LMS block.

instead to rely on the *perfect knowledge* of the noise signal (presented in detail in section 3), to devise a system that would *internally* generate a simpler reference signal that would match the most significant harmonics of the real noise. This idea was tested in a real scenario, that is cancelling the actual full spectrum noise generated by a primary noise source as captured by an error microphone. This technique was named *Reference Synthesis* and it is further described in section 4.

Parallel ANC filtering to reduce siren to stationary noise

The problem with fast-changing signals is not only one of computational performances, but most importantly in this context, is considering the effect they have on how much time an ANC block is given to converge before the noise signal changes, abruptly in case of a siren, and therefore requires the adaptation process to follow suit (section 5 for details).

Two solutions have been implemented to mitigate the above: first, a custom-built electronic board⁵ has been used for noise control; second, but more interesting in terms of innovation, the ANC block was split into two parallel blocks, each of them tasked to cancel only one of the two alternating signals composing the bitonal siren noise, in order to ensure that each adaptive filter would see as an input to be cancelled a simpler *stationary signal*.

This was achieved by having the control algorithm alternatively activating the relevant cancellation filters depending on what pattern of the bitonal siren noise was actually being produced by the primary noise source at any given time (see section 3). This technique was named *Switching FxNLMS*, and it is described in section 5.

3 Deconstruction and synthesis of siren's signal

In [1] the characteristics of the same bitonal siren's signals also used in this paper were first presented, as experimentally measured (figure 2); from those measurements the siren signal was deconstructed and then synthesised (figure 3); the main purposes and benefits have been the following:

1. The two *pulse wave signals*, of figure 3 composing the bitonal siren are *stationary noises*, unlike the periodic siren, so dealing with them independently greatly simplify the adaptation process;
2. The primary noise could be reproduced in a controlled fashion, one pulse wave at the time, using laboratory equipment.

⁵ Developed by an industrial partner, based on the high-performance STM32H7 microcontroller, it has two complete channels of audio processing, from microphone pre-amplification, to power audio output for two loudspeakers.

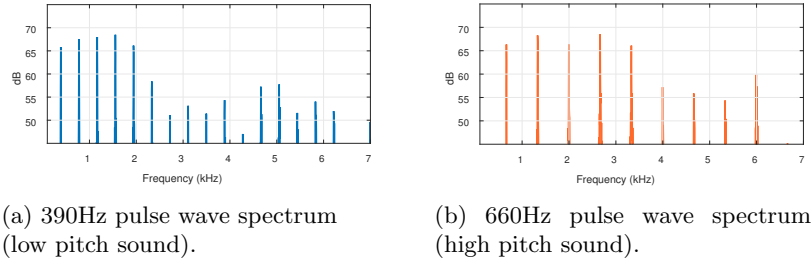


Fig. 2: Siren component signals in the frequency domain.

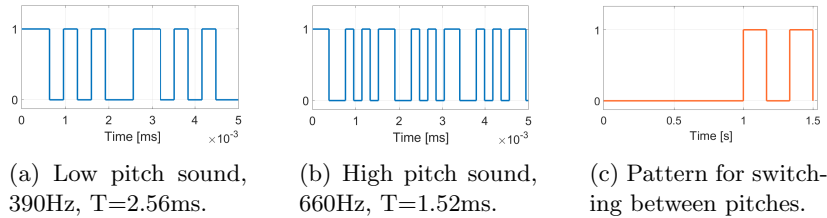


Fig. 3: Siren's component pulse waves in the time domain. In 3c, 0='siren plays the low pitch sound', 1='plays the high pitch sound'.

Selectivity and cancellation targets

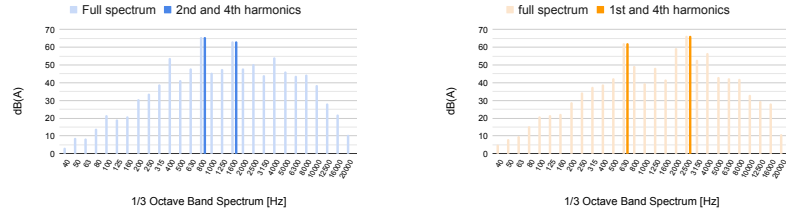
By measuring the spectra of 3a and 3b, using a calibrated *sound level meter* (details in section 6), it was confirmed that the largest contribution to the overall sound pressure level of each of the siren's pulse waves was attributable to 2 harmonic components, in particular: 1) **89.6% of the 390Hz** pulse train's sound level was produced by the **second and fourth harmonics** (780 and 1560Hz respectively, figure 4a); 2) **76.3% of the 660Hz** pulse train's sound level was produced by the **first and fourth harmonics** (660 and 2640Hz respectively, figure 4b).

On that basis, an approach was devised for obtaining satisfactory cancellation performances of the individual pulse waves composing the siren, by selectively tackling a reduced number of frequencies to be cancelled, the ones deemed to be contributing the most to the overall sound levels perceived by the human ear⁶.

4 Reference Signal Synthesis

This technique relies on having complete knowledge of the noise signal that needs cancelling, which is true in the case of a bitonal ambulance siren as demonstrated

⁶ This also means that the sound levels measured in this study have been subjected to A-weighting, to account for relative loudness perceived by the human ear, and it is reflected in measurements expressed in dB(A).



(a) 390Hz pulse wave's most significant harmonics, 2nd (780Hz) and 4th (1560Hz), highlighted over the whole spectrum.

(b) 660Hz pulse wave's most significant harmonics, 1st (660Hz) and 4th (2640Hz).

Fig. 4: Waves' spectra were measured with a sound level meter, so the exact frequency value is combined into discrete *one-third octave* bands.

in section 3. Even though we expect that in operating conditions the siren noise will be subjected to modifications, as the vehicle will be moving in a real environment, for the purpose of this study we propose to demonstrate the working principle under laboratory conditions, and defer to tackling those potential challenges in the next phase of development.

The proposed algorithm is a modified implementation of the FxNLMS that uses an internally generated *synthesised reference signal*, $x_s(n)$ created as a sum of a subset of the individual harmonics composing the original siren, and use such synthetic reference to feed the ANC block (see figure 5 for an example of using only the fundamental frequency of the noise). This algorithm therefore requires neither a reference microphone nor a reference signal directly derived from the electronics of the siren.

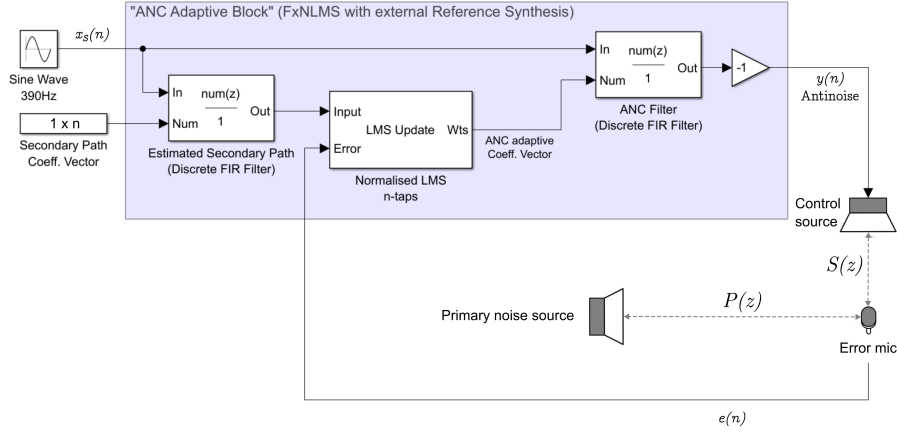
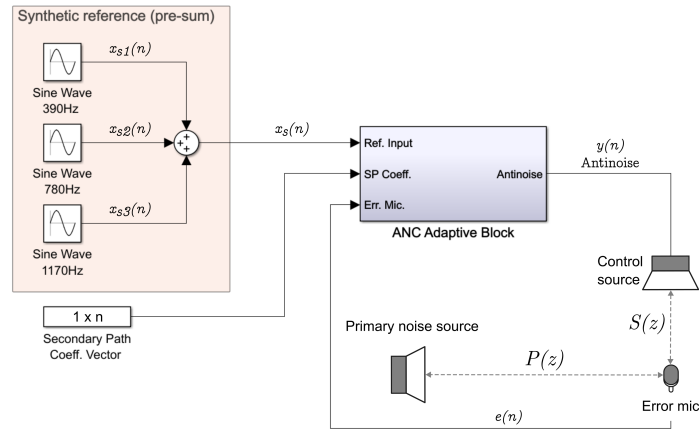


Fig. 5: Basic building block to generate a synthetic reference signal, $x_s(n)$, for a single harmonic at 390Hz. The Primary noise source plays the full-spectrum siren, generated by an independent hardware.

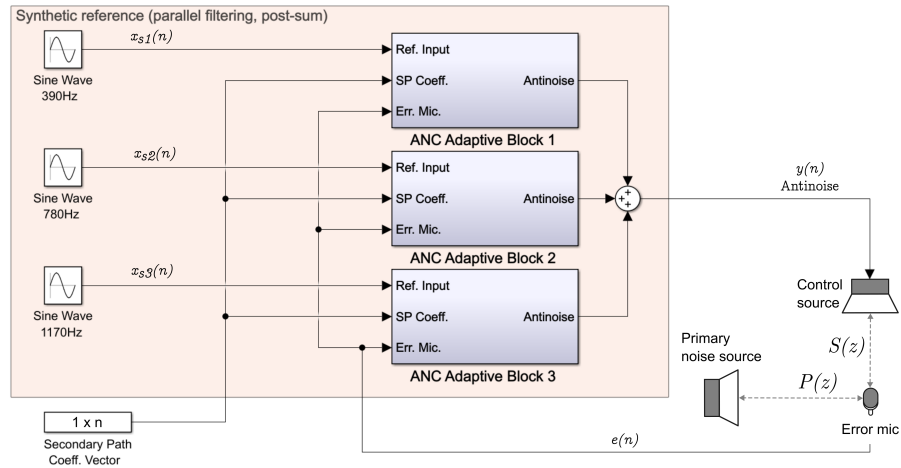
An independent loudspeaker is used as primary noise source, emitting the pulse trains of figures 3a and 3b generated by a computer⁷, rather than using a real siren, to be able to play individual pulse waves rather than the full siren when necessary, but also simply for ease of controlling the noise’s volume inside the laboratory. For testing purposes this is equivalent to using the real siren as the spectra are comparable and in neither configuration it is required to connect the siren to our control algorithm.

In its simplest form, the reference signal $x_s(n)$ is therefore a single sine wave at the fundamental frequency of the noise that needs cancelling, but to obtain a significant cancellation across the whole spectrum of a complex pulse train, as shown at the end of section 3, two or more sinusoidal component are needed; there are at least two ways of combining them: 1) adding them up before inputting the combined signal to a single ANC block (figure 6a) 2) replicating the same structure for each harmonic, de-facto parallelising the processing of each harmonic (figure 6b).

⁷ Unless differently specified, this is not the same control hardware, but a different computer. For the 2-channel configuration, the siren is in fact generated by the control hardware itself, for reasons explained at the end of section 5



(a) 1 ANC filter, 3 harmonics of signal reference summed before input.



(b) 3 ANC filter, antinoise contribution summed before output.

Fig. 6: Two approaches for synthesising a reference signal with multiple harmonics.

Even though the second method is perhaps less efficient, it proved to be working, and in fact at the time of writing it represented the only way to make the cancellation work during testing: whenever the harmonics were added together before being applied as a reference to a single LMS optimiser, the block would either become unstable, or it wasn't able to cancel. Further investigation into why this is happening is ongoing.

In essence, the Reference Synthesis is comparable to applying a low-pass filter to the reference signal $x(n)$, and provided that a finite number of harmonics are deemed capable of obtaining significant overall cancellation, it offers the following features and advantages:

- It provides the ability to precisely select the exact spectral components we aim to cancel, down to the single harmonic of a known noise;
- It requires no hardware to acquire a reference signal;
- It is computationally less intensive to generate sinusoidal waves, rather than having to implement digital FIR filters within the control algorithm to pre-process the reference signal.

In figure 7 is an example of the synthesised reference signals used for cancelling the first three harmonics of the 390Hz pulse wave; the amplitude of each sinusoidal component of the synthetic signal is considered of secondary importance, because of the adaptive nature of the cancellation algorithm which modifies that to obtain cancellation.

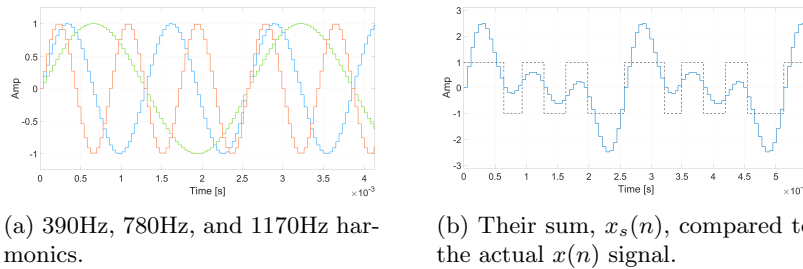


Fig. 7: Example of the first 3 harmonics used as synthetic reference signal for the siren’s 390Hz pulse train.

5 Switching FxNLMS

The Switching FxNLMS was devised starting from the realisation that whenever a single ANC adaptive FxNLMS system is employed with a fast-switching signal like the siren under consideration (figure 3), we are demanding the algorithm to very rapidly adapt the same set of FIR coefficients back and forth between *two otherwise stationary configurations*.

Such siren periodically repeats every 1500ms, of which the higher pitch (figure 3b) lasts only for two spikes of 166.66ms each (figure 3c), but crucially, the adaptive process will always optimise the same set of coefficients for the $W(z)$ filter, for both pitches; practically speaking, this is how the cancellation coefficients change during one periodic cycle:

1. For the first time segment (1000ms) the ANC block is adapting them to minimise the 390Hz pulse train of figure 3a;
2. For the next segment (166.66ms) it needs to complete the convergence of those *same coefficients* to now minimise an essentially new and different 660Hz pulse train;
3. For the next segment (166.66ms) it switches back to adapting them to minimise 390Hz;
4. For the last segment (166.66ms) it switches back to adapting them for 660Hz;

It then starts repeating the entire process from the beginning. The fact that both alternating optimisation happen on the same set of coefficients of $W(z)$ is believed to be the cause that leads to overall failure to cancel either of the siren's distinct pulse trains in [1], and even leads to system instability sometimes, as the block repeatedly tries to adapt to different noises in rapid succession.

But since it is known that both pulse trains taken independently are stationary noises, and that by employing Reference Synthesis cancellation of those individual pulse trains can be obtained (see section 7 for details), we can exploit this knowledge to devise a modification of the FxNLMS that would tackle the siren.

In fact, provided that we can design control algorithms independently capable of cancelling each of the two stationary pulse trains, by implementing two separate and independent ANC blocks, each with one FIR filter⁸ dedicated to one of the siren's pulse waves (i.e. $W_1(z)$ and $W_2(z)$ respectively for the 390Hz and 660Hz pulse trains), it was proven that we can obtain cancellation of the actual siren signal in real tests, as long as we can *track exactly when the siren is switching* between the two different pulse trains.

⁸ In the real implementation it is a bank of filters, as each individual harmonic is processed in parallel, but for the sake of explaining the concept, it could be assumed to have one ANC filter per pulse train.

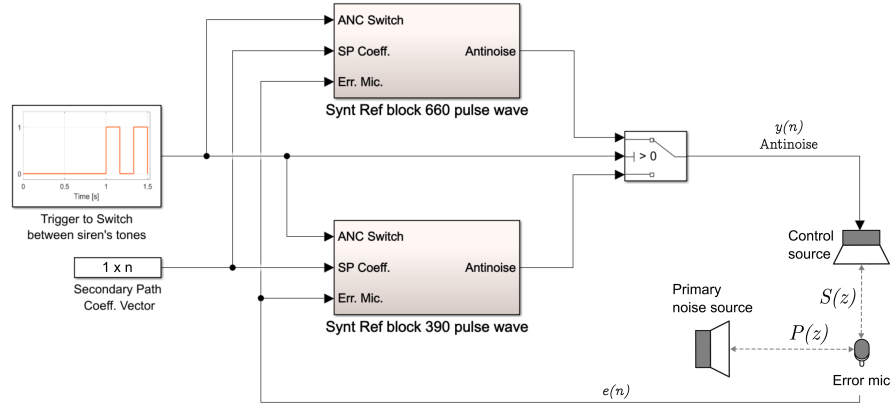


Fig. 8: Block diagram illustrating the Switching FxNLMS variation, where a trigger signal is used to synchronise the enabling of cancellation filter with the siren pattern (see again figure 3c).

To further prove the reason of the effectiveness of such solution, it is useful to take a closer look at the cancellation coefficients behaviour over time (figure 9), for both $W_1(z)$ and $W_2(z)$; there it is shown that when an ANC block is disabled, which happens while the noise produced by the primary noise source is not the one that that particular filter is designed to cancel, the adaptive convergence process for that filter is *suspended*, meaning the coefficient values remain untouched whenever the siren switches to the other noise pitch. This can be seen as having the algorithm simply switching to a parallel process that works independently on a different set of coefficients, which means the cancellation performance experienced with both stationary pulse waves taken on their own (section 7.1 and 7.2) is not negatively affected by the switching, and can in fact be combined to achieve overall cancellation of an alternating noise like the real siren.

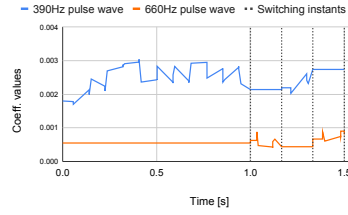


Fig. 9: Evolution of two ANC FIRs' coefficient, one for the 390 and one for the 660Hz pulse wave: while switching between the siren pitches, note that the convergence is suspended, not lost.

It is important to reiterate that for the Switching FxNLMS to work, the cancellation filters $W_1(z)$ and $W_2(z)$ need to be alternatively enabled/disabled by a trigger signal that precisely tracks the siren's pattern. For the tests presented in this paper, this has been guaranteed by generating the siren internally with the same hardware that runs the control algorithms. It is understood that a solution would be needed to synchronise the control board with the real siren, and ideas on how to detect those changes of pitch proposed in section 8.

6 Setting up the laboratory experiment

In this paper the focus was on implementing the control algorithm in a 1-channel configuration to demonstrate the working principle of the modifications proposed for the FxNLMS algorithm. Therefore one control speaker and one error microphone were used, as output and input of the control board, respectively. Figure 10 depicts the scenario:

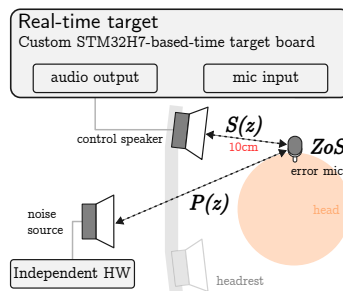


Fig. 10: General laboratory setup, used for results of sections 7.1 and 7.2. For the Switching tests, as explained in this section, the noise source was also connected to the real time target audio output. Primary and secondary acoustic paths, $P(z)$ and $S(z)$, as well as zone of silence, are highlighted.

A prototype of the driver’s headrest was used to mount the control speaker and the error microphone, which was placed in the vicinity of where the driver’s ear would be. A sound-absorbing obstacle was installed in place of where the head would be. The primary noise source was placed about 1m away from the headrest, but this parameter is of secondary importance, the system would work independently of this particular location.

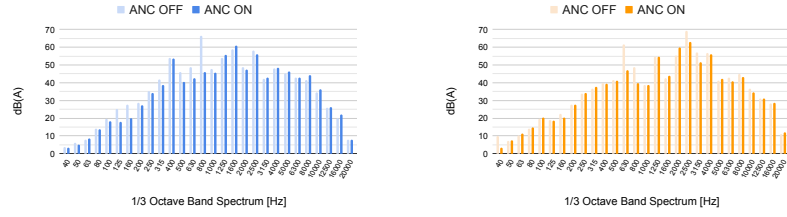
Only for the test where the full bitonal siren was to be cancelled (figure 12) the siren was generated by the same target machine running the control algorithm, because as already introduced in section 5, the switching algorithm needs to be synchronised with the siren alternating between the two pulse waves. For all the other tests, the noise was generated by an independent hardware and played by the primary noise source, but still synthetically reconstructed, to enable the reproduction of the individual component of the siren independently.

To carry out measurements of the signals’ spectra, to verify the noise cancellation at the specific location (*ZoS* near the ear position in the headrest), a precision class 1 measurement chain was used, consisting of a noise signal analyser equipped with a pre-amplifier and pre-polarized class 1 precision capacitive microphones. In order to account for human perception of relative loudness, all results of such measurements have been weighted using the A-weighting curve and are therefore presented as dB(A).

7 Experimental results

The most important result of the experiments has been to demonstrate that approximately 4.5dB(A) of cancellation can be obtained across the entire spectrum of both of siren’s pulse waves, taken independently, by employing selective harmonic cancellation, using an internally synthesised reference signal, working with a 1-channel configuration, as shown in figure 11, therefore demonstrating the effectiveness of FxNLMS with *Reference Synthesis*.

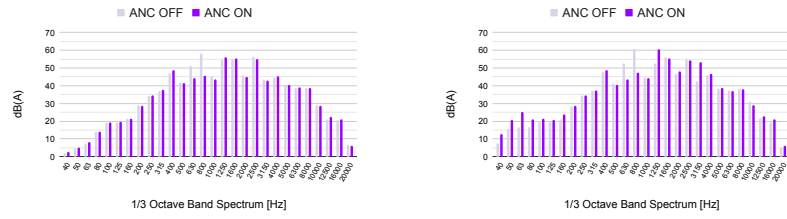
Equally important has been to demonstrate that we could combine the results of the individual pulse waves composing the siren to get the system to cancel the full siren itself in real time, of approximately 2dB(A) across the entire spectrum, as presented in figure 12a, by only cancelling 1 harmonic component for each pulse wave, therefore demonstrating the effectiveness of the *Switching FxNLMS* algorithm. In figure 12b we present the results of cancelling two major contributions for each pulse waves, which turned out to provide worse overall cancellation, but further investigation is necessary to understand this counterintuitive result.



(a) 390Hz pulse wave, cancelling 780Hz and 1560Hz harmonics: 4.2dB(A), over the full spectrum.

(b) 660Hz pulse wave, cancelling 660Hz and 2640Hz harmonics: 4.7dB(A), over the full spectrum.

Fig. 11: Noise reduction over the full spectrum, for each pulse wave composing the siren, obtained by selectively cancelling the most significant harmonics, as identified in section 3.



(a) 2^{nd} harmonic for 390Hz pulse wave (12.8dB(A)), 1^{st} for 660Hz (6.1dB(A)): 1.9dB(A) over the full spectrum.

(b) 2^{nd} and 4^{th} for the 390Hz (13.3dB(A) and (0.8dB(A)) respectively), 1^{st} and 4^{th} for 660Hz (8.8dB(A) and (0.8dB(A)) respectively): 0.4dB(A) over full spectrum.

Fig. 12: Siren reduction over the complete spectrum (in bracket the cancellation over each single harmonic) using the full Switching FxNLMS with Reference Synthesis.

Results of figure 11 were obtained with the FxNLMS algorithm implemented with Reference Synthesis, running the control on a custom target board based on the STM32H7 microcontroller, programmed using Simulink. The model was running at the sample frequency of 17,160Hz, each of the cancellation filters was of the 10-th order (10 taps) for the individual pulse waves, and the ANC filters were built in the parallel configuration shown in figure 6a.

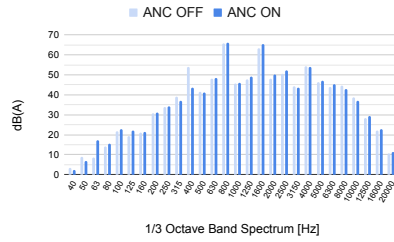
Whereas results of figure 12 were obtained with the full Switching variant of the FxNLMS, using 8-th order ANC filters with the same Reference Synthesis configuration as above, with the control algorithm running on the same hardware, but this time the siren noise was also internally generated and reproduced

by the control hardware via a primary speaker connected to the target hardware's output, to ensure the switching of the control was synchronised with the switching of the alternating siren's tones.

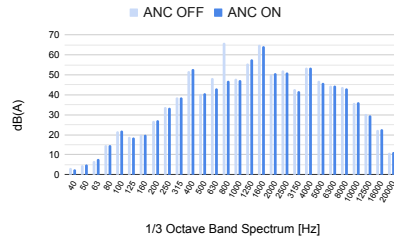
In the following sections results will be presented for more combination of experiments, and in order to better highlight the ability of the proposed Reference Synthesis technique to selectively cancel specific harmonics, another set of results will also be presented, where cancellation is shown on a frequency by frequency basis, rather than over the full spectrum; as calculated via fft processing using a digital spectrum analyser within the Simulink environment; such results are expressed in dB, rather than dB(A).

7.1 390Hz pulse train, 1-channel

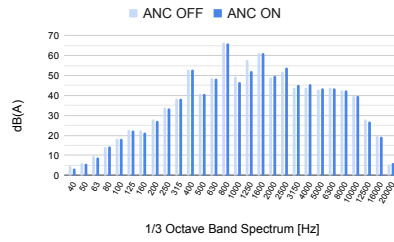
In figures 13 and 14 cancellation results of the 390Hz pulse wave are shown. It is systematically proven that FxNLMS with Reference Synthesis can selectively reduce individual components, by choosing which frequencies to provide as reference signal $x_s(n)$. The test configuration is the same of the experiments presented in figure 11. Figure 13 displays results measured using a sound level meter, whereas figure 14 displays the cancellation measured on the single harmonics the Simulink's spectrum analyser, for sake of comparison.



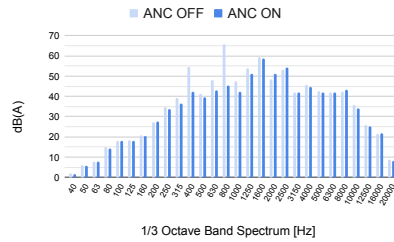
(a) 390Hz pulse wave, 1st harmonic cancellation: 10.5dB(A).



(b) 2nd harmonic, 780Hz: 19dB(A).



(c) 3rd harmonic, 1170Hz: 2.7dB(A). Also note that the adjacent frequency band is reduced by 5.6dB(A).



(d) 1st, 2nd and 3rd harmonic (individual cancellation 12.3dB(A) 20.5dB(A) 5.2dB(A) respectively), 6dB(A) cancellation over full spectrum.

Fig. 13: Noise reduction over the individual components, selectively cancelling harmonics of the 390Hz pulse wave (low pitch component of the bitonal siren), from measurements obtained with the sound level meter.

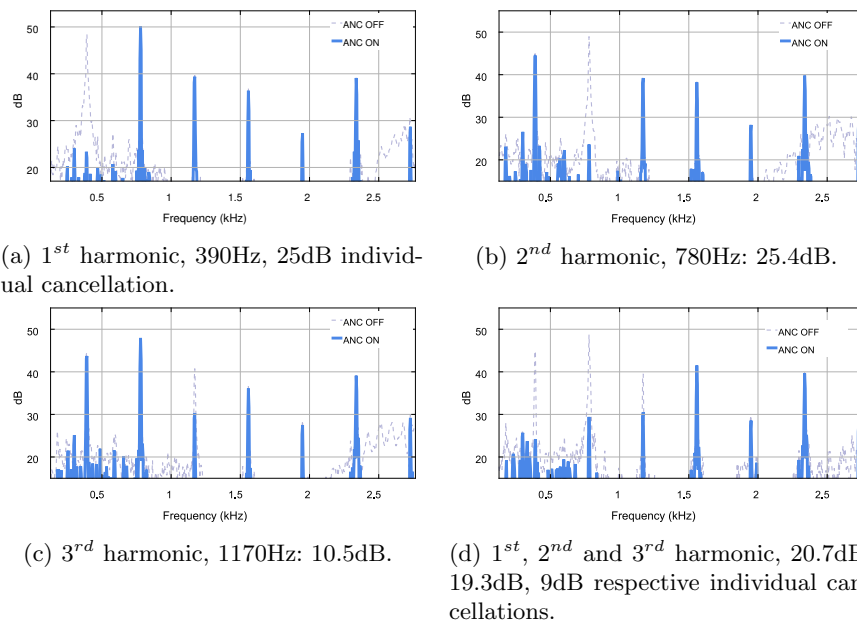
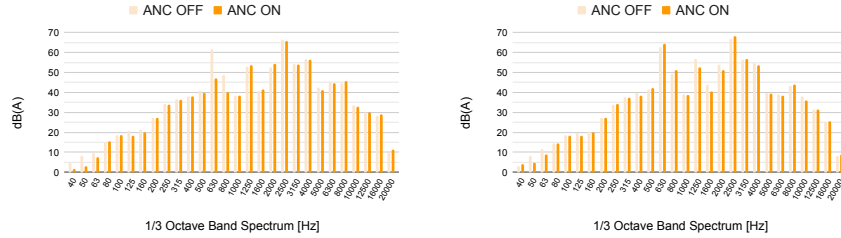


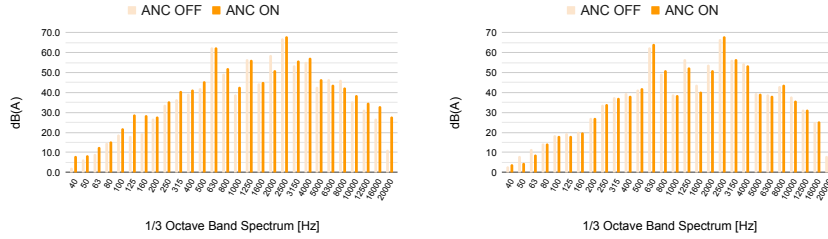
Fig. 14: Noise reduction of individual harmonic components of the 390Hz pulse wave (low pitch component of the bitonal siren) selectively cancelled, measured with Simulink's spectrum analyser.

7.2 660Hz pulse train, 1-channel

Analogously to the section above, figures 15 and 16 show the results of the individual 660Hz pulse wave cancellation.



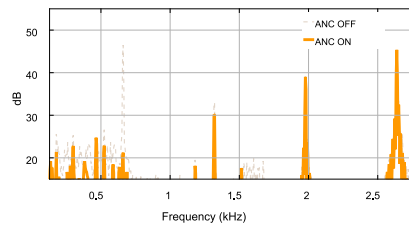
- (a) 660Hz pulse wave, 1st harmonic cancellation: 14.5dB(A). Also note that the adjacent frequency band is reduced by 8.7dB(A).
- (b) 2nd harmonic, 1320Hz: 4dB(A). Also note that the adjacent frequency bands are reduced by 3.4 and 2.5dB(A).



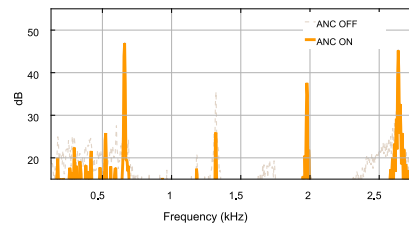
- (c) 3rd harmonic, 1980Hz: 7.9dB(A).
- (d) 1st, 2nd and 3rd harmonic (individual cancellation -1.6dB(A) 4.0dB(A) 7.6dB(A) respectively), -0.6dB(A) cancellation over full spectrum.

1

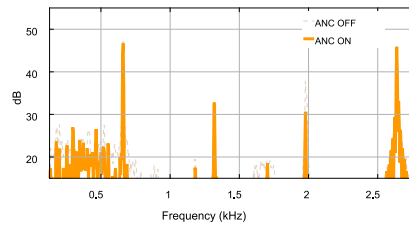
Fig. 15: Noise reduction over the individual components, selectively cancelling harmonics of the 660Hz pulse wave (high pitch component of the bitonal siren), from measurements obtained with the sound level meter.



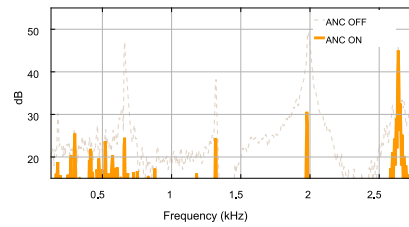
(a) 1st harmonic, 660Hz, 25.3dB individual cancellation.



(b) 2nd harmonic, 1320Hz: 9.9dB.



(c) 3rd harmonic, 1980Hz: 6.3dB.



(d) 1st, 2nd and 3rd harmonic, 22.6dB, 14.2dB, 18.1dB respective individual cancellations.

Fig. 16: Noise reduction of individual harmonic components of the 660Hz pulse wave (high pitch component of the bitonal siren) selectively cancelled, measured with Simulink's spectrum analyser.

8 Conclusions

We wanted to overcome the poor cancellation performance we experienced with complex noises (fast and with long spectrum).

The goal of the work presented in this paper was to improve on a previous implementation of FxLMS to cancel an ambulance's siren noise using real time hardware. Two developments to the classic FxNLMS algorithm are proposed and are proven to be achieving the cancellation task: 1) *Reference Synthesis* is applied to internally generate a smoother reference signal that is proven to allow for selective cancellation of harmonic content of a known noise; 2) *Switching FxLMS* is applied to be able to cancel a complex noise that alternates between two otherwise stationary noise-components.

Both techniques are showing promising results, in deleting single harmonics up to around 25dB in some of the presented configuration, for the individual harmonic cancellation, and obtaining cancellation of the order of 5dB across the whole spectrum of both pulse wave signals under test (the 390 and 660Hz components of the bitonal siren pitches).

The real time siren noise is also proven to be cancelled, in the vicinity of the error microphone, in real time, provided that the Switching FxNLMS algorithm is synchronised with the siren, following the alternating pattern of the low and high pitch sound.

Future development

With the ultimate intention of having the noise cancelling system installed aboard an actual ambulance, it is foreseen to further develop the control board in order to *have two dedicated microcontrollers*, one for each channel of the stereo cancellation, installed on an active headrest; each microcontroller will therefore drive one control speaker with one error microphone. This will also allow the generation of more synthetic harmonics as reference signal, since the hardware will double its current capacity, allowing for more broad noise cancellation, which was currently limited by the amount of FIR filters the algorithm was capable of supporting, in terms of real time computation capacity. What is more, having two independent, and simpler, 1-channel ANC blocks had also been identified as an option since, during tests, it was evident that the cross-secondary paths⁹ were contributing very little to the cancellation performance, likely because of the presence of the obstacle (head) in between the channels, reducing the acoustic cross-interaction to almost zero.

Reference Synthesis technique will require further studies to better define how to best implement the creation of the reference signal itself: even though parallel ANC filters were effective in cancelling the noises in the presented tests, it would be ideally better if it were possible to reduce the overall number of adaptive filters needed. This is also necessary because ultimately we should aim

⁹ The two acoustic paths between control speaker 1 and error microphone 2, and control speaker 2 and error microphone 1.

to cancel 5-6 harmonics per pulse wave, and currently the system is not capable of doing so in a reliable fashion, so improvements and optimisations are necessary to be able to create a successful practical implementation of the technique here presented.

Switching FxNLMS technique will require to devise a way to extract the trigger signal from the siren itself, either from the hardware of the siren itself, or by pre-processing the siren signal in order to extract the required information (when is the siren switching between the low and high pitch, and vice versa). Both options could be comprised of both a hardware and software component to be added to the system used in this paper.

The cancellation measured in the test here presented was localised in the vicinity of the error microphone. Especially for higher frequency components, this is very evident, so for a system that could work on board of an ambulance, *the ZoS must be expanded*, the presence of physical microphones in the vicinity of a driver's ear is not feasible for health & safety and comfort reasons, so a *virtual microphone solutions* should be implemented in order to install the error microphones safely within the headrest. Having an array of virtual microphones could potentially help to also solve the expansion of *ZoS*, but this will require more investigating.

Finally, once the algorithm would satisfy all the above proposal, it could be implemented with a lower level programming language, to *optimise the code* running on the target hardware and this is believed to further help in improving cancellation performances.

Acknowledgement

The publication was made by a researcher with a research contract co-funded by the European Union - PON Research and Innovation 2014-2020 in accordance with Article 24, paragraph 3a), of Law No. 240 of December 30, 2010, as amended and Ministerial Decree No. 1062 of August 10, 2021. Special thanks to our contributing partner, Mariani Fratelli Srl.

References

1. Buttarazzi, M.G., Borchi, F., Mambelli, A., Carfagni, M., Governi, L., Puggelli, L.: An active noise control system for reducing siren noise inside the ambulance. In: ADM International Conference, pp. 630–640. Springer International Publishing, Florence, Italy (2023)
2. Widrow, B., Stearns, S.D.: Adaptive Signal Processing. Prentice-Hall Signal Processing Series, Upper Saddle River, New Jersey, USA (1985)
3. Kuo, S.M., Morgan, D.R.: Active Noise Control Systems Algorithms and DSP Implementations. Wiley, New York, USA (1996)
4. Ardekani, I.T., Abdulla, W.H.: FxLMS-based active noise control: A quick review. In: Proceedings of Asia-Pacific Signal and Information Processing Association Annual Summit and Conference, vol. 1, pp. 1–11. Xi'an, China (2011)

5. Buttarazzi, M.G., Bartalucci, C., Borchì, F., Carfagni, M., Paolucci, L.: Analysis of Possible Algorithms for Active Noise Control of Siren Noise into an Ambulance. In: International Conference on Design, Simulation, Manufacturing: The Innovation Exchange, pp. 630–640. Cham: Springer International Publishing, Rome, Italy (2021)
6. Singh, S., Sharma, M.K., Agrawal, S.: Ambulance siren noise reduction using psychoacoustic active noise control system with A-weighting filter. In: International Conference on Computing, Communication & Automation, pp. 990–993. Greater Noida, India (2015)
7. Pal, R., Sharma, M.K., Thangjam, S.: Ambulance Siren Noise Reduction Using Virtual Sensor based Feedforward ANC System. In: Proceedings 2nd International Conference on Advances in Computing and Communication Engineering, Dehradun, India (2015)
8. Gupta, P., Sharma, M.K., Thangjam, S.: Ambulance siren noise reduction using noise power scheduling based online secondary path modeling for ANC System. In: International Conference on Signal Processing, Computing and Control (ISPCC), pp. 63–67. Wagnaghat, India (2015)
9. Sharma, M.K., Vig, R.: Ambulance Siren Noise Reduction using LMS and FXLMS Algorithms. *Indian Journal of Science and Technology* **9**(47), 1–6 (2016)
10. Akhtar, M.T., Abe, M., Kawamata, M.: Adaptive filtering with averaging-based algorithm for feedforward active noise control systems. In: *IEEE Signal Processing Letters*, vol. 11, no. 6, pp. 557–560 (2004)